2020-04-30

# Rit2-Dependent Dopamine Transporter Endocytosis: Intrinsic Mechanism and In Vivo Impact

Rita R. Fagan
*University of Massachusetts Medical School*

# RIT2-DEPENDENT DOPAMINE TRANSPORTER ENDOCYTOSIS: INTRINSIC MECHANISM AND *IN VIVO* IMPACT

A Dissertation Presented

By

RITA FAGAN

Submitted to the Faculty of the
University of Massachusetts Graduate School of Biomedical Sciences, Worcester
in partial fulfillment of the requirements for the degree of

DOCTOR OF PHILOSOPHY

APRIL 30, 2020

NEUROSCIENCE

# RIT2-DEPENDENT DOPAMINE TRANSPORTER ENDOCYTOSIS: INTRINSIC MECHANISM AND *IN VIVO* IMPACT

A Dissertation Presented

By

RITA FAGAN

This work was undertaken in the Graduate School of Biomedical Sciences

Program in Neuroscience

Under the mentorship of

Haley Melikian, Ph.D., Thesis Advisor

Patrick Emery, Ph.D., Member of Committee

Mary Munson, Ph.D., Member of Committee

David Lambright, Ph.D. Member of Committee

Jonathan Javitch, M.D., Ph.D., External Member of Committee

Paul Gardner, Ph.D., Chair of Committee

Mary Ellen Lane, Ph.D.
Dean of the Graduate School of Biomedical Sciences

April 30, 2020

## ACKNOWLEDGEMENTS

First, I thank my thesis advisor, Haley Melikian. I joined Haley's lab in 2013 (it was my third rotation, and I never left). I was blown away by her enthusiasm for science and mentorship. I remember her training me herself at the bench on my first day, and thinking that I wasn't going to find better graduate training anywhere. Not only that, but Haley clearly had very high expectations for her students and trainees, so I knew she would push me to become a good scientist. When I started in Haley's lab, I had only just graduated from college the year before, so I knew I had a lot to learn. Over the years, our weekly meetings went from me trying to not be show how nervous I was that I didn't know the answer to her questions, to weekly chats about new data and hypotheses.

They say that the road to a PhD is not a straight line from start to finish, and this is certainly true for me. Throughout the course of my graduate work, there were some ups and a lot of downs, but Haley's optimism and guidance never appeared to waver. Together, we designed a new project from a couple pieces of data, which turned into a cohesive story and became my very first first-author publication. Haley's mentorship shaped me into the scientist I am today, and I am forever grateful. As soon as I started asking, "what's the biological question?" during my peers' practice presentations, I knew her influence had fully solidified. Wherever I go and whatever I do next, I will always remember the things she taught me.

I also need to thank the women scientists from the lab I worked in during my undergraduate years at UMass Amherst. Especially Maggie Shen, Chris Devine, and Tuba Ozacar. Without your support, I might never have pursued science or gone on to graduate school. I was only just one of many undergraduates who cycled through the lab while you were there, but you all inspired and encouraged my love for scientific discovery, and I am so grateful.

I would also like to acknowledge my TRAC and DEC members, Patrick Emery, Mary Munson, Paul Gardner, Vivian Budnik, and David Lambright. Your guidance and support throughout my PhD journey were absolutely essential. Thank you, also, to Jonathan Javitch for serving as the external examiner on my committee.

None of the work presented in this thesis was done in isolation, and I am so grateful to everyone who contributed to the research.

*Chapter II:* Thank you so much to the team of people who contributed valuable data to this story. To Brian and Lauren, thank you so much for keeping the ball rolling on these experiments. Your data helped inspire many of the hypotheses and interpretations we made. To Harald Sitte and his team of researchers, I am so grateful to you for sharing your expertise and resources with us so that we could elevate this story. A huge thanks to Patrick, of course, for doing so many experiments, and being incredibly flexible when Haley and I needed data and

figures presented in one way one week, and another the next. Again, this paper would not be what it is without your contributions. Finally, I thank Carolyn for devoting years and years to developing and optimizing tools essential to this story. This chapter represents the culmination of our heartache and pain over whether “Rit2 was even in these cells”, and where our projects would be going during that uncertain and extremely difficult time. I am so happy and proud that it finally came together in the end, and it would not have been possible without your hard work. *Chapter III*: This project would not have been possible without the guidance and support from Patrick Emery and his lab. Taking on a project outside of the expertise of my thesis mentor was only possible because of the wonderful collaboration between our labs. I would like to specifically thank Ratna Chaturvedi for answering my many questions about flies and sleep, and helping me set up experiments, never without a smile.

Thank you so much to my lab mates. All of you helped make me the scientist and person I am now. Thank you to Allyson, Brian, Lauren, Tucker, and Nick. You all brighten the lab and make coming to work that much better. To Sijia and Carolyn: you were the only (full-time) members of the lab when I rotated, and the environment and culture we had together in the lab was a huge part of why I joined. Sijia, thank you for not only answering all my questions and talking about science and experiments with me, but for being a great friend (and also, of course, for “the gossips”). Carolyn, I can’t imagine sharing a bay or sitting next to anyone else for

so long. We always had each other's backs, and it was definitely an adjustment when you left. Thank you for always listening and supporting me, even when I doubted myself. Patrick, so much has happened over the past few years, and I'm so glad we could weather the storm(s) together. It would not have been the same without you, so thank you for always being there and handling the hassles with me.

To all my wonderful grad student friends I've had over the years, thank you so much. Ciearra, we've been friends since our 2nd year, and I honestly can't imagine going through my PhD without you. I feel like we've been in this together the whole way, and your friendship means so much to me. Thank you to Monika and Erica who always listen to me and have made working on the 7th floor that much more entertaining and fun. I'm so glad that we got the chance to become better friends.

To my friends and family, thank you so much for all your love and support throughout the years. To my mom and dad (Marie and Jay): I am so lucky to have such understanding parents; the fact that neither of you ever once asked when I would be finished with my PhD means so much to me. I love you. Thank you for everything!

## ABSTRACT

Dopamine (DA) governs movement, sleep, reward, and cognition. The presynaptic dopamine transporter (DAT), clears released DA, controlling DA signaling and homeostasis. Genetic DAT ablation causes hyperactivity, sleep reduction, and altered psychostimulant response. DAT surface expression is dynamic; DAT constitutively internalizes and recycles to and from the plasma membrane, and acute PKC activation stimulates DAT endocytosis. Cell line experiments demonstrated that PKC-stimulated DAT endocytosis requires Ack1 inactivation and the GTPase, Rit2. How Rit2 controls PKC-dependent DAT internalization, or whether regulated DAT endocytosis impacts behavior, is unknown. Here, I present data supporting that PKC activation stimulates Rit2/DAT dissociation, mediated by the DAT N-terminus. Further, Ack1 and Rit2 function independently to facilitate PKC-stimulated DAT internalization. Moreover, PKC-stimulated DAT endocytosis was limited to ventral striatum in *ex vivo* slice preparations, and required Rit2. Our lab previously demonstrated that certain DA-dependent behaviors required DAergic Rit2 in mice, however whether this was due to perturbed PKC-stimulated DAT internalization, or DAT-independent Rit2 function(s) remains untested. To address this, I turned to *Drosophila* and its Rit2 homolog Ric. I found that Ric and dDAT proteins interact in cell lines, and that constitutively active Ric (RicQ117L) increased dDAT function in cultured cells and *ex vivo* whole fly brains. However, neither DAergic Ric knockdown nor RicQ117L altered overall locomotion or sleep,

suggesting that these fundamental behaviors do not require DAergic Ric. Together, these results expand our understanding of intrinsic mechanisms controlling DAT endocytosis, and their impact on behavior.

TABLE OF CONTENTS

TITLE PAGE i

REVIEWER PAGE ii

ACKNOWLEDGEMENTS iii

ABSTRACT vii

TABLE OF CONTENTS ix

LIST OF TABLES xiii

LIST OF FIGURES xiv

COPYRIGHTED MATERIALS PRODUCED BY THE AUTHOR xvi

SYMBOLS AND ABBREVIATIONS xvii

Preface to Chapter I 1

CHAPTER I 2

Introduction 2

I.A Dopamine Signaling and Circuitry 2

Basal Ganglia and Striatal Circuitry 3

DA release and reuptake 8

I.B The Dopamine Transporter 9

Psychostimulant Pharmacology 12

DAT Animal Models 13

Disease-Associated DAT Coding Variants 17

I.C DAT Endocytic Regulation 25

Forward, biosynthetic trafficking 26

PKC-stimulated DAT trafficking 28

Constitutive DAT Trafficking 35

Post-endocytic DAT localization 40

Substrate-mediated DAT endocytosis 42

Receptor-mediated DAT trafficking 44

DAT Protein-Protein Interactions 50
Membrane potential-dependent DAT trafficking 59
DAT lateral mobility and plasma membrane distribution 59
I.D Rit2 GTPase 62
Rit subfamily of small GTPases 62
Rit subfamily cellular function 65
Rit2 genetic variations in neuropsychiatric diseases and disorders 67
Rit2 function in DA-dependent behavior 70
I.E Summary 71
Preface to Chapter II 73
CHAPTER II 74
Dopamine transporter trafficking and Rit2 GTPase: Mechanism of action and *in vivo* impact 74
II.A Summary 74
II.B Introduction 75
II.C Results 78
Rit2 cellular expression and antibody specificity 78
Rit2 is required for PKC-stimulated, but not basal, DAT internalization 84
Rit2 is required for striatal steady state DAT surface expression and PKC-stimulated DAT internalization in a region- and sex-specific manner 87
Releasing the PKC-sensitive DAT endocytic brake drives DAT-Rit2 dissociation at the plasma membrane 94
The DAT amino terminus is integral to the DAT-Rit2 interaction and PKC-stimulated dissociation 99
The DAT N-terminus is required for PKC-stimulated DAT internalization 103
Rit2 and Ack1 independently converge on DAT in response to PKC 107
II.D Discussion 110
II.E Experimental Procedures 115
Preface to Chapter III 129
CHAPTER III 130

Ric GTPase activity regulates dopaminergic function and sleep quality in a dopamine transporter-dependent manner in *Drosophila melanogaster* 130
III.A Summary 130
III.B Introduction 131
III.C Results 134
Ric interacts with dDAT 134
Constitutively active Ric increases dDAT function and surface levels 138
DAergic RicQ117L expression increases DA uptake ex vivo 138
DAergic Ric activity does not impact locomotor activity or total sleep 142
DAergic Ric expression is not required for locomotor activity or sleep 144
DAergic Ric activity decreases sleep bout consolidation 147
dDAT is required for the RicQ117L sleep fragmentation phenotype 149
III.D Discussion 151
III.E Experimental Procedures 157
CHAPTER IV 164
Discussion and Future Directions 164
IV.A Rit2 is required for PKC-stimulated DAT endocytosis 165
Endogenous PKC activation 168
Is Rit2 required for AMPH's actions at DAT? 169
IV.B Rit2-dependent DAT endocytic mechanism 171
Rit2 and Ack1 independently facilitate PKC-stimulated DAT internalization 174
Ack1 inactivation 175
IV.C Applications for the BBS-DAT pulldown approach 176
IV.D *In vivo* impact of regulated DAT endocytosis 179
Trafficking-dysregulated DAT mutants 182
Drosophila DAT and SERT MPH affinity 185
IV.E Rit2 GTPase function and expression 186
DA neuron-independent Rit2 function 187
DAT-independent Rit2 function 188
Rit2 sexual dimorphisms in DA signaling and behavior 189
Rit2 in PD and neuronal viability 190

IV.F Concluding remarks 191
Bibliography 193

## LIST OF TABLES


| | | |
|---|---|---|
| Table I.1 | Disease-associated DAT Coding Variants | 19 |
| Table I.2 | DAT Protein-Protein Interactions | 51 |
| Table I.3 | Neuropsychiatric diseases and disorders associated with Rit2 genetic variations | 69 |
| Table II.1 | Rit2 expression in mammalian cell lines and rodent brain regions | 80 |

## LIST OF FIGURES


| | | |
|---|---|---|
| Figure I.1 | Dopamine projections in the mouse brain. | 5 |
| Figure I.2 | PKC-stimulated DAT trafficking and endocytic brake model. | 32 |
| Figure II.1 | Rit2 protein is specifically detected by clone 4B5, but not clone 27G2, αRit2 antibodies. | 83 |
| Figure II.2 | Rit2 is required for PKC-stimulated DAT internalization in SK-N-DZ cells. | 85 |
| Figure II.3 | PKC-induced DAT internalization in females is limited to ventral striatum and requires Rit2. | 89 |
| Figure II.4 | PKC-induced DAT internalization in males is limited to ventral striatum and requires Rit2. | 92 |
| Figure II.5 | Surface DAT associates with Rit2 and Ack1, but not Rit1. | 99 |
| Figure II.6 | PKC-mediated endocytic brake release drives DAT-Rit2 dissociation at the plasma membrane. | 98 |
| Figure II.7 | The SERT N-terminus promotes the DAT-Rit2 interaction and blocks PKC-stimulated DAT-Rit2 dissociation. | 101 |
| Figure II.8 | The DAT N-terminus is required for PKC-stimulated DAT internalization. | 105 |
| Figure II.9 | Rit2 and Ack1 independently converge on DAT downstream of PKC activation. | 109 |
| Figure III.1 | Ric interacts with dDAT. | 137 |
| Figure III.2 | Ric activity increases dDAT function and surface expression. | 140 |
| Figure III.3 | Ric activity in DA neurons is not required for baseline locomotor or sleep behavior. | 143 |
| Figure III.4 | Ric expression in DA neurons is not required for locomotor or sleep behavior. | 145 |
| Figure III.5 | DAergic Ric activity modulates sleep bout frequency. | 148 |

Figure III.6 RicQ117L-dependent wake and sleep bout fragmentation is dDAT-dependent. 150

## COPYRIGHTED MATERIALS PRODUCED BY THE AUTHOR

Portions of Chapter I were previously published in:

Fagan, RR, Kearney, PJ, and Melikian HE (2020) In situ regulated dopamine transporter trafficking: There's no place like home. Neurochem Res, in press. DOI: 10.1007/s11064-020-03001-6.

Chapter II of this dissertation was previously published in:

Fagan, RR, Kearney, PJ, Sweeney, CG, Leuthi, D, Uiterkamp, FES, Schicker, K, Alejandro, BS, O'Connor, LC, Sitte, HH, and Melikian, HE (2020) Dopamine transporter trafficking and Rit2 GTPase: Mechanism of action and *in vivo* impact. J Biol Chem, in press. DOI: 10.1074/jbc.RA120.012628.

## SYMBOLS AND ABBREVIATIONS

| | |
|---|---|
| σ1R | sigma receptor 1 |
| 5-HT | serotonin |
| AAV | adeno-associated virus |
| Ack1 | activated by cdc41 kinase 1 |
| ADE | anomalous DA efflux |
| ADHD | attention-deficit/hyperactive disorder |
| Akt | protein kinase B |
| AMPH | amphetamine |
| ASD | autism spectrum disorder |
| BBS | bungarotoxin binding site |
| BIM I | bisindolylmaleimide I |
| BPD | bipolar disorder |
| BRET | bioluminescence resonance energy transfer |
| BTX | bungarotoxin |
| CA | constitutively active |
| CaMKII | calmodulin kinase II |
| CFP | cyan fluorescent protein |
| CIN | cholinergic interneuron |
| CNV | copy number variation |
| Co-IP | co-immunoprecipitation |
| COMT | catechol-O-methyltransferase |
| CPP | conditioned place preference |
| CTX | cholera toxin |
| DA | dopamine |
| DAergic | dopaminergic |
| DAG | diacylglycerol |
| DAT | dopamine transporter |
| DAT-CI | cocaine-insensitive DAT |

| | |
|---|---|
| DAT/C-S | DAT1-583/SERT601-630 |
| dDAT | *Drosophila melanogaster* DAT |
| DHPG | Dihydroxyphenylglycine |
| DN | dominant negative |
| DRD1-5 | dopamine receptor type 1-5 |
| DREADD | designer receptor exclusively activated by designer drugs |
| DS | dorsal striatum |
| dSERT | *Drosophila melanogaster* SERT |
| DTDS | dopamine transporter deficiency syndrome |
| EGF | epidermal growth factor |
| EL | extracellular loop |
| Epsin | epidermal growth factor pathway substrate |
| ER | endoplasmic reticulum |
| ERK | extracellular signal-regulated kinase |
| Flot1 | flotillin-1 |
| FRAP | fluorescence recovery after photobleaching |
| FRET | fluorescence resonance energy transfer |
| FSCV | fast-scan cyclic voltammetry |
| GABA | -aminobutyric acid |
| GAP | GTPase activating protein |
| GAT | GABA transporter |
| GDNF | glial cell-line derived neurotrophic factor |
| GDP | guanosine diphosphate |
| GEF | guanine nucleotide exchange factor |
| GFP | green fluorescent protein |
| GIRK | G-protein coupled inwardly-rectifying potassium channel |
| GLYT | glycine transporter |
| GPCR | G-protein coupled receptor |
| GPe | globus pallidus external segment |

| | |
|---|---|
| GPi | globus pallidus internal segment |
| GST | glutathione S-transferase |
| GTP | guanosine triphosphate |
| GWAS | genome wide association study |
| hDAT | *Homo sapiens* DAT |
| HEK | human embryonic kidney cells |
| IL | intracellular loop |
| IPD | infantile parkinsonism-dystonia |
| IRES | internal ribosomal entry site |
| KOR | kappa opioid receptor |
| L-DOPA | L-Dihydroxyphenylalanine |
| LAP | lipoic acid acceptor peptide |
| LeuT | leucine transporter |
| LplA | lipoic acid ligase |
| mβCD | methyl-β-cyclodextrin |
| M5 | muscarinic acetylcholine receptor 5 |
| MDCK | madin-darby canine kidney cells |
| mGluR | metabotropic glutamate receptor |
| MPH | methylphenidate |
| $MPP^+$ | 1-methyl-4-phenylpyridinium |
| MSN | medium spiny neurons |
| N-S/DAT | SERT1-78/DAT60-620 |
| n.c. | no change |
| n.d. | not determined |
| N2a | Neuro-2a cells |
| NE | norepinephrine |
| Nedd4-2 | neural precursor cell expressed developmentally downregulated 4-2 |
| NET | norepinephrine transporter |
| NGF | nerve growth factor |
| NK-1 | neurokinin 1 receptor |

| | |
|---|---|
| NMDA | N-methyl-D-aspartate |
| PAE | porcine aortic endothelial |
| PC6, PC12 | pheochromocytoma cells |
| PD | Parkinson's Disease |
| PDZ | postsynaptic density protein, drosophila discs large tumor suppressor, zonula occludens-1 protein domain |
| PI3-K | phosphoinositide 3-kinase |
| PICK1 | protein interacting with C kinase 1 |
| PKA | protein kinase A |
| PKC | protein kinase C |
| PKG | protein kinase G |
| PMA | phorbol 12-myristate 13-acetate |
| PRIME | PRobe Incorporation Mediated by Enzyme |
| RACK1 | receptor for activated C kinase 1 |
| Ric | Ras-like protein which interacted with calmodulin |
| Rit1 | Ric-related gene expressed throughout the organism |
| Rit2 | Ric-related gene expressed in neuronal tissues |
| Rit2-KD | Rit2 knockdown |
| RT-qPCR | reverse transcription quantitative polymerase chain reaction |
| RTK | receptor tyrosine kinase |
| S/DAT/S | SERT1-78/DAT60-583/SERT601-630 |
| SEM | standard error of the mean |
| sEPSP | spontaneous excitatory postsynaptic potential |
| SERT | serotonin transporter |
| shRNA | short hairpin ribonucleic acid |
| SLC6 | solute carrier family 6 |
| SNc | substantia nigra pars compacta |

| | |
|---|---|
| SNP | single nucleotide polymorphism |
| SNr | substantia nigra pars reticulata |
| STN | subthalamic nucleus |
| STORM | stochastic optical reconstruction microscopy |
| Syn1A | syntaxin 1A |
| TfR | transferrin receptor |
| TH | tyrosine hydroxylase |
| TIRF | total internal reflection fluorescence |
| TMD | transmembrane domain |
| TPA | 12-O-Tetradecanoylphorbol 13-acetate |
| TRE | tetracycline responsive element |
| tTA | tetracycline transactivator |
| Veh | vehicle |
| VMAT | vesicular monoamine transporter |
| VNTR | variable number of tandem repeats |
| Vps | vacuolar protein sorting-associated |
| VS | ventral striatum |
| VTA | ventral tegmental area |
| WT | wildtype |
| YFP | yellow fluorescent protein |

# Preface to Chapter I

Portions of this chapter were previously published in:

Fagan, RR, Kearney, PJ, and Melikian HE (2020) In situ regulated dopamine transporter trafficking: There's no place like home. Neurochem Res, in press. DOI: 10.1007/s11064-020-03001-6.

Author contributions:

Rita R. Fagan and Haley E. Melikian wrote original manuscript.

# CHAPTER I

## Introduction

### I.A Dopamine Signaling and Circuitry

Dopamine (DA) is a catecholamine neurotransmitter synthesized from the essential amino acid, tyrosine. Tyrosine hydroxylase (TH) hydroxylates the tyrosine phenol ring, generating L-dihydroxyphenylalanine (L-DOPA), which is then decarboxylated by DOPA decarboxylase to produce DA (Blaschko, 1952). In noradrenergic neurons, DA is further processed by dopamine β-hydroxylase into norepinephrine (NE; noradrenaline) (Molinoff and Axelrod, 1971). Though initially thought to simply serve as a precursor to NE, DA was later proposed to be a neurotransmitter itself, due to its high levels in the brain and ability to rescue reserpine-mediated tranquilization and akinesia in mice (Carlsson et al., 1957; Carlsson et al., 1958; Carlsson, 1959). These results, coupled with the discovery that DA concentrations are drastically reduced in Parkinson's disease (PD) patients, led to the development of L-DOPA as a clinical treatment for PD patients (Cotzias et al., 1967; Carlsson, 2002). DA is required for a wide variety of behaviors and cognitive functions such as movement, sleep, learning, memory, and reward (Wise, 2004; Hyman et al., 2006), and disruptions in DA signaling are implicated in many neuropsychiatric diseases and disorders, including PD (Geibl et al., 2019), attention deficit/hyperactivity disorder (ADHD) (Swanson et al., 2007), autism spectrum disorder (ASD) (Paval, 2017), schizophrenia (Owen et al., 2016), and bipolar disorder (BPD) (Ashok et al., 2017). Moreover, DA neurotransmission is an

essential component in reward and development of addiction (Hyman et al., 2006; Schultz, 2007b; Sulzer, 2011). Given its central role in behavior and disease, it is imperative to better understand the mechanisms underlying DA neurotransmission. In this section, I provide a broad overview of DA circuitry and the mechanisms fundamental to DA release and reuptake.

*Basal Ganglia and Striatal Circuitry*

Early experiments characterized the presence of high DA levels in the mammalian caudate and lentiform nuclei, which are core components of the basal ganglia (Carlsson, 1959; Moore and Bloom, 1978). The subcortical nuclei comprising the basal ganglia are the dorsal striatum (DS, or caudate nucleus and putamen), ventral striatum (VS, or nucleus accumbens), globus pallidus internal (GPi) and external (GPe) segments, subthalamic nucleus (STN), thalamus, substantia nigra pars compacta (SNc) and pars reticulata (SNr), and ventral tegmental area (VTA) (Smith et al., 1998; Bolam et al., 2000; Gerfen and Surmeier, 2011). Dopaminergic neurons form three major projections within the basal ganglia originating from the VTA and SNc. VTA DA neurons that terminate in the VS (mesolimbic pathway) are critical for reward and goal-directed behavior (Di Chiara and Imperato, 1988; Morales and Margolis, 2017). VTA DA neurons also project to the prefrontal cortex (PFC; mesocortical pathway), and are involved in executive function and cognitive control (Miller and Cohen, 2001). SNc DA neurons project to the DS (nigrostriatal pathway), and are involved in complex behaviors, such as movement initiation and

habit formation (Faure et al., 2005; Kravitz and Kreitzer, 2012). Subpopulations of VTA DA neurons also project to the interpeduncular nucleus (Molas et al., 2017), hippocampus (Gasbarri et al., 1997), amygdala (Inglis and Moghaddam, 1999), anterior cingulate nucleus (Narita et al., 2010), and olfactory tubercle (Voorn et al., 1986). The STN also receives DAergic input from the SNc (Cragg et al., 2004). Finally, another population of DA neuron cell bodies resides in the hypothalamus and projects to the pituitary, forming the tuberoinfundibular pathway (Stagkourakis et al., 2016) (Figure I.1).

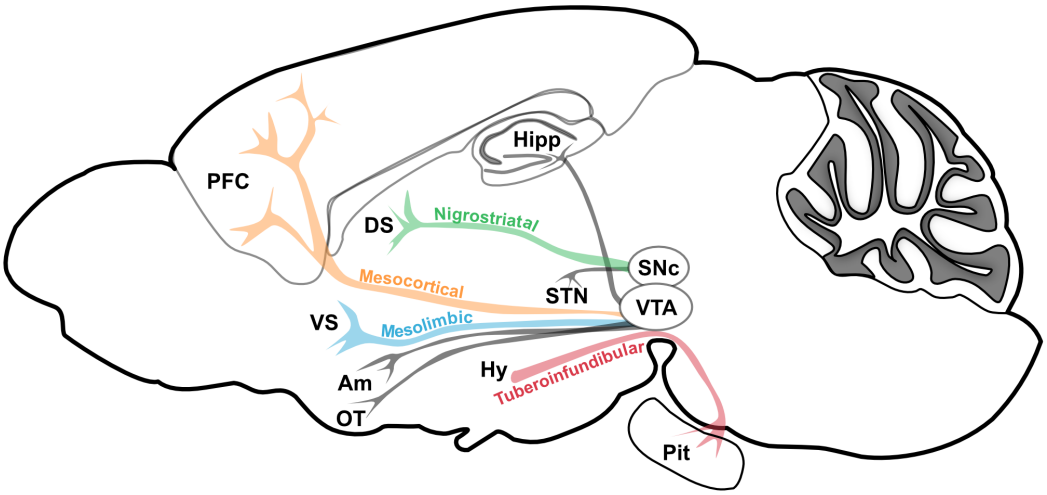


**Figure I.1 Dopamine projections in the mouse brain.** Major DA projections originate in the ventral midbrain regions. Ventral tegmental area (VTA) DA neurons form two main projections: the mesolimbic pathway, which projects into the ventral striatum (blue, VTA → VS), and the mesocortical pathway, which terminates in the prefrontal cortex (orange, VTA → PFC). Substantia nigra pars compacta (SNc) DA neurons terminate in the dorsal striatum, forming the nigrostriatal pathway (green, SNc → DS). There are also DA neuron cell bodies in the hypothalamus (Hy), which project to the pituitary gland (Pit), and constitute the tuberoinfundibular pathway (red). Subpopulations of DA neurons project from the VTA into the olfactory tubercule (OT), amygdala (Am), and hippocampus (Hipp), as well as from the SNc to the subthalamic nucleus (STN).

The striatum also receives input from numerous other, non-DAergic brain nuclei, including cortex, thalamus, hippocampus, and amygdala (Burke et al., 2017). Input to the DS is then transmitted one of two ways within the basal ganglia: the “direct” or “indirect” pathways, which are comprised of inhibitory γ-aminobutyric acid (GABA) projection neurons, or medium spiny neurons (MSNs) (Smith et al., 1998; Bolam et al., 2000). The direct pathway transmits inhibitory information via a single synapse to the inhibitory SNr and GPi regions, thereby disinhibiting the thalamus, and stimulating locomotion. The indirect pathway involves an inhibitory projection directly into the GPe, which releases its inhibition of the STN, facilitating STN-mediated excitation of the SNr and GPi, and thus maintaining baseline motor inhibition (Smith et al., 1998). In general, direct pathway MSNs express the $D_1$ DA receptor subtype and neuropeptides substance P and dynorphin, whereas indirect MSNs express the $D_2$ subtype and the neuropeptide enkephalin (Gerfen et al., 1990; Smith et al., 1998). Some studies have reported $D_1$ and $D_2$ co-expression, nevertheless, the majority of evidence supports that the direct and indirect pathways signal through $D_1$ and $D_2$ receptor subtypes, respectively (Bertran-Gonzalez et al., 2010).

DA receptors are G-protein coupled receptors (GPCRs) that signal through G-proteins to modulate adenylyl cyclase (AC) activity and downstream cyclic AMP production (Kebabian et al., 1972; Kebabian and Calne, 1979; Vallone et al., 2000; Beaulieu and Gainetdinov, 2011). The $D_1$ receptor subtype consists of DA receptors 1 and 5 (DRD1 and DRD5), which stimulate AC activity via $G_s$-coupled

cascades. DRD1 is expressed on direct pathway MSNs in the striatum, as mentioned previously, as well as in the SN, olfactory bulb, amygdala, frontal cortex, hippocampus, cerebellum, thalamus, and hypothalamus. DRD5 is lowly expressed in multiple brain areas that include the PFC, striatal MSNs, SN, and hippocampus (Beaulieu and Gainetdinov, 2011). On the other hand, $D_2$ receptors are coupled to $G_{i/o}$ signaling pathways and therefore inhibit AC activity. This subtype includes DA receptors 2, 3, and 4 (DRD2, DRD3, and DRD4), and while DRD3 and DRD4 have relatively limited expression patterns in the brain, DRD2 is highly expressed on indirect MSNs in the striatum, and in SN, VTA, olfactory tubercle, amygdala, hippocampus, and hypothalamus (Missale et al., 1998; Gerfen and Surmeier, 2011). In addition to expressing postsynaptically on MSNs, DRD2 and DRD3 are also present presynaptically on DA neurons where they function as autoreceptors (Missale et al., 1998). Additionally, DA neurons express DRD2 and DRD3 in the somatodendritic region, and these receptors modulate DA neuron activity via activation of G protein-gated inwardly rectifying $K^+$ (GIRK) channels (McCall et al., 2016).

GABAergic and cholinergic interneurons are also present in the striatum. These neurons express DA receptors, and are therefore also sensitive to DA release (Kreitzer and Malenka, 2008). Moreover, DA terminals express both glutamate and cholinergic receptors, which in turn can regulate DA neuron activity and release (Cachope et al., 2012; Sulzer et al., 2016). This high level of circuit complexity

likely allows for further shaping of striatal output, beyond simply promoting or suppressing locomotion. For instance, since its initial characterization as a hub of motor behavior, the DS has been implicated in motor planning and habit formation, and the VS is specialized for reward-based learning (Isomura et al., 2013). Given its critical role in controlling myriad behaviors within this complex circuit, it is crucial to understand the mechanisms that control DA signaling and homeostasis.

*DA release and reuptake*

Several factors contribute to striatal DA release, such as neuronal firing rate and receptor activation (Sulzer et al., 2016). DA neurons exhibit two distinct firing patterns: tonic firing (~3-8 Hz), which establishes a baseline DAergic tone, and phasic (or burst) firing (>10 Hz) in response to salient behavioral stimuli (Grace and Bunney, 1984; Grace, 1991; Sulzer, 2011). Rewarding stimuli increase phasic firing, and phasic DA neuron firing suffices to drive behavioral conditioning (Tsai et al., 2009; Keiflin and Janak, 2015). DA release is negatively regulated by the DRD2, presumably functioning cell-autonomously within the DA neuron, however postsynaptic DRD2 activation and downstream indirect mechanisms cannot be completely ruled out (Anzalone et al., 2012). DRD2 reduces TH activity, the rate-limiting enzyme in DA synthesis, via $G_i$-coupled signaling, which decreases cAMP production and protein kinase (PKA)-dependent TH phosphorylation and activity (Kehr et al., 1972; Wolf and Roth, 1990; Pothos et al., 1998). Furthermore, DRD2 expressed in the somatodendritic regions of the DA neurons decreases DA release

probability by hyperpolarizing the DA neuron via GIRK channel activation (Schmitz et al., 2002; Schmitz et al., 2003).

Once released, extracellular DA must be cleared in order to terminate the signal. Originally, Axelrod and colleagues proposed that this process was governed by metabolism via the enzymes monoamine oxidase (MAO) and catechol-O-methyltransferase (COMT) for neurotransmitters including DA and NE (Axelrod and Tomchick, 1958; Fowler and Benedetti, 1983; Axelrod, 2003). However, direct COMT inactivation did not cause NE accumulation, indicating the presence of a separate mechanism that functions to clear released transmitter (Axelrod, 2003). Using tritiated monoamines, researchers later discovered the existence of distinct reuptake mechanisms for DA, NE, serotonin (5-HT), and others (Hertting and Axelrod, 1961; Blackburn et al., 1967; Snyder and Coyle, 1969). Below, I will discuss DA uptake in greater detail, focusing on the transport mechanism and *in vivo* consequences for overall DA homeostasis and behavior that result from dysregulated DA uptake function.

## I.B The Dopamine Transporter

Synaptic DA clearance is mediated by the presynaptic dopamine transporter (DAT). DAT is a member of the large solute carrier gene family (SLC) comprised of over 300 distinct transporters classified into 55 subfamilies (Kristensen et al., 2011). DAT is an SLC6 transporter (SLC6A3), as are the neurotransmitter

transporters for 5-HT and NE (SERT and NET, respectively), two glycine transporters (GLYT1, GLYT2), and four GABA transporters (GAT1, GAT3, GAT4, and BGT1) (Kristensen et al., 2011). Despite numerous studies characterizing the behavioral relevance and function of these transporters, the rodent and human DAT, SERT, and NET genes were not cloned until the early 1990s (Blakely et al., 1991; Kilty et al., 1991; Giros et al., 1992; Ramamoorthy et al., 1993; Brüss et al., 1997). DAT hydropathy analysis predicted a topology of 12 transmembrane domains (TMDs), 6 extracellular loops (ELs), 5 intracellular loops (ILs), and intracellular N- and C-termini (Giros et al., 1992; Torres et al., 2003a). DAT is expressed exclusively in DA neurons, and resides outside of synaptic active zones (i.e. perisynaptically), therefore DAT is particularly well-positioned for its critical function: spatially and temporally limiting DA neurotransmission (Nirenberg et al., 1996; Hersch et al., 1997). DAT translocates DA via an “alternating-access” mechanism in which extracellular DA interacts with its substrate binding pocket when DAT is outwardly-facing, and releases into the cytoplasm following DAT’s conformational change to inwardly-facing. DAT’s affinity for DA has been measured in an array of model systems, and ranges from approximately 0.25-5.25μM, depending on the expression context. The transport cycle is completed when DAT re-establishes its outwardly-facing conformation, translocating on average 0.75-2.0 DA molecules per second (Kristensen et al., 2011; Pramod et al., 2013).

Although the mammalian DAT structure remains unsolved, solution of the evolutionarily related bacterial leucine transporter (LeuT) supported the predicted topology and substrate translocation process of mammalian SLC6 transporters (Yamashita et al., 2005). The crystal structure of the *Drosophila melanogaster* DAT (dDAT), which shares more than 50% sequence identity with human DAT (Porzgen et al., 2001), was recently reported by the Gouaux group. The dDAT crystal structure solution was a major breakthrough in the field's understanding of inhibitor binding and substrate translocation process for the SLC6 transporter family. Previous studies established that SLC6 transporters require cotransport of extracellular $Na^+$ and $Cl^-$ ions for substrate reuptake. Moreover, when DA transport properties were measured in transfected cells, researchers found that $Na^+$-dependent DA uptake rate was sigmoidal, indicating participation of multiple $Na^+$ ions (Gu et al., 1994). Penmatsa and colleagues indeed found all three ions bound to dDAT, and also observed an interaction with a cholesterol molecule (Penmatsa et al., 2013). The dDAT crystal structure confirmed the predicted topology and also revealed 1) a kink in TMD12 which oriented distal residues away from the core of the transporter, and 2) that the C-terminus is stabilized via hydrogen bonds with sites in IL1, forming a latch-like structure. Given the critical role of the C-terminus in DAT endocytic regulation and protein-protein interactions (discussed in detail in "*DAT Endocytic Regulation*"), these structural data shed light on how conformational changes may impact DAT's ability to undergo functional or surface expression changes.

*Psychostimulant Pharmacology*

DAT is the primary molecular target for addictive and therapeutic psychostimulants, which include cocaine, amphetamine (AMPH), and methylphenidate (MPH; Ritalin). Although all rewarding drugs increase extracellular DA in the VS, psychostimulants specifically increase extracellular DA by competitively inhibiting DAT with sub-micromolar potency, further potentiating DA neurotransmission (Han and Gu, 2006; Sulzer, 2011). Typical psychostimulant behavioral phenotypes include increased locomotor activity, arousal, attention, and wakefulness (Wood et al., 2014). While these drugs also target other neurotransmitter reuptake systems (NET and SERT), DAT is absolutely essential for their hyperlocomotive and rewarding effects (discussed in further detail in "*Cocaine-insensitive DAT*").

Cocaine and MPH bind to DAT and inhibit DA reuptake, but AMPH is a DAT substrate that also facilitates reverse DA transport (efflux) through DAT once inside the cell (Fischer and Cho, 1979; Kantor and Gnegy, 1998; Sitte et al., 1998; Khoshbouei et al., 2003). Typically, the vesicular monoamine transporter 2 (VMAT2) loads synaptic vesicles with DA. However, in order for AMPH to cause DA release through DAT, it must redistribute DA out of synaptic vesicles. The mechanism underlying how AMPH mobilizes DA from vesicles into the cytosol has been the subject of debate in the field. One possible explanation for how AMPH

causes DA release is the “weak base hypothesis”, in which AMPH disrupts the vesicular pH gradient required for VMAT2-mediated DA transport, and increases cytosolic DA levels. Freyberg and colleagues tested this hypothesis *in vivo* for the first time using a false fluorescent neurotransmitter and pH biosensor, dVMAT-pHluorin, in whole *Drosophila* brain preparations. Investigators determined that AMPH dose-dependently alkalizes DA terminal vesicles in a dDAT- and dVMAT-dependent manner, by genetically and pharmacologically disrupting the transporters (Freyberg et al., 2016). Notably, MPH had no effect on vesicular pH, indicating that the alkalization is specific to substrates of dDAT and dVMAT. However, 1-methyl-4-phenylpyridinium ($MPP^+$), a substrate for both transporters, but not a weak base, also alkalized the synaptic vesicles, suggesting that the antiport of 2 $H^+$ ions by VMAT, which occurs during substrate translocation, is sufficient for vesicle alkalization (Freyberg et al., 2016). Thus, AMPH increases the pH of synaptic vesicles, which consequently increases cytoplasmic DA levels (via an unknown mechanism) and promotes reverse DA transport through DAT. While these data illustrate DAT’s requirement for psychostimulant actions at DAergic synapses, genetic DAT ablation animal models (described below) provide further evidence of DAT’s critical role in regulating DA homeostasis and the *in vivo* response to psychostimulants.

*DAT Animal Models*

*DAT*$^{-/-}$ Mice

The DAT knockout (*DAT*$^{-/-}$) mouse line was generated and characterized over twenty years ago (Giros et al., 1996). These mice are slightly underweight and die earlier compared to wildtype littermates, but are fertile despite the reported reduction in maternal behavior. Locomotor activity is dramatically increased in *DAT*$^{-/-}$ mice, and habituation to a novel environment takes twice as long as *DAT*$^{+/+}$ and *DAT*$^{+/-}$ mice (Giros et al., 1996). Moreover, using fast-scan cyclic voltammetry (FSCV), Giros and colleagues found that *DAT*$^{-/-}$ mice have reduced DA release, slower DA reuptake kinetics, and no AMPH-stimulated DA efflux. Accordingly, *DAT*$^{-/-}$ mice also do not display acute hyperactivity following psychostimulant injection (Giros et al., 1996). In a follow-up study, researchers confirmed the critical role of DAT in maintaining presynaptic DA stores. Quantitative microdialysis experiments revealed markedly increased extracellular DA concentrations and decreased tissue DA stores in *DAT*$^{-/-}$ animals (Gainetdinov et al., 1998). Interestingly, DA synthesis rates in *DAT*$^{-/-}$ mice were increased two-fold (Jones et al., 1998), indicating that DA synthesis by TH cannot suffice to maintain synaptic DA stores in the absence of DAT.

In order to test whether DAT is required for psychostimulant-induced addictive behaviors, researchers measured self-administration in *DAT*$^{-/-}$ mice. The self-administration behavioral paradigm involves training animals to learn to perform an action in order to receive an intravenous injection of a drug, and measures the animal's drug-seeking behavior. To the researcher's surprise, *DAT*$^{-/-}$ mice self-

administered cocaine, although they required significantly more sessions to meet acquisition criteria (5 versus 10 sessions, on average) (Rocha et al., 1998). Additionally, DA concentrations did not increase in *DAT*$^{-/-}$ mice during cocaine administration as measured by *in vivo* microdialysis (Rocha et al., 1998). Taken together, researchers hypothesized that other catecholamine systems, such as 5-HT, suffice in absence of DAT for cocaine-dependent reward. Alternatively, DAT may not be as critical for psychostimulant reward as previously thought.

Cocaine-insensitive DAT

Given the result that DAT was not required for cocaine self-administration in mice, (Rocha et al., 1998), scientists were prompted to take an alternative approach to test the specific requirement for DAT in cocaine reward. To do this, Chen and colleagues screened for DAT residues required for cocaine binding, but not DA reuptake and identified L104V, F105C, and A109V, within TM2 of DAT (Chen et al., 2005). The cassette containing these mutations was inserted into the endogenous mouse DAT gene to generate a cocaine-insensitive DAT (DAT-CI) mouse model. Protein expression and DA transport in DAT-CI mice were comparable to wildtype (Chen et al., 2006). Importantly, the cocaine affinity of DAT-CI mice was approximately 35μM, almost two orders of magnitude less potent than in wildtype mice (0.39μM) (Chen et al., 2006). As predicted, *in vivo* microdialysis measurements of DA concentrations revealed that the DAT-CI mice were insensitive to cocaine-mediated increases. This was specific to cocaine, as

AMPH treatment elevated DA levels in both wildtype and DAT-CI mice (Chen et al., 2006).

Finally, acute i.p. cocaine injection no longer increased locomotor activity in DAT-CI mice; in fact, these mice had significantly reduced locomotion following cocaine treatment (Chen et al., 2006). Consistent with the microdialysis experiments, AMPH- and morphine-induced hyperactivity remained intact. Cocaine-mediated reward was also disrupted in the DAT-CI mouse model. Cocaine preference, measured by conditioned place preference (CPP), and self-administration were completely absent in DAT-CI mice, whereas AMPH-dependent reward remained intact (Chen et al., 2006; Thomsen et al., 2009). Thus, despite the initial conclusion that DAT is not required for cocaine-dependent behavior, the DAT-CI mouse revealed that DAT is, in fact, indispensable for cocaine-mediated hyperactivity and reward.

*DAT$^{fmn}$ Drosophila melanogaster*

In addition to mammalian animal models, DAT-dependent behaviors can be modeled in *Drosophila melanogaster* (Kaun et al., 2012; Martin and Krantz, 2014). Of the three monoamine transporters, *Drosophila* only express DAT and SERT (Demchyshyn et al., 1994; Porzgen et al., 2001). A null mutation in the *Drosophila* DAT (dDAT) gene was serendipitously discovered and characterized by Kume and colleagues (Kume et al., 2005). These flies exhibit significantly more locomotor

activity and reduced sleep (Kume et al., 2005). Given the sleepless nature of these flies, the mutant allele was dubbed "*fumin*" (*fmn*), the Japanese translation for "sleepless". In addition, whereas wildtype flies show sleep rebound (increased sleep following mechanical sleep deprivation for 2, 4, or 6 hours), *fmn* flies did not, indicating a requirement for dDAT in homeostatic sleep (Kume et al., 2005). Remarkably similar phenotypes were observed in flies fed methamphetamine (Andretic et al., 2005), further highlighting the conserved role of DA and DAT in regulating locomotor and sleep behavior. Importantly, dDAT is also required for psychostimulant-induced hyperlocomotion, as demonstrated by loss of AMPH- and MPH-dependent hyperactivity in *fmn* larvae (Pizzo et al., 2013). These data support that the DAergic system is highly conserved, and regulates similar functions and behaviors in invertebrates and mammals.

*Disease-Associated DAT Coding Variants*

DAT genetic variation has been studied in the context of human patients with neuropsychiatric diseases and disorders. Variable number of tandem repeats (VNTRs) in the downstream 3' region of the *DAT* gene are tenuously linked to patients with schizophrenia, PD, ADHD, and alcoholism (Fuke et al., 2001; Hahn and Blakely, 2007). *DAT* missense mutations and single nucleotide polymorphisms (SNPs) have also been found in patients with these diseases, as well as in infantile parkinsonism-dystonia (IPD) patients, a degenerative neurological disorder (Table I.1). DAT mutations found in IPD cause almost

complete or total loss-of-function, with very little to no DAT protein expressed, hence this disorder is also referred to as dopamine transporter deficiency syndrome (DTDS) (Kurian et al., 2009; Kurian et al., 2011; Pramod et al., 2013; Ng et al., 2014; Asjad et al., 2017). Of particular interest, researchers have characterized more subtle changes in DAT function and expression in ADHD, ASD, BPD, and schizophrenia patients (described in further detail below) that, in some cases, significantly disrupt DA-dependent behaviors. Overall, these coding variants highlight DAT's fundamental role in controlling DA synaptic homeostasis and behavior.

## Table I.1 Disease-associated DAT Coding Variants

| Disorder | DAT Variant | Functional Effect(s) | | | Behavioral Phenotype(s) | References |
|---|---|---|---|---|---|---|
| | | *DA uptake* | *Surface expression* | *DA efflux* | | |
| **ADHD** | V55A | ↓ ($K_m$) | n.c. | n.d. | n.d. | Lin and Uhl (2003) |
| | V382A | ↓ ($V_{max}$) | ↓ | n.d. | n.d. | Lin and Uhl (2003), Mazei-Robison and Blakely (2005) |
| | A559V | ↓ ($V_{max}$; DS only) | ↑ (DS only), ↑ lateral mobility | ADE; blocked by AMPH | ↓ rearing, ↑ darting, ↓ MPH & AMPH hyperactivity | Mazei-Robison et al. (2005), Mazei-Robison et al. (2008), Gowrishankar et al. (2018), Thal et al. (2019) |
| | R615C | ↓ ($V_{max}$) | ↑ trafficking, ↑ lateral mobility | n.c. | n.d. | Sakrikar et al. (2012), Kovtun et al. (2015), Wu et al. (2015) |
| **ASD** | R51W | n.c. | n.d. | ↓ AMPH-stim efflux | ↓ AMPH hyperactivity (Dmel) | Cartier et al. (2015) |
| | T356M | ↓ ($V_{max}$) | n.c. | ADE | ↓ baseline & AMPH hyperactivity (Dmel, Mmus) | Neale et al. (2012), Hamilton et al. (2013), DiCarlo et al. (2019) |
| | A559V | | | | | Bowton et al. (2014) |
| **BPD** | A559V | | | | | Grünhage et al. (2000) |
| | E602G | n.c. | n.c. | n.d. | n.d. | Herborg et al. (2018) |
| **IPD** | R85L | ↓↓ | ↓ | n.d. | n.d. | Asjad et al. (2017) |
| | V158F* | ↓↓ | ↓ | n.d. | reduced sleep (Dmel) | Asjad et al. (2017) |

| | | | | | | |
|---|---|---|---|---|---|---|
| | L224P | ↓↓ | ↓ | n.d. | n.d. | Asjad et al. (2017) |
| | A314V | ↓↓ | ↓ | n.d. | n.d. | Asjad et al. (2017) |
| | G327R* | ↓↓ | ↓ | n.d. | reduced sleep (Dmel) | Asjad et al. (2017) |
| | L368Q* | ↓↓ | ↓ | n.d. | n.d. | Kurian et al. (2009); Asjad et al. (2017) |
| | G386R | ↓↓ | ↓ | n.d. | n.d. | Asjad et al. (2017) |
| | P395L | ↓↓ | ↓ | n.d. | n.d. | Kurian et al. (2009); Asjad et al. (2017) |
| | R445C | ↓↓ | ↓ | n.d. | n.d. | Asjad et al. (2017) |
| | Y470S | ↓↓ | ↓ | n.d. | n.d. | Asjad et al. (2017) |
| | R521W | ↓↓ | ↓ | n.d. | n.d. | Asjad et al. (2017) |
| | P529L | ↓↓ | ↓ | n.d. | n.d. | Asjad et al. (2017) |
| | P554L | ↓↓ | ↓ | n.d. | n.d. | Asjad et al. (2017) |
| **Unknown** | R237Q | n.c. | n.c. | n.c. | n.d. | Mazei-Robison et al. (2005) |

n.c. no change; n.d. not determined; ADE: anomalous DA efflux; ↓: reduced $V_{max}$; ↓↓: virtually undetectable DA uptake; *loss of uptake reduced with pharmacochaperoning; Dmel: *Drosophila melanogaster*; Mmus: *Mus musculus*

V382A, V55A, R237Q, and E602G

DAT coding variants V382A, V55A, R237Q, and E602G were originally found in human patients with ADHD or BPD (Cargill et al., 1999; Vandenbergh, 2000). These mutations only mildly, if at all, affect DAT function or expression. The ADHD-associated mutation in DAT EL4, V382A, displayed reduced DA transport activity and surface expression, but has not yet been linked to behavioral phenotypes (Lin and Uhl, 2003). The missense variant in the DAT N-terminus, V55A, was also found in an ADHD proband, but had no effect on DAT surface expression or total DA uptake (Lin and Uhl, 2003). R237Q-DAT, a TMD4 mutation originally identified in a screen for single nucleotide polymorphisms (SNPs), was later demonstrated to function and express equally to wildtype DAT in all parameters tested (DA uptake kinetics, psychostimulant affinity, DAT surface expression, and PKC-stimulated DAT functional downregulation) (Cargill et al., 1999; Mazei-Robison and Blakely, 2005; Mazei-Robison et al., 2008). Finally, in a screen of patients with BPD, the DAT C-terminal mutation E602G was identified (Grünhage et al., 2000), however E602G did not alter DAT function or surface expression (Mazei-Robison and Blakely, 2005).

R51W

The R->W substitution at position 51 in the DAT N-terminus was identified in siblings with ASD, and while R51W-DAT functioned similar to wildtype, it exhibited reduced AMPH-stimulated DA efflux, proposed to be due to reduced syntaxin 1A

(Syn1A) binding (Cartier et al., 2015). Given this loss in AMPH-stimulated DA efflux, the researchers tested whether this mutation altered AMPH-dependent hyperactivity. Using *Drosophila*, Cartier and colleagues replaced endogenous dDAT with either wildtype hDAT or R51W-hDAT and measured locomotion in adult flies fed 1mM AMPH. Flies expressing R51W-hDAT displayed normal levels of baseline locomotor activity, but had significantly reduced AMPH-stimulated hyperactivity compared to hDAT-expressing flies (Cartier et al., 2015).

A559V

Interestingly the TMD12 DAT mutation, A559V, was identified independently in patients with BPD (Grünhage et al., 2000), ADHD (Mazei-Robison et al., 2005), and ASD (Bowton et al., 2014). While, A559V-DAT did not disrupt DAT function or steady-state surface expression in transfected COS-7 cells (Mazei-Robison and Blakely, 2005), A559V-DAT displayed significantly higher rates of lateral membrane diffusion as measured by single quantum dot imaging, potentially denoting a general destabilization of A559V-DAT (Thal et al., 2019). In a follow-up report, researchers determined that the A559V mutation altered DAT surface expression when expressed in the appropriate context. Using A559V-DAT knock-in mice, Gowrishankar and colleagues found that A559V-DAT expressed on the cell surface significantly more than wildtype DAT, but only in the DS, and retained normal surface expression in the VS (Mergy et al., 2014; Gowrishankar et al., 2018). Moreover, A559V-DAT supported anomalous DA efflux (ADE), in which the

transporter constitutively effluxes DA backwards out of the cell (Mazei-Robison et al., 2008). Of note, AMPH treatment completely abolished A559V-DAT-mediated ADE (Mazei-Robison et al., 2008). Furthermore, while AMPH stimulates wildtype DAT internalization and surface loss (discussed further in "DAT endocytic regulation"), AMPH had no effect on A559V-DAT surface expression, which was further shown to be due to the inability of A559V-DAT to translocate AMPH into the cell (Bowton et al., 2014). In accordance with these results, A559V-DAT knock-in mice exhibited a blunted locomotor response to acute AMPH injection (3 mg/kg) compared to wildtype mice (Mergy et al., 2014).

T356M

The first ASD-associated DAT coding variant identified was a threonine to methionine substitution (T356M) (Neale et al., 2012). T356M-DAT had significantly decreased transport velocity compared to wildtype DAT, but equal steady-state surface expression when measured in transfected CHO cells (Hamilton et al., 2013). Similar to the A559V-DAT mutation, the T356M-DAT also exhibited ADE that was significantly blocked by AMPH (Hamilton et al., 2013). Because T356M-DAT displayed reduced DA uptake, investigators predicted that this mutation would cause hyperactivity due to increased extracellular DA concentrations. In fact, fruit flies expressing T356M-DAT were significantly hyperactive compared to hDAT-expressing controls (Hamilton et al., 2013). This hyperactive phenotype was recapitulated in a follow-up study in which the T356M mutation was knocked into

the mouse *SLC6A3* (DAT) gene and expressed under the endogenous DAT promoter (DiCarlo et al., 2019). Using carbon fiber amperometry, DiCarlo and colleagues observed T356M-DAT mice had significantly decreased rate of DA reuptake but no overall difference in overall DAT protein, confirming earlier results obtained in cell culture models, (DiCarlo et al., 2019). These data indicate that the behavioral hyperactivity phenotype is likely due to reduced synaptic DA clearance by T356M-DAT.

R615C

The variant R615C was identified in an ADHD proband, and displays the most profound trafficking defect of the coding variants identified to date (Sakrikar et al., 2012). AMPH-stimulated efflux was unaffected by the R615C mutation, in contrast to other disorder-associated variants. Instead, the mutation caused a significant loss in DAT function, surface expression, and AMPH- and PKC-stimulated endocytosis (Sakrikar et al., 2012; Wu et al., 2015) (described in detail in "DAT Endocytic Regulation"). Like the A559V-DAT mutation, R615C-DAT also demonstrated increased membrane mobility compared to wildtype DAT, further supporting that DAT lateral mobility may be important for proper DAT function and regulation (Kovtun et al., 2015). However, it remains unknown whether R615C-DAT alters DA-dependent behaviors or DAergic signaling *in vivo*.

## I.C DAT Endocytic Regulation

DAT plasma membrane presentation is regulated by a variety of cellular mechanisms that include kinase signaling, protein-protein interactions, transporter substrates, and cellular activity. DAT surface expression changes are often a result of altered rates of endocytosis (internalization), plasma membrane insertion (recycling), or both. DAT can also move laterally between membrane domains (Adkins et al., 2007; Navaroli and Melikian, 2010; Gabriel et al., 2013; Kovtun et al., 2015). Both DAT intracellular termini critically control DAT surface expression and regulated endocytic trafficking (Torres et al., 2003b; Miranda et al., 2004; Holton et al., 2005). Kinases including protein kinase A (PKA), Akt, protein kinase C (PKC), and protein kinase G (PKG) stimulate DAT trafficking (Bermingham and Blakely, 2016). Many of these kinases function downstream of cell surface receptor activation, such as GPCRs and receptor tyrosine kinases (RTKs) (Chen et al., 2013; Zhu et al., 2015). Additionally, DAT substrates DA and AMPH can also alter DAT surface expression and endocytic rates (Saunders et al., 2000; Chi and Reith, 2003). Finally, membrane potential can also influence DAT trafficking (Richardson et al., 2016). Altogether, since DAT function and expression exert fine control over DA homeostasis, it is likely that intrinsic mechanisms that alter DAT surface expression contribute to DA-dependent behaviors *in vivo*. However, despite decades of evidence defining the molecular mechanisms that control DAT surface expression, this hypothesis remains untested. In this section, I highlight many of the mechanisms underlying regulated DAT trafficking to illustrate the complexity of

this phenomenon, and to explore the possibility that DAT trafficking may occur *in vivo* in response to various stimuli to acutely regulate DA neurotransmission.

*Forward, biosynthetic trafficking*

DAT function relies on its proper localization to the plasma membrane. DAT exit from the endoplasmic reticulum (ER) has been shown to rely on specific residues and domains, as well as the protein transport protein, SEC24 (Sucic et al., 2011). SEC24 is a component of the coat protein complex II (COPII), and is responsible for vesicle formation off of ER membranes (Barlowe, 1994). Specifically, in HeLa cell experiments, DAT, NET and GAT1 ER export required the SEC24D isoform, whereas SERT required SEC24C (Farhan et al., 2007; Sucic et al., 2011; Sucic et al., 2013).

DAT domains, in particular the amino and carboxy termini, contribute to DAT plasma membrane delivery. Increasingly large truncations of the DAT N-terminus (the first 11, 20, 48, or 60 amino acids) progressively decreased DAT function, culminating in a complete loss of DA reuptake by the $\Delta$60 mutant, likely due to improper biosynthetic processing leading to reduced plasma membrane expression (Torres et al., 2003b). Sorkina and colleagues demonstrated that YFP replacement of the N-terminus (1-65) also reduced DAT surface levels and increased endosomal localization (Sorkina et al., 2009). Early termination mutations at amino acids Q611, R601, L591, or S582 in the DAT C-terminus

significantly also reduced DAT plasma membrane insertion (Torres et al., 2003b). In fact, the largest truncation (S582) exhibited virtually no uptake function nor surface expression (Torres et al., 2001; Torres et al., 2003b). Sorkin's group also reported DAT terminal truncations beginning at 598 and 586 also drastically reduced surface expression and increased intracellular DAT (Miranda et al., 2004), and the point mutation G585A-DAT did not express on the cell surface in heterologous models and cultured primary DA neurons due to ER retention (Miranda et al., 2004).

Of note, multiple DAT mutants associated with IPD (*discussed above*) exhibit significant decreases in DA uptake function due to protein misfolding and failure to exit the ER (Kasture et al., 2016; Asjad et al., 2017). The deficit in transport function and the sleeplessness phenotype caused by some of these mutants when expressed in *Drosophila* were both rescued by treatment with the drug noribogaine, a DAT ligand that binds the inward-facing DAT conformation, and presumably assisted in its protein folding and ER exit (Kasture et al., 2016; Asjad et al., 2017). These mutants provide further evidence to support that DAT's expression at the plasma membrane is required for proper spatial and temporal regulation of DA reuptake and behavior.

*PKC-stimulated DAT trafficking*

Early studies in *Xenopus laevis* oocytes, COS cells, and striatal synaptosomes demonstrated that the $V_{max}$ of DA uptake rapidly decreases in response to acute protein kinase C (PKC) activation with phorbol esters (Huff et al., 1997; Zhu et al., 1997; Pristupa et al., 1998), suggesting that DAT may be subject to either PKC-mediated catalytic inactivation, decreased surface expression, or both. Subsequent studies in heterologous expression systems demonstrated that acute PKC activation decreases DAT surface expression (Daniels and Amara, 1999; Melikian and Buckley, 1999), and that the shift in DAT from the cell surface to endosomal loci is mediated by increased DAT internalization combined with decreased plasma membrane delivery (Pristupa et al., 1998; Loder and Melikian, 2003; Hong and Amara, 2013) (Figure I.2). Although PKC activation leads to phosphorylation of serine residues within the DAT N-terminus (Foster et al., 2002; Cervinski et al., 2005; Gorentla et al., 2009; Moritz et al., 2013), and mutating Ser7 to alanine significantly blocked PKC-mediated DAT phosphorylation and functional loss, PKC-mediated DAT phosphorylation is not required for PKC-stimulated DAT surface loss (Moritz et al., 2015).

PKC-stimulated DAT internalization is clathrin- and dynamin-dependent. In an early report, investigators speculated that PKC-stimulated DAT internalization requires clathrin via overexpression of the dominant negative dynamin mutant, K44E (Daniels and Amara, 1999). Additionally, siRNA-mediated clathrin heavy chain or dynamin knockdown blocked constitutive and PKC-stimulated DAT

endocytosis in transfected porcine aortic endothelial (PAE) cells measured using fluorescence microscopy (Sorkina et al., 2005). A later study similarly reported a significant reduction in PKC-mediated DAT downregulation with the K44A dynamin mutant (Foster et al., 2008). In experiments performed in intact DA terminals, PKC-mediated DAT surface loss was blocked by pre-treatment with the noncompetitive dynamin inhibitor, Dynole (Gabriel et al., 2013). Moreover, direct clathrin inhibition with pitstop2 abolished PKC-stimulated DAT internalization in the DAergic human neuroblastoma SK-N-MC cells stably expressing DAT (Wu et al., 2015).

PKC-stimulated DAT internalization requires residues and domains in both intracellular termini. The DAT C-terminus is required for PKC-stimulated DAT endocytosis. Alanine mutations of residues 587-589 (“FRE”) in the DAT C-terminus significantly increased DAT internalization rates basally, but did not block PKC-dependent endocytosis. However, just one additional alanine mutation (587-590, “FREK”) significantly increased basal DAT internalization, and also abolished PKC-stimulated endocytosis (Boudanova et al., 2008b). These data suggest that residues 587-590 constitute a negative regulatory mechanism, or “endocytic brake”, that curbs DAT internalization rates in the absence of stimuli. Alanine substitutions at these amino acids increased basal DAT endocytosis to levels equivalent to PKC-stimulated wildtype DAT, indicating a possible ceiling effect to stimulated DAT internalization. In argument against this hypothesis, Boudanova and colleagues found that residues 587-590 were not required for AMPH-

stimulated endocytosis (Boudanova et al., 2008a), and AMPH exposure in combination with PKC activation can additively stimulate DAT internalization rates (Hong and Amara, 2013).

The N-terminus also contributes to the DAT endocytic brake mechanism that tempers basal endocytosis. Initial reports found that deleting DAT's first 22 amino acids (Granas et al., 2003) or the whole amino terminus (residues 1-65) (Sorkina et al., 2005) did not block PKC-stimulated DAT surface loss. However, these data were later challenged by follow-up studies by Sorkin's group. Sorkina and colleagues found that replacing the N-terminus with a YFP tag significantly increased internal DAT localization, suggesting that the N-terminus negatively regulates constitutive internalization and is required to stabilize DAT surface expression (Sorkina et al., 2009). Furthermore, N-terminal DAT lysines 19 and 35 were found to be ubiquitinated following PKC activation (Miranda et al., 2005), and Miranda and colleagues found that the triple mutation (K19R/K27R/K35M) blocked PKC-stimulated DAT ubiquitination and surface loss (Miranda et al., 2007). These data indicate that residues within the DAT N-terminus are also required for PKC-mediated endocytic brake release.

Recently, our lab identified two of the proteins required for PKC-mediated DAT endocytic brake release. PKC activation reduces phosphorylation and activity of the nonreceptor tyrosine kinase, Ack1 (activated by cdc42 kinase 1; Tnk2),

(Linseman et al., 2001; Wu et al., 2015). Moreover, direct Ack1 inactivation with AIM-100 significantly increases DAT internalization rates and decreases DAT surface expression in transfected cells and *ex vivo* striatal slices. Using a constitutively-active Ack1 mutant (S445P-Ack1), our lab demonstrated that Ack1 inactivation is absolutely required for PKC-stimulated DAT internalization (Wu et al., 2015). Thus, at basal states Ack1 activity negatively regulates DAT endocytosis (Figure I.2). The R615C-DAT mutant internalizes and recycles at significantly higher rates than wildtype DAT (Sakrikar et al., 2012), suggesting that R615C-DAT is destabilized in the membrane due to a lack of endocytic braking. In support of this hypothesis, our lab found that we could restore R615C-DAT internalization rates to wildtype levels by overexpressing S445P-Ack1, imposing the Ack1-dependent endocytic brake (Wu et al., 2015). These results suggest a potential therapeutic route to reinstate normal endocytosis for trafficking-defective DAT mutants. However, it remains unknown whether the R615C-DAT alters DA-dependent behaviors, including locomotor activity or psychostimulant response, or whether suppressing the trafficking dysfunction via Ack1 activity *in vivo* would ameliorate any behavioral phenotypes.

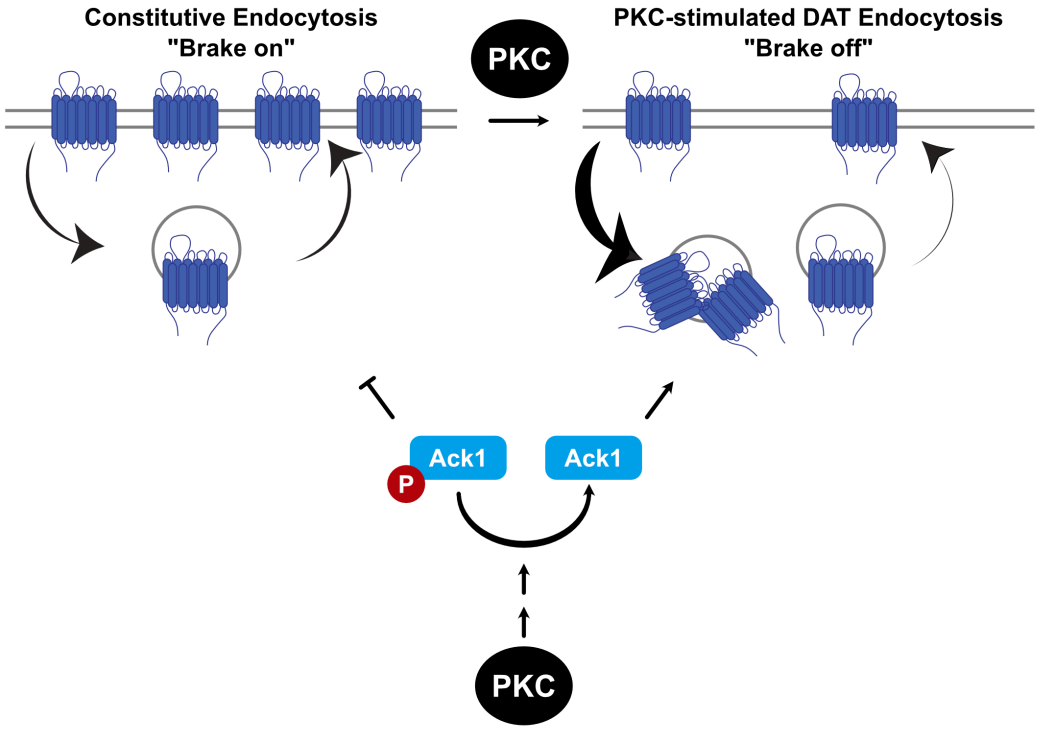


**Figure I.2 PKC-stimulated DAT trafficking and endocytic brake model.** Under basal conditions, DAT undergoes slow rates of internalization and surface delivery. PKC activation increases the DAT internalization rate and decreases the DAT recycling rate, leading to reduced overall DAT surface expression. The slower DAT endocytic rate is referred to as “brake on”, and relies on residues within the DAT N and C termini, as well as Ack1 activity. PKC activation indirectly dephosphorylates and inactivates Ack1 (“brake off”), stimulating DAT internalization, and reducing DAT surface expression (Adapted from Wu et al., 2015).

In addition, our lab discovered that the DAT binding protein, Rit2, a neuronal GTPase (*see "Rit2 GTPase" section*) plays an integral role in PKC-dependent DAT endocytosis (Navaroli et al., 2011). The DAT-Rit2 interaction was originally identified in a yeast two-hybrid screen using the DAT C-terminal "FREKLAYAIA" domain as bait. Given its role in PKC-dependent and constitutive DAT internalization (discussed below), Rit2 was hypothesized to contribute to PKC-stimulated endocytic brake release. In support of this prediction, putatively dominant-negative Rit2 mutant, S34N, blocked PKC-stimulated DAT internalization in transfected PC12 cells (Navaroli et al., 2011). We further hypothesized that if Rit2 was a component of the endocytic brake, then the DAT-Rit2 interaction would be disrupted by a) PKC activation, and b) mutating DAT residues required for braking ("FREK"). Paradoxically, however, co-immunoprecipitation (co-IP) experiments demonstrated that both of these manipulations increased the DAT-Rit2 association. Given these conflicting results, Rit2's exact role in the DAT endocytic brake mechanism remains unclear.

Which PKC isoform mediates DAT trafficking? PKCβ is required for D2-dependent DAT insertion (see "*D2-dependent DAT Plasma Membrane Insertion*" below), however it remains unknown which PKC isoform(s) are required for PKC-stimulated DAT internalization in response to phorbol ester treatment. The vast majority of studies to date (including those described above) use phorbol 12-myristate 13-acetate (PMA) to study PKC-dependent trafficking. PMA activates

two diacylglycerol (DAG)-sensitive PKC isozyme subtypes: classical (DAG- and $Ca^{2+}$-dependent) and novel (DAG-dependent, $Ca^{2+}$-independent) PKCs (Steinberg, 2008). Candidate PKCs can be further narrowed, as PMA-stimulated DAT internalization is blocked by the PKC inhibitor, bisindolylmaleimide I (BIM I, GF 109203X, Gö 6850) (Melikian and Buckley, 1999; Gorentla and Vaughan, 2005; Boudanova et al., 2008a), which is selective for $\alpha$, $\beta$I, $\delta$, $\varepsilon$, and $\zeta$ PKC isozymes. However, PKC$\zeta$ is not DAG-dependent, and therefore not activated by PMA. Thus, PKC-stimulated DAT internalization likely requires either PKC$\alpha$, $\beta$I, $\delta$, or $\varepsilon$.

What are the physiological mechanisms that drive PKC-stimulated DAT internalization? Conventional and novel PKCs are typically activated in response to stimulating Gq-coupled GPCRs (G-protein-coupled receptors), which activate PKC and release $Ca^{2+}$ from intracellular stores, in parallel, downstream of phospholipase C activation. However, it still is not clear whether activating endogenously expressed, Gq-coupled GPCRs stimulates DAT internalization in intact DA terminals. Studies in transfected HEK293 and N2a cells demonstrated that activating the Gq-coupled receptor neurokinin (NK)-1 with its endogenous ligand, substance P, reduced DAT surface expression in a PKC-dependent manner (Granas et al., 2003), providing a possible candidate for endogenous PKC-dependent DAT endocytosis. However, substance P-dependent DAT internalization has not yet been reported in DAergic terminals. The Gq-coupled,

Group I metabotropic glutamate receptor 5 (mGluR5) has also been implicated in DAT functional downregulation. DHPG, a Group I selective mGluR agonist, decreased DAT function in rat striatal synaptosomes, which was blocked by the mGluR5-specific antagonist, MPEP, as well as the PKC inhibitor, Ro-31-8220 (Page et al., 2001). However, Ro-21-8220 was used at a relatively high concentration that can also inhibit other kinases (e.g. GSK3β, MAPKAP-K1β), raising the possibility that mGluR5-mediated DAT downregulation may be mediated via signaling pathways other than PKC. Fast-scan cyclic voltammetry studies from Alvarez and colleagues recently found that activating the muscarinic receptor M5, a Gq-coupled GPCR selectively expressed in DA neurons (Bendor et al., 2010; Foster et al., 2014), significantly decreased DA clearance rates in VS (Shin et al., 2015). Given that mGluR5, and possibly M5, receptors are expressed on other cell types throughout the striatum, such as cholinergic interneurons and medium spiny neurons, it is unclear whether or not mGluR5 and M5-mediated DAT downregulation occur cell autonomously. Thus, whether activating a Gq-coupled GPCR expressed on DA terminals can stimulate PKC-dependent DAT internalization, and whether this mechanism is subject to regional differences, remains to be tested.

*Constitutive DAT Trafficking*

Constitutive DAT internalization and recycling has been reported in a variety of heterologous expression systems (Loder and Melikian, 2003; Holton et al., 2005; Furman et al., 2009a; Eriksen et al., 2010b; Sakrikar et al., 2012; Gabriel et al.,

2013; Wu et al., 2017), as well as in primary DAergic neuronal cultures (Eriksen et al., 2010b; Hong and Amara, 2013), as measured using biochemical and imaging approaches (Loder and Melikian, 2003; Holton et al., 2005; Sorkina et al., 2005; Eriksen et al., 2010b; Navaroli et al., 2011; Sakrikar et al., 2012; Gabriel et al., 2013; Hong and Amara, 2013; Wu et al., 2015). Constitutively internalized DAT can reportedly target to several endocytic compartments (discussed in further detail in the following section), including those positive for EEA1, rab4, rab5, and the Vps35 retromer complex component. DAT also targets, albeit to a lesser extent, to rab11- and rab7-positive loci (Eriksen et al., 2010b; Hong and Amara, 2013; Wu et al., 2017). Moreover, Vps35 is required for constitutive DAT recycling to the plasma membrane (Wu et al., 2017).

In contrast to PKC-stimulated DAT internalization, constitutive DAT trafficking is clathrin-independent. Inhibiting dynamin in acute striatal slices with Dynole significantly reduced steady-state DAT surface levels. This result indicates that constitutive DAT internalization is dynamin-independent, whereas constitutive DAT surface delivery, or recycling, is dynamin-dependent (Gabriel et al., 2013). Another report from the same year further supported this conclusion by demonstrating that the dominant negative dynamin K44A mutant did not alter constitutive DAT internalization when transfected into cultured midbrain DA neurons (Rickhag et al., 2013b). In a follow-up study, our laboratory also demonstrated that directly inhibiting clathrin with pitstop2 also had no effect on DAT constitutive internalization rates (Wu et al., 2015).

The DAT domains required for constitutive internalization are distinct from those necessary for PKC-stimulated endocytosis. Whereas the amino terminus contains residues critical for PKC-mediated DAT internalization and endocytic braking (Miranda et al., 2007), the domain as a whole is not sufficient to drive basal endocytosis. This was demonstrated using a peptide fusion approach in which the DAT N-terminus (residues 1-44) failed to induce endocytosis when fused to an endocytic-deficient transferrin receptor (TfR) (Holton et al., 2005). The DAT C-terminus is also required for plasma membrane expression, and contains an intrinsic endocytic signal. As discussed earlier, C-terminal truncations result in DAT ER retention and loss of surface expression. However, DAT residues 587-596 (FREKLAYAIA) suffice to drive constitutive endocytosis of the endocytic-deficient interleukin 2$\alpha$ receptor (Holton et al., 2005), demonstrating that constitutive DAT internalization occurs via a nonclassical endocytic determinant. Specifically, mutating amino acid L591, Y593, or I595 to alanine significantly reduced DAT basal endocytosis, but had no effect on PKC-mediated functional or surface downregulation (Holton et al., 2005).

Constitutive DAT trafficking in intact DA terminals has proven difficult to assess. In cell lines, basal DAT endocytic trafficking can be readily measured using reversible biotinylation assays (Gabriel et al., 2009). However, the rapid and dramatic temperature shifts required for this approach are not optimal for acute brain slice

viability, creating a sizable obstacle in measuring DAT internalization in *bona fide* DAergic terminals. Using cultured rat midbrain DA neurons and the fluorescent cocaine analog JHC 1-64, which selectively labels DAT (Eriksen et al., 2009), Gether and colleagues found that native DAT indeed constitutively internalizes (Eriksen et al., 2010b). Hong and Amara further confirmed this finding, and found that internalized DAT co-localizes with Rab11+ recycling endosomes in rat embryonic mesencephalic primary cultured neurons (Hong and Amara, 2013). To track DAT internalization in DAergic terminals *in situ*, Sorkin and colleagues generated a DAT knock-in mouse, in which an HA epitope was engineered into the DAT extracellular loop 2 (HA-EL2-DAT), and used this mouse to monitor DAT internalization by tracking anti-HA antibody internalization in *ex vivo* striatal slices. They found only sparse intracellular HA immunoreactivity via electron microscopy (Block et al., 2015), and therefore concluded that DAT undergoes little, if any, constitutive or regulated endocytosis in axon terminals. This result is in contrast to biochemical studies that demonstrate that various stimuli can modulate DAT surface expression in *ex vivo* striatal slices, and raises the possibility that technical obstacles may have impacted their study. For example, studies were performed in 800 μm brain slices, which are relatively thick in comparison to the standard 250-400 μm thickness typically prepared, which maximizes tissue oxygenation for *ex vivo* studies. Moreover, several recent reports demonstrated that large immunoglobulins cannot efficiently penetrate thick tissue slices beyond 50-100μm (Biermann et al., 2014; Wakayama et al., 2017). Similarly, our laboratory recently

reported that although PRIME (PRobe Incorporation Mediated by Enzyme) labeling can efficaciously label surface DAT and track its internalization in monolayer culture, it cannot be used to successfully label DAT in 300μm acute brain slices, presumably due to an inability of the lipoic acid ligase (LpIA) enzyme to effectively penetrate the slice (Wu et al., 2017). Given that the HA-EL2-DAT mouse study did not present controls for either slice viability or antibody access to deep tissue loci, it is not clear whether the approach used was able to accurately measure endogenous DAT trafficking events.

In summary, the mechanisms underlying constitutive DAT endocytosis are distinct from stimulated endocytosis. Additionally, multiple approaches have detected the existence of an internal DAT population in DA terminals, and DAT can internalize in acute striatal slices in the absence of stimulation (Gabriel et al., 2013), indicating that DAT indeed constitutively internalizes in the striatum. Despite support of constitutive DAT internalization via biochemical methods, researchers have not yet been able to visualize basal DAT trafficking in intact DA neurons. Recent studies using super-resolution microscopy techniques such as PALM (photoactivated localization microscopy) and STORM (stochastic optical reconstruction microscopy) have allowed researchers to more precisely measure DAT surface dynamics in cultured DA neurons (Rahbek-Clemmensen et al., 2017), however this type of high-resolution approach has not yet been employed to study basal or stimulated DAT trafficking in DA terminals.

*Post-endocytic DAT localization*

DAT endocytic sorting following constitutive and stimulated internalization has been a subject of contention within the field. Does DAT degrade once internalized, or can it be recycled back to the plasma membrane? Does PKC-stimulated endocytosis alter DAT's intracellular fate? Early reports found DAT associated with early endosome markers EEA1 and rab5 (Daniels and Amara, 1999; Melikian and Buckley, 1999), as well as lysosomes (Daniels and Amara, 1999), opening up the field to numerous follow-up reports. DAT recycling and cell surface insertion was demonstrated, either by colocalization with recycling endosomes (rab11+), or by biochemical measurements, in a wide variety of cell types and models (Loder and Melikian, 2003; Lee et al., 2007; Boudanova et al., 2008a; Furman et al., 2009b; Furman et al., 2009a; Eriksen et al., 2010b; Rao et al., 2011; Sakrikar et al., 2012; Chen et al., 2013; Gabriel et al., 2013; Hong and Amara, 2013; Richardson et al., 2016; Vuorenpaa et al., 2016; Wu et al., 2017). Moreover, DAT can also be ubiquitinated and targeted to late endosomes and lysosomes (Miranda et al., 2005; Sorkina et al., 2006; Miranda et al., 2007; Eriksen et al., 2010b; Hong and Amara, 2013; Vuorenpaa et al., 2016; Wu et al., 2017). On the other hand, some groups reported little or no change in DAT targeting following PKC activation (Melikian and Buckley, 1999; Loder and Melikian, 2003; Rao et al., 2011), whereas others found that PKC increased DAT ubiquitination, enhanced its lysosomal targeting, and led to degradation (Daniels and Amara, 1999; Miranda et al., 2005; Sorkina et al., 2006; Miranda et al., 2007; Hong and Amara, 2013). Nevertheless, neither DAT

ubiquitination nor PKC-mediated degradation has been confirmed in DA terminals, where DAT protein is not artificially overexpressed.

DAT protein levels are fairly stable (Kimmel et al., 2000), seemingly in contradiction with its propensity to colocalize with late endosomes in transfected AN27 cells (approx. 20% of DAT colocalized with the late endosome marker rab7 after 30 minutes, compared with only approx. 5% colocalized with rab11 after the same amount of time, under basal conditions (Wu et al., 2017)). Moreover, DAT only colocalized with lysosomal markers after drug treatment (Hong and Amara, 2013), indicating that rab7 colocalization may not be indicative of lysosomal targeting. Recently, rab7 was implicated in retromer-dependent cargo selection (Rojas et al., 2008; Seaman et al., 2009). Although originally characterized for its role in endosome-to-trans golgi trafficking (Seaman et al., 1997), retromer has now come to light as a critical component of recycling and endocytic sorting (Kleine-Vehn et al., 2008; Temkin et al., 2011; Seaman, 2012). The mammalian retromer complex is comprised of a trimer of vacuolar protein sorting-associated (Vps) proteins: Vps35, Vps26, and Vps29 (Seaman et al., 1997; Seaman, 2004), which facilitates cargo selectivity (Seaman et al., 1998), and a sorting nexin (SNX) dimer (Rojas et al., 2007). Using the PRIME labeling technique described above our group tested whether DAT traffics through a retromer-dependent mechanism. DAT colocalized with retromer component Vps35 in cultured cells, midbrain DA neuron cell bodies, and striatal DA terminals. Moreover, Vps35 knockdown via shRNA significantly

reduced DAT protein expression and recycling rate in cells (Wu et al., 2017). Finally, stimulating DAT internalization via Ack1 inhibition did not dramatically alter DAT/Vps35 colocalization over time in cells, indicating that under basal and stimulated conditions DAT traffics through a retromer-dependent mechanism (Wu et al., 2017).

*Substrate-mediated DAT endocytosis*

DA-dependent

DAT substrates have additionally been demonstrated to regulate DAT trafficking and surface expression. DA itself induced DAT functional and surface downregulation, though the mechanism by which this change occurs is unknown (Daniels and Amara, 1999; Chi and Reith, 2003). Chi and colleagues found that exposure for 1 hour with at least 10μM DA decreased DAT function in HEK-293 cells transfected with hDAT and in rat striatal synaptosomes (Chi and Reith, 2003). Researchers further found that DA decreased DAT surface expression in their cell culture experiments (Chi and Reith, 2003). In contrast, a separate team observed no differences in DAT surface levels after DA treatment (10μM, 10min) in MDCK cells stably expressing hDAT (Daniels and Amara, 1999). This disparity may have arisen from the treatment times or cell lines employed in these experiments. In support of the latter possibility, a follow-up study found that DA increased DAT surface levels via total internal reflection fluorescence (TIRF) microscopy in N2A cells, and that this occurred within a very short time frame (10μM, 120sec) (Furman

et al., 2009b). Moreover, surface biotinylation in rat striatal synaptosomes confirmed that DA increased DAT surface expression after 1 minute in a DRD2-dependent manner (Furman et al., 2009b). The MDCK cells used in the earlier study, in contrast, are canine kidney cells that may not endogenously express DRD2, thereby precluding DA-dependent increases in DAT surface expression in this system (see "*DRD2-mediated DAT surface delivery*" section).

AMPH-stimulated

Amphetamine (AMPH) is an addictive psychostimulant that increases extracellular DA concentrations via multiple actions at the DA terminal (as described earlier). In addition, AMPH exposure induces DAT internalization from the plasma membrane, thus decreasing surface DAT availability (Saunders et al., 2000; Sandoval et al., 2001; Gulley et al., 2002; Johnson et al., 2005b; Kahlig et al., 2006; Boudanova et al., 2008a; Hong and Amara, 2013; Wheeler et al., 2015; Underhill et al., 2019).

AMPH-stimulated DAT surface loss was originally characterized in HEK293 cells treated with AMPH (Saunders et al., 2000), and was later demonstrated to be CaMKII-dependent (Wei et al., 2007). This result was later replicated in synaptosomes made from whole rat striatum (Johnson et al., 2005b) and in primary DA neuronal cultures (Wheeler et al., 2015). AMPH-stimulated DAT endocytosis is likely not a clathrin-mediated process, as AMPH treatment did not stimulate appreciable DAT and clathrin light chain colocalization in transfected neuronal SK-N-SH cells (Wheeler et al., 2015). AMPH-induced DAT internalization was further

demonstrated in *ex vivo* mouse midbrain slices, and was dependent on Rho GTPase activity downstream of the trace amine-associated receptor (TAAR) 1 (Wheeler et al., 2015; Underhill et al., 2019).

It is still unknown whether AMPH stimulates DAT internalization in *bona fide* DA terminals. Using the HA-EL2-DAT and electron microscopy techniques, Block and colleagues found that i.p. AMPH injection did not subsequently affect DAT surface distribution in axon terminals or DA cell bodies. However, it is unclear whether the DAT labeling method employed was sufficient to detect drug-induced changes (see "*Constitutive Internalization*" section above) (Block et al., 2015). Finally, trafficking dysregulated DAT mutant, R615C-DAT, does not internalize in response to AMPH (Sakrikar et al., 2012), further implicating the DAT C-terminus in mediating DAT's endocytosis in response to various stimuli.

*Receptor-mediated DAT trafficking*

DRD2-mediated DAT surface delivery

Multiple lines of evidence, both from *ex vivo* and transfected cell line studies, support that DRD2 activation increases DAT function and plasma membrane expression. Initial studies in rat striatal synaptosomes revealed that the DRD2-like agonist, quinpirole, increased DA uptake as measured by rotating disk voltammetry (Meiergerd et al., 1993). Moreover, *in vivo* chronoamperometry demonstrated that DA clearance decreased following systemic injection with the

broad-spectrum DRD antagonist, haloperidol (Meiergerd et al., 1993). Subsequent kinetic studies in *Xenopus* oocytes co-expressing DAT and DRD2 observed both increased DA uptake $V_{max}$ and [$^3$H]WIN35,428 whole cell binding $B_{max}$, suggesting that DRD2 activation may increase DAT activity via enhanced surface expression (Mayfield and Zahniser, 2001). DRD2-mediated DAT functional upregulation was further confirmed by Liu and colleagues (Lee et al., 2007), who reported that DRD2 associates with DAT in isolated protein complexes from rat striatal lysates, and that DAT residues 1-26 were sufficient to recover DRD2 *in vitro*. One potential confound in studies using [$^3$H]DA uptake to measure how DRD2 activation impacts DAT function, is that the inherent addition of DA to the assay will also activate DRD2. To eliminate this potential pitfall, Shippenberg and colleagues leveraged the fluorescent DAT substrate, 4-[4-(diethylamino)-styryl]-*N*-methylpyridinium iodide ($ASP^+$), which is taken up by DAT, but does not activate DRD2 (Bolan et al., 2007). Using $ASP^+$ uptake, these studies found that DRD2-mediated increases in DAT function required ERK1/2, but not PI3-kinase, activity (Bolan et al., 2007) in HEK and N2a cells. Further, using bioluminescence resonance energy transfer (BRET) they confirmed the DRD2-DAT association, but co-IP experiments suggested that DAT N-terminal residues 1-55 were not required for the DRD2-DAT association. Taken together, these initial studies clearly demonstrated that DRD2 increases DAT activity, and were consistent with the hypothesis DRD2-mediated DAT upregulation was likely due to enhanced surface expression. However, the

influence of the DRD2-DAT interaction on DRD2-dependent DAT surface delivery, and the DAT domains required for the interaction remain unknown.

DRD2-mediated DAT surface delivery in DA terminals was first directly demonstrated by Gnegy and colleagues, using a surface biotinylation approach in *ex vivo* mouse striatal synaptosomes prepared from total striatum that included both DS and VS (Chen et al., 2013). Moreover, using both PKCβ-specific inhibitors and *PKCβ*$^{-/-}$ mice, they found that DRD2-mediated DAT surface delivery requires PKCβ (Chen et al., 2013; Luderman et al., 2015).

These landmark results have opened the door to a variety of new potential questions regarding DRD2-mediated DAT trafficking: Is DRD2-activated DAT trafficking mediated by DRD2 autoreceptors, or is there a retrograde signaling contribution via DRD2 receptors expressed throughout the striatum? Are there regional differences in DRD2-mediated DAT surface delivery? Blakely and colleagues recently reported that DRD2-dependent DAT trafficking differs between DS and VS in *ex vivo* slices, where the DRD2 agonist, quinpirole, significantly increased DAT surface expression in DS, but had no effect on DAT surface levels in VS (Gowrishankar et al., 2018). The mechanisms governing these regional differences remain unknown. However, it should be noted that quinpirole can activate all D2-like receptors (i.e. DRD2, DRD3, DRD4; Ki~4.8, 24, and 30nM, respectively), as well as DRD1 (1.9μM). Since their study used 1μM quinpirole,

there is a possibility that region-specific effects reported may reflect a net integrated signal from multiple DRDs, which would be equally interesting to discern. Alternatively, region-specific, DRD2-mediated DAT trafficking could arise from distinct DRD2 signaling, which is differentially sensitive to DA in the DS vs. VS (Marcott et al., 2018).

Does DRD2-dependent DAT trafficking occur *in vivo*? *In vivo* chronoamperoetric studies revealed that hypoinsulinemic rats exhibit reduced DA clearance, due to decreased insulin receptor-mediated PI3K/Akt signaling (Owens et al., 2005). Interestingly, DAT activity in hypoinsulinemic rats was restored in a DRD2-dependent manner by treating with AMPH (Owens et al., 2012), which drives DA efflux through the DAT (Sitte et al., 1998; Sulzer et al., 2005). These results strongly suggest that DRD2-mediated DAT membrane insertion occurs *in vivo,* in response to elevated extracellular DA.

Kappa opioid receptor

The κ-opioid receptor (KOR) is a $G_i$-coupled GPCR expressed in DA neurons (Svingos et al., 2001) that also interacts with and regulates DAT activity and expression. Studies from Shippenberg and colleagues found that KOR activation increased DA uptake and DAT surface expression in cell lines and synaptosomes, and likewise found that KOR activation increased DA uptake in minced striatal preparations, using rotating disk voltammetry (Kivell et al., 2014a). KOR-mediated

DAT upregulation was further found to require ERK1/2 signaling. Researchers also demonstrated a direct interaction between DAT and KOR using co-IP, BRET, and fluorescence resonance energy transfer (FRET) techniques (Kivell et al., 2014a). Further, KOR activation increased the DAT/KOR FRET signal, suggesting that KOR activation may anchor DAT at the plasma membrane, precluding it from constitutively internalizing, and thereby increasing overall DAT surface levels. Interestingly, KOR-dependent DAT regulation is reminiscent of DRD2-mediated DAT trafficking. DRD2 is also a $G_i$-coupled GPCR that binds to DAT and stimulates DAT plasma membrane insertion, raising the possibility that this DAT trafficking event may be a general phenomenon of $G_i$-coupled, ERK1/2-dependent signaling cascades. However, whether DAT's interaction with either DRD2 or KOR also contributes to their influence on DAT surface expression remains unknown. Finally, KOR activation has aversive properties, thus KOR-mediated DAT trafficking is poised as a pivotal interaction point between the opiate and reward circuitry, and may have future therapeutic potential (Kivell et al., 2014b).

Receptor Tyrosine Kinases

DAT surface expression is also regulated by RTKs. Broad-spectrum tyrosine kinase inhibitors, such as genistein, tyrphostin 23, and tyrphostin 25, significantly decreased DAT function in DS synaptosomes and *Xenopus* oocytes (Simon et al., 1997; Doolen and Zahniser, 2001). Additional studies indicate that direct RTK activation modulates DAT surface expression (Carvelli et al., 2002; Garcia et al.,

2005; Hoover et al., 2007; Zhu et al., 2015). Insulin-like growth factor receptor (IGFR-1) activation increased DAT function and surface expression in transfected cell lines, and was dependent on PI3-kinase and Akt activity, as defined with PI3-kinase and Akt inhibitors (Carvelli et al., 2002; Garcia et al., 2005). Moreover, hypoinsulinemia induced either by streptozotocin treatment or high fat diet significantly reduced DA clearance rates, DA reuptake, and DAT surface expression compared to controls, as measured in rat striatal synaptosomes (Owens et al., 2005; Williams et al., 2007; Speed et al., 2011), consistent with the results obtained in cell lines.

Glial cell line-derived neurotrophic factor (GDNF) also regulates DAT surface expression through receptor Ret activation and downstream signaling (Zhu et al., 2015). *GDNF*$^{+/-}$ mice exhibited increased DA uptake in the VS, but not DS, as measured via *in vivo* chronoamperometry, and reduced striatal DA tissue content in both VS and DS (Littrell et al., 2012). Furthermore, a similar, regional-specific increase in DA levels and DAT function was observed in synaptosomes prepared from *Ret*$^{+/-}$ DS and VS (Zhu et al., 2015). GDNF/Ret-dependent negative regulation of DAT surface expression was demonstrated to require Vav2, a guanine exchange factor (GEF) that activates Rho and Rac GTPases (Zhu et al., 2015). In striatal synaptosomes prepared from *Vav2*$^{-/-}$ mice, DAT exhibited enhanced DA uptake and surface expression specifically in the VS, but not DS. Moreover, GDNF-dependent Ret activation increased Vav2 phosphorylation, and Ret co-

expression increased the DAT-Vav2 interaction, suggesting that Ret RTK signaling may negatively regulate DAT surface expression through Vav2 activation (Zhu et al., 2015).

*DAT Protein-Protein Interactions*

DAT exists at the plasma membrane as part of a multi-protein complex. Over twenty proteins have been identified to directly interact or associate with DAT. A number of these interactions play critical roles in regulating DAT function or surface expression, as well as DA-dependent behaviors (Table I.2). Some of these proteins have already been discussed, given their roles in stimulated DAT trafficking (e.g. Rit2 and DRD2). However, DAT's interactions with proteins such as CaMKII$\alpha$ (Fog et al., 2006; Steinkellner et al., 2012; Rickhag et al., 2013a), Epsin/Eps15 (Sorkina et al., 2006), Flot1 (Cremona et al., 2011), Nedd4-2 (Sorkina et al., 2006), PICK1 (Torres et al., 2001; Bjerggaard et al., 2004), RACK1 (Lee et al., 2004; Franekova et al., 2008), and Syn1A (Lee et al., 2004; Binda et al., 2008; Cervinski et al., 2010) have also been studied in the context of regulated DAT endocytosis. Overall, these data highlight the importance of the DAT interactome in maintaining appropriate DAT function, trafficking, and psychostimulant response.

## Table I.2 DAT Protein-Protein Interactions

| Protein | DAT Interaction Domain(s) | Impact on DAT function and/or expression | References |
|---|---|---|---|
| α-synuclein | C-terminus (598-620) | Increased DA uptake & DAT surface expression, increased AMPH-stimulated DA efflux | Lee et al. (2001), Moszczynska et al. (2007), Butler et al. (2015) |
| $\sigma_1$R | n.d. | Increased DA uptake, blocked METH-stimulated DA efflux and hyperactivity | Hong et al. (2017), Sambo et al. (2017) |
| 14-3-3ζ | n.d. | Required for DAT protein expression | Ramshaw et al. (2013) |
| CaMKIIα | C-terminus (612-617) | Required for AMPH-stimulated DA efflux and hyperactivity | Fog et al. (2006), Steinkellner et al. (2012), Steinkellner et al. (2014) |
| Carboxy-peptidase E | C-terminus (583-620) | Increased DAT function | Zhang et al. (2009) |
| Ctr9 | C-terminus (577-579) | Increased DAT function | De Gois et al. (2015) |
| DRD2 | N-terminus (1-15)* | D2 activation increased DAT function & surface expression | Lee et al. (2007), Bolan et al. (2007)* |
| Disc1 | n.d. | Mutant Disc1 increased surface DAT | Trossbach et al. (2016) |
| DJ-1 | IL4 | Increased DA uptake | Luk et al. (2015) |
| Epsin/Eps15 | n.d. | Required for PKC-stimulated DAT endocytosis | Sorkina et al. (2006) |
| Flot1 | n.d. | Required for PKC-stimulated DAT endocytosis and AMPH-stimulated efflux and hyperactivity | Cremona et al. (2011), Sorkina et al. (2013)[+], Pizzo et al. (2013) |
| GPR37 | n.d. | GPR37-KO mice have increased DA uptake & DAT surface expression | Marazziti et al. (2007) |
| Gβγ | C-terminus (587-590) | Decreased DA uptake, promoted DA efflux (AMPH-independent) | Garcia-Olivares et al. (2013), Garcia-Olivares et al. (2017) |
| Hic-5 | C-terminus (571-580) | Decreased DAT function & surface expression | Carneiro et al. (2002) |
| KOR | n.d. | Increased DAT function | Kivell et al. (2014a) |
| Kv2.1 | n.d. | Decreased DAT function, internalization & lateral mobility | Lebowitz et al. (2019) |
| Nedd4-2 | n.d. | Required for PKC-stimulated DAT endocytosis and ubiquitination | Sorkina et al. (2006) |
| Parkin | C-terminus (583-620) | Increased DA uptake[a], decreased DA uptake[b] | Jiang et al. (2004)[a], Moszczynska et al. (2007)[b] |

| | | | |
|---|---|---|---|
| PICK1 | C-terminus (618-620) | Increased DA uptake, required for DAT protein expression | Torres et al. (2001), Bjerggaard et al. (2004), Madsen et al. (2012), Rickhag et al. (2013b) |
| PKCβI, PKCβII | n.d. | Required for D2-dependent DAT surface delivery, AMPH-stimulated efflux | Johnson et al. (2005a) |
| PP1/2Ac | n.d. | Decreased DAT function | Bauman et al. (2000), Yang et al. (2019) |
| RACK1 | N-terminus (1-65) | n.d. | Lee et al. (2004), Franekova et al. (2008) |
| Rit2 | C-terminus (587-596) | Required for PKC-stimulated DAT endocytosis and acute cocaine hyperactivity | Navaroli et al. (2011), Sweeney et al. (2020) |
| Syn1A | N-terminus (1-33) | Potentiated AMPH-stimulated DA efflux, decreases DA uptake | Lee et al. (2004), Binda et al. (2008), Cervinski et al. (2010) |
| Synaptogyrin-3 | N-terminus (1-60) | Increased DAT function | Egana et al. (2009) |

n.d. not determined; *N-terminus not required for co-IP; ⁺No association detected

CaMKIIα

A yeast two-hybrid screen with the DAT C-terminal domain as bait identified calmodulin kinase II α (CaMKIIα) as a direct DAT interactor, which was later confirmed via GST fusion proteins *in vitro* and demonstrated to require amino acids 612-617 of the DAT C-terminus (Fog et al., 2006). Moreover, researchers demonstrated DAT/CaMKIIα colocalization in midbrain DAergic neurons. Interestingly, although CaMKIIα did not interact with the DAT N-terminus, CaMKIIα phosphorylated DAT N-terminal peptides (Fog et al., 2006; Gorentla et al., 2009). Importantly, CaMKIIα activity and interaction with DAT were both found to be required for AMPH-stimulated efflux and internalization, but not steady-state DAT surface expression (Fog et al., 2006; Wei et al., 2007; Steinkellner et al., 2012; Rickhag et al., 2013a). The *in vivo* impact of CaMKIIα on DAT function was more closely investigated in CaMKIIα knock-out (CaMKIIα-KO) mice. These mice exhibited baseline hyperactivity compared with wildtype controls, which could be attributed to their elevated extracellular DA concentrations and DA release (Steinkellner et al., 2014). Furthermore, the CaMKIIα-KO mice displayed significantly less, if any, AMPH-stimulated DA efflux or locomotor hyperactivity (Steinkellner et al., 2014).

Flot1

The caveolar-associated protein, Flotillin-1/Reggie-2 (Flot1), associates with DAT and is required for PKC-stimulated DAT endocytosis (Cremona et al., 2011). In

stably-transfected HEK293 cells and cultured mouse midbrain DA neurons siRNA-mediated knockdown of endogenous Flot1 blocked PMA-induced DAT internalization, as measured by both confocal microscopy and cell surface biotinylation methods. Flot1 knockdown did not affect DAT steady-state surface expression. Co-IP experiments defined an association between Flot1 and DAT that was increased upon PKC activation. Interestingly, Flot1 silencing in DA neurons also blocked AMPH-stimulated DA efflux, indicating that Flot1-dependent DAT regulation is broader than trafficking alone(Cremona et al., 2011).

In contrast, Sorkina and colleagues reported that Flot1 knockdown did not block PKC-dependent DAT endocytosis in HEK293 or HeLa cells, and were further unable to recapitulate a specific protein-protein association (Sorkina et al., 2013). Instead, researchers found that Flot1 knockdown resulted in increased DAT lateral mobility using FRAP (fluorescence recovery after photobleaching), suggesting a role for Flot1 in regulating DAT plasma membrane compartmentalization. Discrepancies in methodology likely explain the differing results across these two studies. Importantly, Cremona et al. measured PKC-stimulated DAT trafficking in DA neurons, the more physiologically relevant model (Cremona et al., 2011).

Finally, the best evidence that Flot1 regulates DAT comes from *in vivo* experiments done in *Drosophila* larvae. To test whether Flot1 was required for DAT-dependent behavior *in vivo*, researchers fed larvae psychostimulants MPH and AMPH and

observed significantly increased larval crawling speed that was dose-dependent (Pizzo et al., 2013). Importantly, flies lacking DAT did not display psychostimulant-induced hyperactivity. Researchers knocked down Flot1 in DA neurons using cell-specific RNAi and found that DAergic Flot1 was required for AMPH-stimulated hyperlocomotion, but not MPH-induced. Given that Flot1 silencing blocked both PKC-stimulated DAT trafficking and AMPH-stimulated DA efflux (Cremona et al., 2011), it cannot be distinguished whether DAT trafficking or DA efflux causes the behavioral disruption. However, as the phenotype appears to be specific to AMPH and can be rescued with phosphomimetic mutations at DAT residues required for AMPH-stimulated efflux, it can likely be attributed to the loss of DA efflux.

Nedd4-2, Epsin, and Epsin15

The neuronal E3 ubiquitin ligase, Nedd4-2 (neural precursor cell expressed, developmentally downregulated 4-2) was identified in an RNAi screen for proteins required for PKC-stimulated DAT endocytosis (Sorkina et al., 2006). Sorkina and colleagues further proposed that this was due to the concomitant loss of PMA-induced DAT ubiquitination, that they previously demonstrated to be required for PKC-dependent DAT surface loss (Miranda et al., 2005; Miranda et al., 2007). Moreover, Nedd4-2 co-immunoprecipitated with DAT. Epsin (epidermal growth factor pathway substrate) and Epsin clone 15 (Eps15) were also identified in this screen. Epsins are important for endocytosis of ubiquitinated membrane proteins (Chen et al., 1998), and pooled siRNAs targeted against Epsin/Eps15/Eps15R

blocked PKC-stimulated DAT endocytosis (Sorkina et al., 2006). Eps15 colocalized with DAT in rat DA neuron cultures, and both Epsin and Eps15 associated with DAT as measured by co-IP. However, whether the Nedd4-2 or Epsin association with DAT is required for PKC-stimulated internalization remains untested.

PICK1

Multiple DAT domains have been identified that are required either 1) to maintain DAT surface expression, or 2) to promote biosynthetic (i.e. “forward”) DAT trafficking (described above). The final carboxy terminal amino acids of DAT, “LKV”, constitute a PDZ-binding domain, and are required for DAT binding to the PDZ protein, PICK1 (protein interacting with C kinase 1) (Torres et al., 2001). Initial studies in HEK293 cells and cultured DA neurons found that PICK1 potentiated DAT function in an LKV-dependent manner. Moreover, truncating the LKV residues from the DAT carboxy terminus substantially reduced DA uptake and DAT axonal targeting, suggesting that the PDZ domain, possibly through the PICK1 association, is required for DAT surface delivery (Torres et al., 2001). A subsequent study by Gether and colleagues confirmed that truncating the LKV motif indeed resulted in DAT retention in the endoplasmic reticulum (ER). They further found that replacing the LKV motif with the β2-adrenergic receptor PDZ domain (SLL) sufficed to rescue DAT surface targeting, but not PICK1 binding, indicating that PDZ-dependent plasma membrane targeting may not be solely

dependent upon the DAT-PICK1 interaction (Bjerggaard et al., 2004). Moreover, using an alanine substitution mutant (DAT-AAA), our laboratory recently found that the LKV PDZ domain is required for retromer-dependent, DAT endosomal surface delivery in the rat mesencephalic cell line, AN27 (Wu et al., 2017). However, DAT-AAA relative surface levels were comparable to wildtype DAT, indicating that the DAT LKV motif, *per* se, might not be required for DAT biosynthesis and forward trafficking in AN27 cells (Wu et al., 2017).

In order to address the role of the LKV motif *in situ*, Gether and colleagues generated a knock-in mouse expressing DAT-AAA, which had significantly reduced affinity for purified PICK1 protein (Rickhag et al., 2013b). The DAT-AAA mouse had a striking loss in striatal DAT protein. Furthermore, DAT-AAA was not retained in the ER in neuronal cultures made from the knock-in mouse, in agreement with their previous cell line report (Bjerggaard et al., 2004). However, PICK1 was not required *in vivo* for proper DAT protein levels or axonal targeting, as demonstrated by the PICK1 knockout mouse (Rickhag et al., 2013b). In summary, these data indicate that 1) the DAT PDZ domain is required *in vivo* for DAT protein expression, but not for DAT's overall surface:intracellular distribution, and 2) PICK1, though initially thought to be required for PDZ-dependent DAT plasma membrane targeting, is not required *in vivo* for DAT protein expression.

*RACK1 & Syntaxin 1A*

The receptor for activated C kinase (RACK1) and syntaxin 1A (Syn1A) interact with the DAT N-terminus. These interactions were originally identified in the same yeast two-hybrid screen of a human brain cDNA library and confirmed using a His-tagged DAT N-terminal (1-65) fragment to pulldown RACK1 and Syn1A from rat brain synaptosomes (Lee et al., 2004). The first 33 DAT amino acids were later found to be sufficient for the Syn1A/DAT interaction in a GST pull-down experiment (Binda et al., 2008). Using Co-IP, Lee and colleagues also found an association between Syn1A and RACK1, however the Syn1A/RACK1 association could be a result of the two proteins' interaction with DAT. How or whether RACK1 regulates DAT function or expression remains completely unexplored.

In contrast, researchers demonstrated that Syn1A is required for, or involved in, multiple DAT functions. The membrane protein Syn1A is a neuron-specific isoform of Syntaxin that also interacts with GAT1 (Beckman et al., 1998), SERT (Haase et al., 2001), and NET (Sung et al., 2003) and regulates their function and surface expression. Co-expression of Syn1A significantly decreased DA uptake in $LLCPK_1$ cells and potentiated PKC-dependent DAT functional downregulation (Cervinski et al., 2010). However, PKC-stimulated DAT internalization was not blocked by Syn1A overexpression (Cervinski et al., 2010). Interestingly, co-expression of Syn1A and DAT potentiated AMPH-stimulated DA efflux in both HEK293 cells and cultured mouse midbrain neurons (Binda et al., 2008). Together, these data

indicate that Syn1A is important for mediating the actions of AMPH on DAT, but does not regulate DAT trafficking.

*Membrane potential-dependent DAT trafficking*

Neuronal activity can also regulate DAT function and trafficking. Early studies reported reduced DA uptake in synaptosomes at depolarized states (Woodward et al., 1986) and increased uptake at hyperpolarized potentials in *Xenopus* oocytes (Sonders et al., 1997). In a follow-up report, researchers found that KCl-mediated depolarization decreased DAT surface expression, as measured by TIRF microscopy, surface biotinylation, and JHC 1-64 internalization tracking in cultured cells and primary neurons (Richardson et al., 2016). Shifting the cell to a hyperpolarized state increased DAT surface expression, demonstrating a direct bidirectional effect on DAT surface levels within the same cell mediated by membrane potential. Furthermore, membrane depolarization-stimulated DAT endocytosis required CaMKII$\alpha$, likely activated as a consequence of KCl-mediated $Ca^{2+}$ release (Richardson et al., 2016). Despite the potential relevance to physiological DA neuron firing, it remains untested whether neuronal activity directly controls DAT endocytic trafficking in intact DA neurons.

*DAT lateral mobility and plasma membrane distribution*

DAT not only recycles and internalizes to and from the cell surface, but also moves laterally within the plasma membrane. Numerous reports support that DAT

localizes to particular membrane domains measured by colocalization with cholera toxin (CTX), and fractionation with GM1 glycosphingolipid, markers of lipid rafts (Adkins et al., 2007; Foster et al., 2008; Navaroli et al., 2011; Gabriel et al., 2013; Butler et al., 2015). Evidence that DAT function is influenced by its microdomain association stems from early experiments that described decreased DAT function following cholesterol depletion via methyl-$\beta$-cyclodextrin (m$\beta$CD) treatment (Adkins et al., 2007; Foster et al., 2008; Hong and Amara, 2010). Moreover, DAT lateral diffusion in the membrane was demonstrated by FRAP experiments in live cultured cells and DA neurons (Adkins et al., 2007; Eriksen et al., 2009; Butler et al., 2015; Lebowitz et al., 2019). Finally, quantum-dot labeling experiments have enabled examination of the membrane diffusion dynamics of single DAT molecules in live cells (Kovtun et al., 2015; Kovtun et al., 2019; Thal et al., 2019), revealing signaling- and conformational-dependent changes.

DAT lateral mobility and microdomain localization are altered by a variety of stimuli. PKC activation shifts DAT out of CTX+ microdomains, whereas AMPH redistributes DAT into CTX+ domains (Gabriel et al., 2013; Butler et al., 2015), raising the possibility that the machinery required for stimulated DAT endocytosis is spatially restricted at the plasma membrane. This is consistent with data supporting that PKC- and AMPH-stimulated DAT internalization are mechanistically distinct (Boudanova et al., 2008a; Hong and Amara, 2013; Wheeler et al., 2015), and that DAT's conformational state and its protein-protein

interactions differ depending on its membrane context (Hong and Amara, 2010; Navaroli et al., 2011; Butler et al., 2015). DAT also forms smaller sub-clusters at the plasma membrane, termed DAT “nanodomains” (Rahbek-Clemmensen et al., 2017). NMDA receptor activation can stimulate burst firing of DA neurons, and given DAT’s ability to traffic with changes to membrane potential (Richardson et al., 2016), researchers were prompted to test whether neuronal activity alters DAT membrane distribution. Using stochastic optical reconstruction microscopy (STORM), Rahbek-Clemmensen and colleagues tested whether NMDA receptor activation altered DAT surface distribution in cultured rat midbrain DA neurons. Basally DAT is clustered into cholesterol-sensitive nanodomains, however exposure to 20μM NMDA for 5 minutes significantly reduced DAT clustering (Rahbek-Clemmensen et al., 2017).

Finally, disease-associated DAT mutants exhibit disrupted microdomain localization and baseline lateral mobility. The R615C-DAT variant found in an ADHD patient associates with CTX+ microdomains significantly less than wildtype DAT (Sakrikar et al., 2012) and displayed significantly a higher diffusion rate compared with wildtype DAT, as measured by single-molecule quantum dot labeling at basal states (Kovtun et al., 2015). Both AMPH treatment and cholesterol depletion by mβCD treatment increased wildtype DAT lateral mobility, however R615C-DAT was resistant to further increases in membrane diffusion (Kovtun et al., 2015), supporting that R615C-DAT is mislocalized at the plasma membrane.

A559V-DAT had similarly increased membrane diffusion rates that were likewise insensitive to PKC-stimulated increases observed in wildtype DAT (Thal et al., 2019).

As a whole, these data emphasize that many intrinsic mechanisms within the DA neuron contribute to DAT function and surface expression. Given that DAT surface availability is fundamental to DA homeostasis and psychostimulant action, it is likely that perturbations in DAT endocytic regulation will impact DA-dependent behaviors. However, this hypothesis remains to be tested directly.

## I.D Rit2 GTPase

*Rit subfamily of small GTPases*

The Ras superfamily includes over 150 distinct GTP-binding proteins that function as “molecular switches” in a wide variety of cellular processes, including cell growth, proliferation, differentiation, endocytosis, and exocytosis (Wennerberg et al., 2005). Ras guanosine triphosphate phosphatases (GTPases) bind to GTP and GDP, and generally display higher affinity for downstream effector proteins in the GTP-bound, or active, form. GTPase intrinsic GDP/GTP exchange and GTP hydrolysis rates are very slow, but are accelerated by guanine nucleotide exchange factors (GEFs), which activate Ras GTPases, and GTPase-activating proteins (GAPs), which inactivate GTPases by hydrolyzing the bound GTP for GDP (Vetter and Wittinghofer, 2001). GTPases contain five functional domains

(G1-G5), where G1 and G3 are involved in phosphate binding, the G2 domain binds to downstream effector proteins, and G4 and G5 are involved in GTP binding and hydrolysis (Colicelli, 2004). In most cases, Ras GTPases contain a C-terminal motif, CAAX (C=Cys, A=aliphatic, X=any amino acid), that is required for membrane targeting (Wennerberg et al., 2005).

The Ras superfamily GTPases is divided into five classes based on sequence homology: Ras, Rho, Rab, Ran and Arf (Wennerberg et al., 2005). Contained within the Ras subfamily are the Rit small GTPases, which include the *Drosophila* protein, Ric (Ras-like protein which interacted with calmodulin), and vertebrate homologs, Rit1 (Ric-related gene expressed throughout the organism), and Rit2 (Ric-related gene expressed in neuronal tissues) (Lee et al., 1996; Wes et al., 1996). Ric shares 66% and 71% amino acid identity with Rit1 and Rit2, respectively, and Rit1 and Rit2 are 64% identical. The unique G2 effector domain within this subfamily, however, is absolutely identical between Rit1 and Rit2 (HDPTIEDAY), and differs by only one residue in Ric (HDPTIEDSY) (Shi et al., 2013). The Rit subfamily lack the canonical CAAX domain and instead rely on highly polybasic C-termini for membrane targeting. Moreover, Rit1 and Rit2 require C-terminal tryptophan residues W204 and W202, respectively, and $PI(4,5)P_2$ and $PI(3,4,5)P_3$, lipids for proper membrane localization (Heo et al., 2006). Rit1 and Ric RNA is expressed across all tissues and developmental stages. In contrast, Rit2 RNA is only detected in the brain of human and mouse tissues, and has

considerably greater abundance in adult mice than embryonic, P7 and P21 mice (Lee et al., 1996; Wes et al., 1996; Spencer et al., 2002b). Of note, Rit2 neuronal expression is specifically enriched in the SNc, a DAergic cell body region, as measured by *in situ* hybridization (Zhou et al., 2011).

Ric was originally identified in a screen for *Drosophila* retinal calmodulin-binding proteins (Wes et al., 1996). In this initial report, researchers confirmed, *in vitro*, that Ric binds to calmodulin, but does not require calcium to interact. The Rit2-calmodulin interaction was also demonstrated *in vitro*, however this interaction was calcium-dependent (Lee et al., 1996; Wes et al., 1996). Shortly after the identification of Rit1 and Rit2, Shao et al. confirmed their GTPase functionality *in vitro* using C-terminally truncated GST fusion proteins. Both Rit1 and Rit2 bound GTP$\gamma$S in a $Mg^{2+}$-dependent manner, and were specific for guanine nucleotides (Shao et al., 1999). This study further demonstrated that the putative constitutively active Rit2 mutant (Q78L) and Rit1 mutant (Q79L) had significantly reduced GTP hydrolysis, indicating that they are indeed constitutively active (Shao et al., 1999). Specific GAPs, GEFs, and effector proteins for Rit1, Rit2, and Ric have not yet been identified. Shao and colleagues employed *in vitro* binding assays to test whether C-terminally truncated Rit1 or Rit2 GST fusion proteins interacted with other Ras effector proteins, including RalGDS, RIN1, Raf kinase, RLF, and AF6. Rit1 and Rit2 bound to RalGDS, RLF, and AF6, but not full-length Raf kinase, RIN1, or the catalytic domain of PI3-kinase, p110 (Shao et al., 1999). Another

group later identified a Ral-Ras-binding domain (RBD) interaction with Rit2, again using a truncated protein *in vitro* (Hoshino and Nakamura, 2002). They also proposed that Rit2 interacts with the Ras GEF, mSOS, and the cell adapter protein, PAR6 (Hoshino and Nakamura, 2002; Hoshino et al., 2005). However, these results have not been replicated nor validated in physiologically-relevant conditions. Furthermore, endogenous Rit2 GAPs, GEFs, and effectors remain unknown.

*Rit subfamily cellular function*

Despite the lack of information regarding the Rit1/Rit2/Ric interactome, a role in neurite outgrowth has been described for this family of proteins. EGF (epidermal growth factor)- and NGF (nerve growth factor)-dependent Rit2 activation was demonstrated by two groups who assessed GTP-dependent Rit2 binding to putative effectors as a measure of activation (Hoshino and Nakamura, 2002; Spencer et al., 2002b; Hoshino and Nakamura, 2003). Overexpression of the constitutively active Rit2 (Rit2-Q78L) in PC6 and PC12 cells (but not NIH-3T3 cells) suffices to induce neurite outgrowth to a similar degree as NGF alone (Hoshino and Nakamura, 2003; Shi et al., 2005), and Rit1 activity similarly stimulates neurite outgrowth in PC6 cells (Spencer et al., 2002a). Shi and colleagues further demonstrated that Rit2 interacts with B-Raf in order to activate ERK and p38 MAP kinase, and that this mechanism is required for NGF-dependent neurite outgrowth (Shi et al., 2005). Moreover, the Rit2-dependent outgrowth required calmodulin

and Rac/Cdc42 activity (Hoshino and Nakamura, 2003). Rit2 also associates with the neuronally-expressed plexin B3, which also stimulates neurite outgrowth in NIH-3T3 cells; however, whether Rit2 is required for plexin B3-dependent outgrowth was not examined (Hartwig et al., 2005), and Rit2 is not endogenously expressed in NIH-3T3 cells (see Chapter II). Finally, the Rit2/B-Raf interaction was later confirmed in a report that also demonstrated that Rit2 is required for ERK phosphorylation and cell viability in human neuroblastoma SH-SY5Y cells (Uenaka et al., 2018).

Ric-dependent neurite outgrowth is conserved in *Drosophila*, and was demonstrated *in vivo*. Putative constitutively active Ric mutant, Ric-Q117L, overexpression causes neurite outgrowth in PC6 cells and *Drosophila* wing veins when expressed using a tissue-specific driver (Harrison et al., 2005). Given its initial identification in *Drosophila* retina, researchers also tested whether Ric activity was required for eye formation. They found that Ric-Q117L expression causes eye deformation phenotypes, wherein the eyes were visibly reduced or misshapen (Harrison et al., 2005). Both Ric-Q117L phenotypes are exacerbated by concomitant calmodulin mutations, further supporting the interdependent roles of Ric and calmodulin in regulating cellular outgrowth (Harrison et al., 2005).

*Rit2 genetic variations in neuropsychiatric diseases and disorders*

Numerous reports utilizing genome-wide association studies (GWAS) have identified Rit2 genetic anomalies associated with multiple diseases and disorders, including PD (Bossers et al., 2009; Latourelle et al., 2012; Pankratz et al., 2012; Lin et al., 2013; Emamalizadeh et al., 2014; Nalls et al., 2014; Liu et al., 2015; Lu et al., 2015; Nie et al., 2015; Wang et al., 2015; Zhang et al., 2015; Chan et al., 2016; Chang et al., 2017; Emamalizadeh et al., 2017; Li et al., 2017; Daneshmandpour et al., 2018; Liu et al., 2019), essential tremor (Emamalizadeh et al., 2017), schizophrenia (Glessner et al., 2010; Emamalizadeh et al., 2017), ASD (Liu et al., 2016; Hamedani et al., 2017), BPD (Emamalizadeh et al., 2017), and speech delay (Bouquillon et al., 2011) (Table I.3). Interestingly, all of these disorders are DAergic in nature, further highlighting the importance of appropriate Rit2 expression and function specifically in DA neurons. Both SNPs and copy number variations (CNVs) have been discovered within the Rit2 genomic region, and may be specifically associated with a disease or disorder. In particular, the rs12456492 SNP is associated with PD and essential tremor across different patient populations and in numerous reports (Daneshmandpour et al., 2018). Of note, rs12456492 is not associated with PD patients in studies performed in Taiwanese populations, indicating possible genetic distinctions between populations (Lin et al., 2013; Li et al., 2017; Liu et al., 2019). On the other hand, rs16976358 was associated with schizophrenia, ASD, and BPD, but not PD (Emamalizadeh et al., 2017). Finally, a large (5.3 Mb) chromosomal deletion was

found in two patients with speech delay, and while the closest gene is Rit2, it is not clear whether Rit2 deletion itself is responsible for this cognitive impairment (Bouquillon et al., 2011).

**Table I.3 Neuropsychiatric diseases and disorders associated with Rit2 genetic variations.**

| Associated Disease /Disorder | Genetic Variation | References |
|---|---|---|
| **PD** | Reduced Rit2 mRNA | Bossers et al. (2009) |
| | rs12456492 (SNP) | Pankratz et al. (2012), Lin et al. (2013)*, Emamalizadeh et al. (2014), Nalls et al. (2014)+, Liu et al. (2015), Lu et al. (2015)+, Nie et al. (2015), Wang et al. (2015), Zhang et al. (2015)+, Chan et al. (2016), Chang et al. (2017)+, Emamalizadeh et al. (2017), Li et al. (2017)*, Daneshmandpour et al. (2018)®, Liu et al. (2019)*,+ |
| | rs9948019 (SNP) | Latourelle et al. (2012) |
| **Essential Tremor** | rs12456492 (SNP) | Emamalizadeh et al. (2017) |
| **Schizophrenia** | CNV (deletion) | Glessner et al. (2010) |
| | rs16976358 (SNP) | Emamalizadeh et al. (2017) |
| **ASD** | rs16976358 (SNP) | Liu et al. (2016), Hamedani et al. (2017) |
| | rs4130047 (SNP) | Hamedani et al. (2017) |
| **BPD** | rs16976358 (SNP) | Emamalizadeh et al. (2017) |
| **Speech Delay** | 5.3 Mb chromosomal deletion (18q12.3) | Bouquillon et al. (2011) |

*No association with PD; +Meta-analysis; ®Review

rs12456492: intronic; rs16976358: downstream of Rit2

The mechanism(s) by which Rit2 may influence disease predisposition or progression remain completely unknown. The original report that identified Rit2 as a potential PD risk allele reported that Rit2 was among genes most highly downregulated in the SNc of PD patients, as compared to healthy controls (Bossers et al., 2009). Rit2 gene expression was decreased by approximately 65%, even after accounting for DAergic cell death in the samples. However, it is not known how, or if, the disease-associated SNPs affect Rit2 gene expression or protein function. Given that Rit2 is involved in neurite outgrowth and cell survival, it is possible that these signaling pathways are disrupted by Rit2 genetic variations, thus resulting in reduced DA neuron viability and/or function. This hypothesis, however, has not been tested.

*Rit2 function in DA-dependent behavior*

Given that Rit2 binds to DAT and is somehow involved in PKC-stimulated DAT internalization, our laboratory recently leveraged a conditional and inducible gene knockdown approach to evaluate the behavioral impact of DA neuron-specific Rit2 knockdown (Rit2-KD). We demonstrated that AAV-mediated, conditional Rit2-KD in DA neurons significantly reduced anxiety behaviors in mice. Moreover, we found that DAergic Rit2 modulates the locomotor response to a single cocaine injection (Sweeney et al., 2020). Interestingly, the Rit2-KD phenotype was sexually dimorphic. In male mice, Rit2-KD increased the sensitivity to cocaine such that a previously-determined sub-threshold dose now induced hyperactivity. Conversely,

in female mice Rit2-KD significantly attenuated cocaine-stimulated hyperactivity (Sweeney et al., 2020). Given that DAT is required for cocaine-dependent behavior, we tested whether Rit2-KD altered DAT protein and/or surface expression. Rit2-KD had no effect on overall DAT protein levels in female mice, but significantly decreased DAT protein in male mice by approximately 50% (Sweeney et al., 2020). Whether these phenotypes are driven by Rit2-dependent changes in DAT function, expression, or PKC-stimulated DAT endocytosis remains unknown.

## I.E Summary

DAT critically regulates DA neurotransmission with spatial and temporal precision, and is required for maintaining synaptic DA homeostasis. Mutations that affect DAT function and/or expression disrupt DA-dependent behaviors, highlighting the importance of proper DAT regulation *in vivo*. It is well-established that DAT surface expression is dynamic and highly regulated, yet whether regulated DAT trafficking impacts behavior is not known. Our laboratory discovered that Rit2 interacts with DAT, and its activity is required for PKC-stimulated DAT internalization in transfected PC12 cells (Navaroli et al., 2011). However, questions still remain regarding the cellular mechanisms and *in vivo* impact of regulated DAT trafficking. First, the mechanisms by which Rit2 mediates PKC-dependent DAT endocytosis are unknown. Does Rit2 coordinate its action with the nonreceptor tyrosine kinase, Ack1, to facilitate DAT internalization? What is the influence of the DAT terminal

domains on the DAT/Rit2 interaction and, if relevant, the Rit2-dependent mechanism? Moreover, it remains unknown whether Rit2 is required in DA terminals for PKC-stimulated DAT downregulation. Second, despite multiple decades worth of evidence supporting that DAT trafficking occurs in heterologous cells, as well as in native DA neuron preparations, the physiological impact of regulated DAT endocytosis remains untested. Here, I present the molecular mechanisms of Rit2-dependent DAT trafficking (Chapter II) and use *Drosophila melanogaster* to test whether the DAT-Rit2 interaction is conserved in flies, and whether DAergic Ric and/or regulated DAT trafficking impact DA-dependent behaviors (Chapter III).

## Preface to Chapter II

This chapter was previously published separately in:

Fagan, RR, Kearney, PJ, Sweeney, CG, Leuthi, D, Uiterkamp, FES, Schicker, K, Alejandro, BS, O'Connor, LC, Sitte, HH, and Melikian, HE (2020) Dopamine transporter trafficking and Rit2 GTPase: Mechanism of action and *in vivo* impact. J Biol Chem, in press. DOI: 10.1074/jbc.RA120.012628.

Author Contributions:

Rita R. Fagan, Patrick J. Kearney, Carolyn G. Sweeney, Harald H. Sitte, and Haley E. Melikian designed experiments.

Rita R. Fagan, Patrick J. Kearney, Carolyn G. Sweeney, Dino Leuthi, Florianne E. Schoot Uiterkamp, Klaus Schicker, Brian S. Alejandro, and Lauren C. O'Conner performed experiments.

Rita R. Fagan, Patrick J. Kearney, Carolyn G. Sweeney, Dino Leuthi, Klaus Schicker, Lauren C. O'Conner, Harald H. Sitte, and Haley E. Melikian and analyzed data.

Rita Fagan and Haley Melikian wrote original manuscript draft.

# CHAPTER II

## Dopamine transporter trafficking and Rit2 GTPase: Mechanism of action and *in vivo* impact

Rita R. Fagan, Patrick J. Kearney, Carolyn G. Sweeney, Dino Luethi, Florianne E. Schoot Uiterkamp, Klaus Schicker, Brian S. Alejandro, Lauren C. O'Connor, Harald H. Sitte, and Haley E. Melikian

## II.A Summary

Following its evoked release, dopamine (DA) signaling is rapidly terminated by presynaptic reuptake, mediated by the cocaine-sensitive DA transporter (DAT). DAT surface availability is dynamically regulated by endocytic trafficking, and direct protein kinase C (PKC) activation acutely diminishes DAT surface expression by accelerating DAT internalization. Previous cell line studies demonstrated that PKC-stimulated DAT endocytosis requires both Ack1 inactivation, which releases a DAT-specific endocytic brake, and the neuronal GTPase, Rit2, which binds DAT. However, it is unknown whether Rit2 is required for PKC-stimulated DAT endocytosis in DAergic terminals, or whether there are region- and/or sex-dependent differences in PKC-stimulated DAT trafficking. Moreover, the mechanisms by which Rit2 controls PKC-stimulated DAT endocytosis are unknown. Here, we directly examined these important questions.

*Ex vivo* studies revealed that PKC activation acutely decreased DAT surface expression selectively in ventral, but not dorsal, striatum. AAV-mediated, conditional Rit2 knockdown in DAergic neurons impacted baseline DAT surface:intracellular distribution in DAergic terminals from female ventral, but not dorsal, striatum. Further, Rit2 was required for PKC-stimulated DAT internalization in both male and female ventral striatum. FRET and surface pulldown studies in cell lines revealed that PKC activation drives DAT-Rit2 surface dissociation, and that the DAT N-terminus is required for both PKC-mediated DAT-Rit2 dissociation and DAT internalization. Finally, we found that Rit2 and Ack1 independently converge on DAT to facilitate PKC-stimulated DAT endocytosis. Together, our data provide greater insight into mechanisms that mediate PKC-regulated DAT internalization, and reveal unexpected region-specific differences in PKC-stimulated DAT trafficking in *bona fide* DAergic terminals.

## II.B Introduction

DA neurotransmission is required for motor control, learning, memory, motivation, and reward (Wise, 2004; Iversen and Iversen, 2007). DAergic dysregulation is evidenced in numerous neuropsychiatric disorders, including ADHD, ASD, schizophrenia, BPD, addiction, and PD (Hyman et al., 2006; Sharma and Couture, 2014; Ashok et al., 2017; Howes et al., 2017; Eissa et al., 2018; Geibl et al., 2019). DA signaling is tightly controlled by the presynaptic DAT, which rapidly clears synaptically released DA. DAT is also the primary target for addictive and

therapeutic psychostimulants, including AMPH, cocaine, and methylphenidate (Ritalin), which inhibit DAT as competitive substrates (AMPH) and antagonists (cocaine and methylphenidate) (Kristensen et al., 2011). Genetic DAT deletions in mice and *Drosophila melanogaster* elevate extracellular DA concentrations and evoke hyperactivity (Giros et al., 1996; Gainetdinov et al., 1998; Kume et al., 2005), and human DAT missense mutations have been reported in PD, ADHD and ASD patients (Mazei-Robison and Blakely, 2005; Kurian et al., 2009; Sakrikar et al., 2012; Hamilton et al., 2013; Bowton et al., 2014; Ng et al., 2014; Herborg et al., 2018). Together, these studies underscore that DAT is critical to maintain DAergic homeostasis (Kristensen et al., 2011).

Given its central role in DAergic signaling, intrinsic neuronal mechanisms that alter DAT surface expression and function are likely to significantly impact DAergic transmission. DAT surface availability is dynamically modulated by endocytic trafficking (Melikian, 2004; Eriksen et al., 2010b; Bermingham and Blakely, 2016). A negative regulatory mechanism, or “endocytic brake”, tempers basal DAT endocytosis (Boudanova et al., 2008b; Wu et al., 2015), and acute PKC activation disengages the DAT endocytic brake, stimulates DAT internalization, and rapidly diminishes DAT surface expression (Loder and Melikian, 2003; Gabriel et al., 2013). The DAT N- and C-termini encode residues required to engage the DAT endocytic brake, and, when mutated, markedly accelerate DAT internalization (Boudanova et al., 2008b; Sorkina et al., 2009; Sakrikar et al., 2012). We

previously reported that the nonreceptor tyrosine kinase, Ack1 (AKA: TNK2), is a critical component of the DAT endocytic brake, and that Ack1 inactivation is required for PKC-mediated brake release (Wu et al., 2015).

Rit2 (also known as Rin) is a neuronal small GTPase that lacks a CAAX domain, and associates with the plasma membrane in a phosphoinositide-dependent manner (Lee et al., 1996; Wes et al., 1996; Heo et al., 2006). *RIT2* gene expression is highly enriched in DA neurons (Zhou et al., 2011), and several recent GWAS studies identified *RIT2* SNPs and long tandem repeat variants associated with multiple DA-related disorders, including PD, ASD, and schizophrenia (Glessner et al., 2010; Pankratz et al., 2012; Zhang et al., 2015; Emamalizadeh et al., 2017; Foo et al., 2017; Hamedani et al., 2017). However, despite its disease association, relatively little is known about endogenous DAergic Rit2 function. We previously reported that DAT directly binds to Rit2, and that Rit2 activity is required for PKC-stimulated DAT internalization (Navaroli et al., 2011). Moreover, we recently found that *in vivo* DAergic Rit2 knockdown (Rit2-KD) differentially alters acute cocaine sensitivity in males and females (Sweeney et al., 2020). However, it remains unknown whether PKC-stimulated DAT internalization in DAergic terminals requires Rit2, and whether there are region- or sex-specific differences in DAT's reliance upon Rit2. Further, it is unclear how intrinsic DAT domains influence the DAT-Rit2 interaction, or whether Rit2 and Ack1 coordinate to release the DAT endocytic brake. In the present study, we leveraged biochemical and genetic

approaches, in both cultured cells and *ex vivo* mouse striatal slices, to directly address these salient questions.

## II.C Results

*Rit2 cellular expression and antibody specificity*

In our previous study, in which we initially reported the DAT-Rit2 interaction (Navaroli et al., 2011), there were several paradoxical findings regarding 1) how PKC activation impacted the DAT-Rit2 interaction, and 2) the Rit2 expression profile across various cell lines. In cellular imaging studies, which used CFP-Rit2, Rit2 appeared to remain at the plasma membrane following PKC-stimulated DAT internalization, suggesting that PKC may drive DAT and Rit2 to dissociate. In contrast, parallel co-IP studies found that PKC activation *increased* the DAT-Rit2 interaction in PC12 cells. Furthermore, although Rit2 expression is reportedly restricted to neurons (Lee et al., 1996; Wes et al., 1996; Zhou et al., 2011; Zhang et al., 2013), we detected a single, ~20kDa immunoreactive band by immunoblot in all neuronal and nonneuronal cell lines tested, as well as *RIT2* mRNA expression in these cell lines by standard RT-PCR. The previous studies utilized the anti-Rit2 monoclonal antibody, clone 27G2, and in that report, we additionally confirmed that 27G2 specifically recognizes Rit2, but not Rit1, (the ubiquitously expressed Rit2 homologue) using fluorescently-tagged Rit2 and Rit1 fusion proteins. Recently, we decided to take advantage of highly specific, Rit2-directed, real-time qPCR probes to reassess the Rit2 expression profile across a large panel of human, mouse and rat cell lines, as well as in mouse and rat midbrain, all of which exhibit the single,

20kDa immunoreactive band when probed with the anti-Rit2 27G2. To our surprise, *RIT2* mRNA was undetectable in any of the mouse or rat cell lines tested, whereas a robust *RIT2* mRNA signal was detected in both mouse and rat midbrain controls (Table II.1). Moreover, among the human cell lines tested, *RIT2* mRNA was only detected in SK-N-DZ cells, as reported previously (Zhang et al., 2013), and at low levels in SH-SY5Y cells. However, SK-N-MC and HEK293T cells expressed markedly less/negligible *RIT2* signal than SK-N-DZ cells, ranging from 20-300-fold less (Table II.1).

**Table II.1 Rit2 expression in mammalian cell lines and rodent brain regions**
Rit2 mRNA expression was determined by RT-qPCR and normalized to internal GAPDH values, n=2-4.

| Species/Cell line | Rit2 ($2^{-\Delta Ct}$ x $10^4$ ± S.E.M.) |
|---|---|
| **Mouse** | |
| CAD | 0.02 ± 0.0067 |
| N2a | 0.09 ± 0.052 |
| NIH/3T3 | No signal detected |
| Midbrain | 72.0 ± 12.8 |
| Cortex | 54.8 ± 9.19 |
| **Rat** | |
| AN27 | No signal detected |
| PC12 | No signal detected |
| Midbrain | 110.0 ±0.51 |
| **Human** | |
| HEK293T | 0.40 ± 0.34 |
| SH-SY5Y | 1.3 ± 0.56 |
| SK-N-MC | 0.09 ± 0.07 |
| SK-N-DZ | 27.2 ± 18.7 |

Our current RT-qPCR results raised the possibility that although 27G2 recognizes Rit2, it also may cross-react with a ubiquitously expressed protein that has an electrophoretic mobility close to that of Rit2. To test this, we screened several newer, commercially available anti-Rit2 antibodies using cell lysates from HEK293T cells transfected with CFP-Rit2. Consistent with our previous report, clone 27G2 identified a single 20kDa band in both transfected and nontransfected cells, and also detected CFP-Rit2 selectively in transfected cells (Figure II.1A). However, when immunoblots were probed with αRit2 clone 4B5, the low molecular weight immunoreactive band was not detected, whereas CFP-Rit2 was detected in transfected cells (Figure II.1A). These results are consistent with our RT-qPCR results and confirm that 27G2 detects an artifactual band with an electrophoretic mobility close to the Rit2 predicted size. We next used 4B5 to assess Rit2 in cells transfected with HA-Rit2 and in mouse DAergic tissues. Clone 4B5 detected a single, ~28kDa immunoreactive band selectively in cells transfected with HA-Rit2, which was identical in mobility to an immunoreactive band detected with αHA, in parallel (Figure II.1B). αHA also detected a higher molecular weight band (~30kDa) specifically in cells transfected with HA-Rit2, which we did not detect using 4B5 (Figure II.1B), suggesting that Rit2 may have multiple isoforms, and that 4B5 may only detect one of these. 4B5 also detected bands at ~24kDa in mouse lysates enriched for either dorsal striatum or ventral midbrain (Figure II.1B). These immunoblot results were consistent with our RT-qPCR results, and confirmed that most cell lines either do not express Rit2, or express Rit2 at negligible levels. They

further support that the 27G2 antibody cannot reliably distinguish between Rit2 and a robust, artifactual, background band. It should also be noted that while 4B5 specifically detects Rit2, it does so with extremely low sensitivity, even when Rit2 is highly overexpressed. Indeed, using the 4B5 antibody, we could only detect Rit2 by immunoblot in lysates from mouse tissues when a very high protein mass was loaded. Moreover, although both hRit2 and mRit2 are predicted to have identical number of amino acids, and a predicted mass of ~24kDa each, the overexpressed hRit2 protein ran slightly higher than the putative mRit2 band. There are two known hRit2 isoforms, variants 1 and 2, which are predicted to be ~24kDa and ~17kDa, respectively, and our hRit2 cDNA codes for variant 1. To date it is unknown whether there are tissue specific Rit2 isoforms in mouse neurons. Given that there is no global $Rit2^{-/-}$ mouse available, we therefore cannot say with absolute certainty that the single immunoreactive band in mouse tissue is definitively Rit2, or possibly a smaller splice variant. Therefore, for the majority of our cell line studies, we opted to use HA-Rit2 for greater sensitivity in cell lines and did not further assess Rit2 protein in tissue.

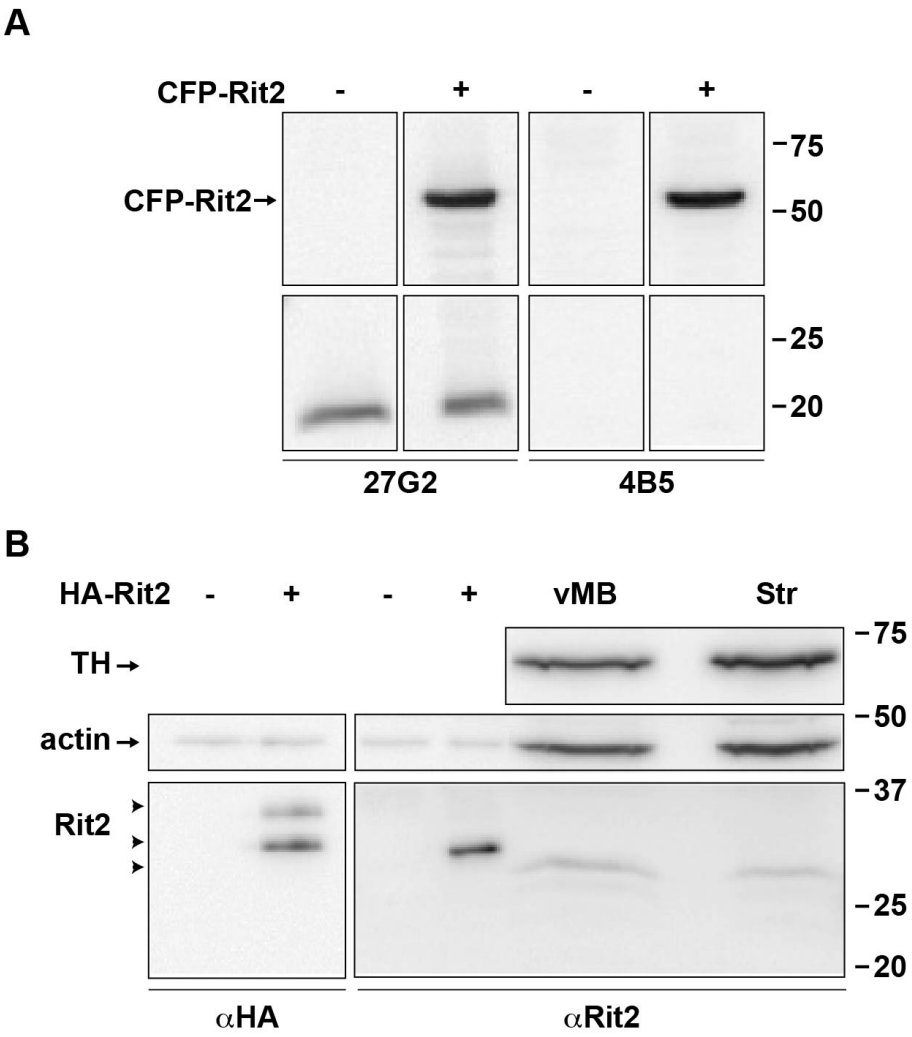


**Figure II.1 Rit2 protein is specifically detected by clone 4B5, but not clone 27G2, αRit2 antibodies. A** and **B**, Rit2 detection in transfected cell lines and mouse tissues by immunoblot analysis. **A**, HEK293T cells were transfected with either vector (-) or CFP-Rit2 (+), and cell lysates were assessed by immunoblot 48 h post-transfection, probing with either αRit2 clones 27G2 (left) or 4B5 (right), as described under "Experimental procedures." Molecular mass markers indicate kDa. **B**, HEK293T cells transfected with vector (-) or HA-Rit2 (+), mouse ventral midbrain (vMB), and striatum (Str) were assessed by immunoblotting, probing with either αHA (left) or αRit2 clone 4B5 (right). 10μg/lane and 100μg/lane were loaded for transfected cell lysates and mouse brain lysates, respectively. Arrowheads, Rit2-immunoreactive bands.

*Rit2 is required for PKC-stimulated, but not basal, DAT internalization*

In our original DAT-Rit2 study (Navaroli et al., 2011), we used shRNA to silence Rit2 in SK-N-MC cells and to test whether Rit2 is required for PKC-stimulated DAT downregulation. In light of our current findings that SK-N-MC cells do not appreciably express Rit2, we were prompted to 1) re-screen Rit2 targeted shRNAs, and 2) reassess whether Rit2 is required for PKC-stimulated DAT internalization in SK-N-DZ cells, which endogenously express Rit2. We screened several candidate human Rit2-directed shRNAs, and identified two shRNAs (shRit2-104 and -107) that significantly silenced CFP-hRit2 protein expressed in Neuro2a cells (Figure II.2A). Additionally, both shRit2-104 and -107 significantly silenced endogenous Rit2 mRNA expression in SK-N-DZ cells (Figure II.2B). We utilized shRit2-107 to ask whether Rit2 is required for PKC-stimulated DAT internalization in SK-N-DZ cells. Rit2-KD significantly blocked PKC-stimulated DAT endocytosis as compared to vector-transduced cells (Figure II.2C), consistent with a requisite role for Rit2 in PKC-stimulated DAT internalization. The ability of shRit2-107 to block PKC-stimulated DAT endocytosis was not likely due to off-target effects, as shRit2-107 did not decrease expression of *RIT1*, the closest homolog to Rit2 (Figure II.2D). To further ensure that shRit2-107 effects were specific, we repeated these studies with shRit2-104. Similar to our findings with shRit2-107, Rit2 silencing with shRit2-104 significantly blocked PKC-stimulated DAT internalization (Figure II.2E).

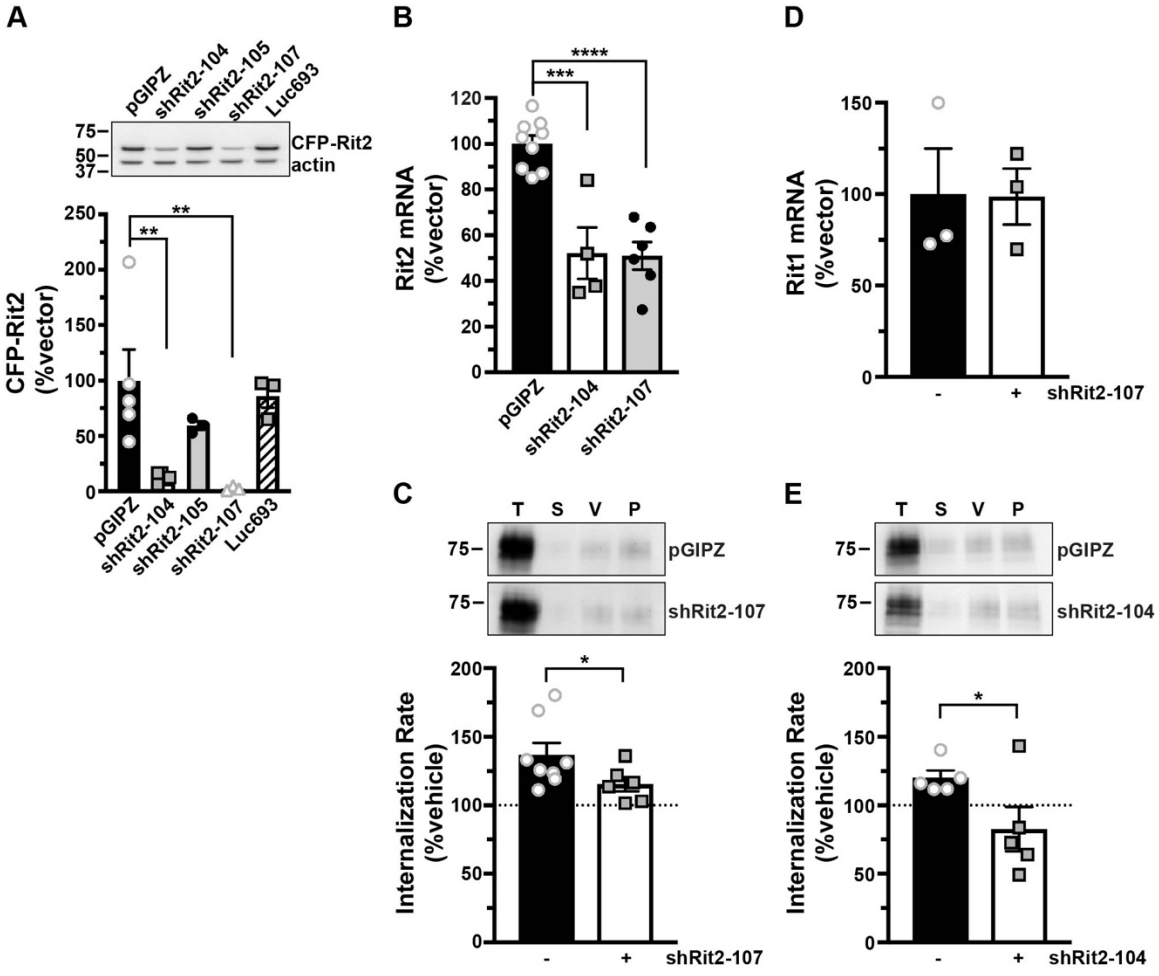


**Figure II.2 Rit2 is required for PKC-stimulated DAT internalization in SK-N-DZ cells. A**, human Rit2 shRNA screen. Mouse N2a cells were co-transfected with human CFP-Rit2 and either pGIPZ vector, luciferase-293 control, or the indicated Rit2 shRNA-pGIPZ plasmids. Top, representative immunoblots. Bottom, average CFP-Rit2 levels, normalized to actin-loading controls, expressed as percentage of pGIPZ vector ±S.E.M. (error bars). Asterisks, significant difference from pGIPZ controls (one-way ANOVA $F_{(4, 14)} = 6.396$, p=0.004; Dunnett's multiple-comparison test, pGIPZ versus shRit2-104: **p=0.005; versus shRit2-105: p=0.36; versus shRit2-107: **p=0.006; versus luc693: p=0.95, n=3-5). **B**, shRit2-mediated knockdown in stable DAT-SK-N-DZ cells. DAT-SK-N-DZ cells were transduced with control, shRit2-104, or shRit2-107 lentiviral particles, and Rit2 mRNA expression was measured by RT-qPCR 96 h post-transduction. Average $\Delta\Delta$Ct values are presented, expressed as percentage of control-transduced values ±S.E.M. Asterisks, significant difference from pGIPZ controls (one-way ANOVA

$F_{(2, 16)}$ = 25.09, p=0.0001; Dunnett's multiple-comparison test: pGIPZ versus shRit2-104: ***p=0.0001; versus shRit2-107: ****p<0.0001, n=4-9). **C**, DAT internalization assay. Stable DAT-SK-N-DZ cells were transduced with the indicated lentiviral particles, and DAT internalization rates were measured at 96 h post-transduction as described under "*Experimental procedures*." Top, representative immunoblots depicting surface DAT expression at t=0 (T), strip control (S), and internalized DAT during either vehicle (V) or 1 μM PMA (P) treatment. Bottom, average DAT internalization rates expressed as percentage of vehicle treated control rates ±S.E.M. *p=0.04, one-tailed Student's t test, n=6-8. **D**, Rit1mRNA expression specificity control. DAT-SK-N-DZ cells were transduced with control or shRit2-107 lentiviral particles, and Rit1 expression was measured by RT-qPCR 96 h post-transduction. Average ΔΔCt values are presented, expressed as percentage of control-transduced values ±S.E.M. shRit2-107 transduction did not significantly affect Rit1 mRNA expression, p=0.965, two-tailed Student's t test, n=3. **E**, DAT internalization assays. Stable DAT-SK-N-DZ cells were transduced with the indicated lentiviral particles, and DAT internalization rates were measured 96 h post-transduction as described under "*Experimental procedures*." Data are presented identically as in **C**. *p=0.03, one-tailed Student's t test, n=5.

*Rit2 is required for striatal steady state DAT surface expression and PKC-stimulated DAT internalization in a region- and sex-specific manner*

PKC-stimulated DAT internalization in response to phorbol ester treatment has been reported by numerous laboratories, in a variety of transfected cell lines (Daniels and Amara, 1999; Granas et al., 2003; Loder and Melikian, 2003; Holton et al., 2005; Sorkina et al., 2005; Cervinski et al., 2010; Sakrikar et al., 2012). Moreover, we previously reported that phorbol 12-myristate 13-acetate (PMA) treatment decreases DAT surface levels in DAergic terminals in *ex vivo* total striatal slices containing both dorsal (DS) and ventral (VS) striatum (Gabriel et al., 2013). However, it is unknown whether PKC-stimulated DAT internalization differs between DAergic terminal regions, such as DS and VS, or between males and females. Moreover, although Rit2 is required for PKC-stimulated DAT internalization in SK-N-DZ cells (Figure II.2), it is unknown whether Rit2 is required for PKC-stimulated DAT endocytosis in DAergic terminals. We recently leveraged the TET-OFF system to achieve conditional, inducible DAergic Rit2-KD in *Pitx3*$^{IRES2\text{-}tTA}$ mice, in which AAV9-shRit2 injection into mouse VTA significantly silenced *RIT2* expression in both VTA and SNc (Sweeney et al., 2020). We found that DAergic Rit2 silencing decreased total striatal DAT protein in males, but not females. Further, although total DAT protein decreased within male total striatum, the DAT surface:intracellular ratio was unchanged in either DS or VS, resulting in less overall surface DAT in both male striatal subregions (Sweeney et al., 2020). In the current study, we extended our *in vivo* Rit2-KD studies and asked whether

Rit2 impacts DAT basal distribution in female DS and VS. We further asked whether PKC-mediated DAT internalization requires Rit2 in male and female DS and VS. Male and female *Pitx3*$^{IRES2\text{-}tTA/+}$ mice VTA were bilaterally injected with either AAV9-TRE-eGFP or AAV9-TRE-shRit2, and DAT surface expression was measured by *ex vivo* slice biotinylation in the VS and DS, following treatment ±1μM PMA, 30 min, 37°C.

We first examined the effect of Rit2 silencing on DAT surface expression in female DS and VS, under both basal and PKC-stimulated conditions. Surprisingly, in DS, PKC activation did not decrease DAT surface expression in control female mice (Figure II.3A). Moreover, DAergic Rit2-KD had no effect on DS DAT surface expression, under either basal or PKC-stimulated conditions (Figure II.3A). In contrast, in female VS, PKC activation significantly reduced DAT surface levels, and DAergic Rit2-KD completely blocked further surface loss in response to PKC activation (Figure II.3B). Moreover, DAergic Rit2-KD significantly reduced the basal DAT surface level in female VS, as compared with control mice (Figure II.3B).

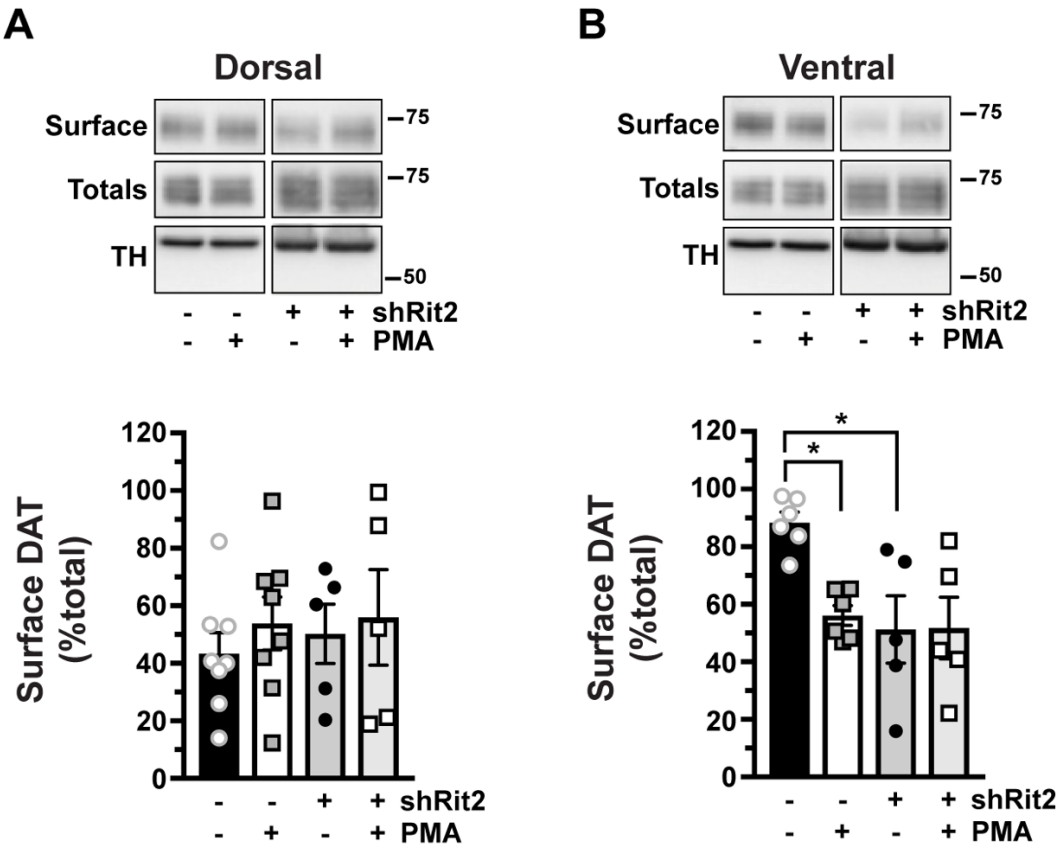


**Figure II.3 PKC-induced DAT internalization in females is limited to ventral striatum and requires Rit2.** Conditional Rit2 silencing in DA neurons and *ex vivo* striatal slice biotinylation. Female *Pitx3*$^{IRES2\text{-}tTA/+}$ mouse VTA were bilaterally injected with either AAV9-TRE-eGFP or -shRit2. Brains were harvested 4-5 weeks postinjection, and DAT surface expression was measured in *ex vivo* striatal slices by surface biotinylation as described under "*Experimental procedures*," following treatment with or without 1 μM PMA for 30 min at 37 °C. Representative blots are shown in the top of each panel, and average data are presented at the bottom of each panel. DAT surface levels are expressed as percentage of total DAT ±S.E.M. (error bars), n=5-8 slices from n=3 independent mice/virus. **A**, Dorsal striatum. Neither PKC activation nor Rit2-KD had an effect on DAT surface expression (two-way ANOVA: interaction: $F_{(1, 22)} = 0.051$, p=0.82; drug: $F_{(1, 22)} = 0.58$, p=0.46; virus: $F_{(1, 22)} = 0.18$, p=0.68). **B**, Ventral striatum. PKC activation and Rit2-KD significantly decreased DAT surface expression, and Rit2-KD blocked PKC-stimulated DAT internalization (two-way ANOVA: interaction: $F_{(1, 18)} = 4.54$, p=0.047; drug: $F_{(1, 18)} = 4.25$, p=0.054; virus: $F_{(1, 18)} = 7.28$, p=0.015. Sidak's multiple comparisons test:

eGFP(veh) versus eGFP(PMA): *p=0.04; eGFP(veh) versus shRit2(veh): *p=0.02; shRit2(veh) versus shRit2(PMA): p>0.99).

Our previous study probed the impact of DAergic Rit2 KD on basal DAT surface levels in males (Sweeney et al., 2020). Therefore, we next asked whether Rit2 was required for PKC-stimulated DAT internalization in male DS and VS. Similar to females, PKC activation had no effect on DAT surface expression in DS, but significantly decreased DAT surface expression in VS, measured in control (eGFP-injected) male mice (Figure II.4A). Also similar to females, DAergic Rit2-KD completely abolished PKC-stimulated DAT internalization in male VS (Figure II.4B). Given that phorbol esters can stimulate a variety of signaling pathways in addition to PKC, we further tested whether PMA-induced DAT internalization in VS was PKC-mediated. Pre-treatment with the PKC-specific inhibitor bisindolylmaleimide I (BIM I; 1μM, 15 min, 37°C) significantly abolished PMA-induced DAT internalization, and treatment with BIM I alone was not significantly different from BIM I/PMA (Figure II.4C), clearly demonstrating that PMA-mediated DAT internalization in DAergic terminals is PKC-dependent.

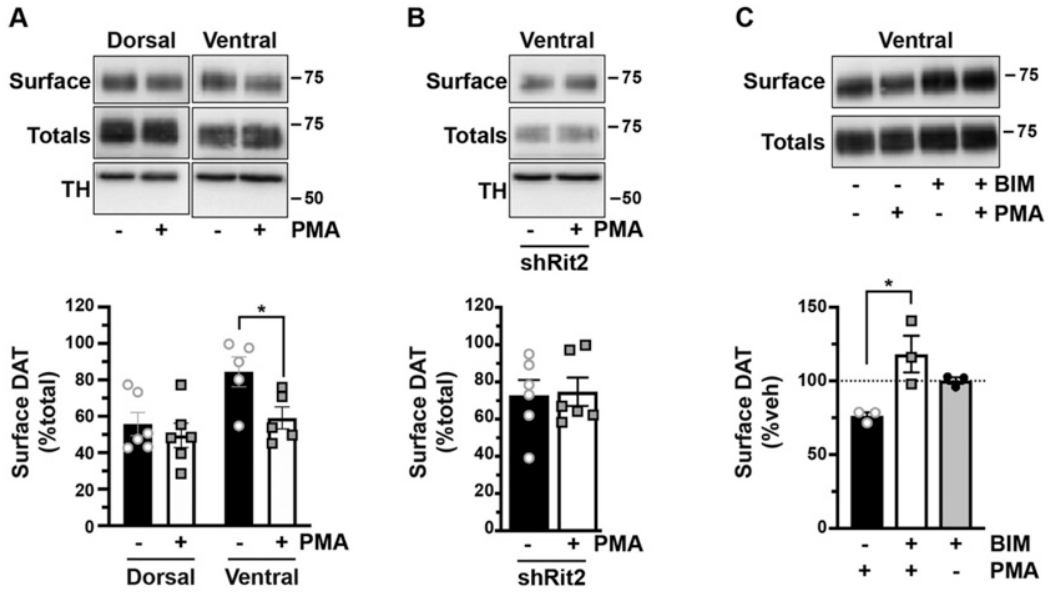


**Figure II.4 PKC-induced DAT internalization in males is limited to ventral striatum and requires Rit2.** Conditional Rit2 silencing in DA neurons and *ex vivo* striatal slice biotinylation. Male *Pitx3*$^{IRES2\text{-}tTA/+}$ mouse VTA were bilaterally injected with either AAV9-TRE-eGFP or -shRit2. Brains were harvested 4–5 weeks postinjection, and DAT surface expression was measured in ex vivo striatal slices by surface biotinylation as described under "*Experimental procedures*," following treatment with or without 1μM PMA for 30 min at 37 °C. Representative blots are shown in the top of each panel, and average data are presented at the bottom of each panel. **A**, effect of PKC activation on DAT surface levels in dorsal versus ventral striatum. DAT surface levels were measured in AAV9-TREeGFP–injected mice and are expressed as percentage of total DAT ±S.E.M. (error bars) PKC activation had no effect on DAT surface expression in dorsal striatum but significantly decreased DAT surface levels in ventral striatum (two-way ANOVA: interaction: $F_{(1, 18)} = 1.96$, p=0.18; region: $F_{(1, 18)} = 7.76$, p=0.01; drug: $F_{(1, 18)} = 5.30$, p=0.03. Sidak's multiple-comparison test (vehicle versus PMA): dorsal: p=0.76; ventral: p=0.043, n=5-6 slices from three independent mice. **B**, Rit2-KD significantly blocked PKC-stimulated DAT internalization in ventral striatum (shRit2: p=0.86, two-tailed Student's *t* test, n=6 slices from three independent mice). **C**, PMA-induced DAT internalization is PKC-mediated. DAT surface expression was measured in *ex vivo* VS slices prepared from C57Bl/6J mice and pretreated with or without 1μM BIM I for 15 min at 37 °C prior to PMA treatment as described above. DAT surface levels are expressed as percentage of vehicle ±S.E.M. BIM I pretreatment significantly abolished PMA-mediated DAT surface

loss (one-way ANOVA $F_{(2, 6)} = 8.08$, $p=0.02$; Sidak's multiple comparison test, PMA versus BIM/PMA: *$p=0.01$, BIM/PMA versus BIM: $p=0.25$, $n=3$ independent mice/condition).

*Releasing the PKC-sensitive DAT endocytic brake drives DAT-Rit2 dissociation at the plasma membrane*

We next sought to decipher the molecular mechanisms by which Rit2 impacts DAT trafficking. We first asked whether driving DAT internalization, by disengaging the PKC-sensitive DAT endocytic brake, impacts the DAT-Rit2 interaction at the plasma membrane. To specifically interrogate the DAT surface population and its associated protein complex, we leveraged a bungarotoxin binding site (BBS)-targeted surface labeling strategy (Sekine-Aizawa and Huganir, 2004; Wilkins et al., 2008; Yang et al., 2010) to label DAT in intact cells. We engineered a BBS into the DAT extracellular loop 2, a site we previously successfully targeted for bio-orthogonal DAT labeling (Wu et al., 2017), and which also tolerates an HA epitope (Sorkina et al., 2006). BBS-DAT expressed and functioned comparably to WT DAT, and PKC activation acutely decreased BBS-DAT function to 67.97 ± 5.9% control levels (Figure II.5A), which is comparable with PKC-mediated DAT downregulation as previously reported by our group and others (Granas et al., 2003; Gorentla and Vaughan, 2005; Navaroli et al., 2011; Bermingham and Blakely, 2016; Wu et al., 2017). We first tested whether BBS-DAT could 1) specifically isolate surface DAT via bungarotoxin labeling and pulldown, and 2) recover DAT-associated proteins. HEK293T cells expressing HA-Rit2 and either BBS-DAT or WT DAT were incubated with $\alpha$-BTX-b, and DAT surface complexes were isolated from cell lysates by streptavidin pulldown. We specifically recovered BBS-DAT, but not WT DAT, following $\alpha$-BTX-b incubation (Figure II.5B),

demonstrating the selectivity of the BBS pulldown approach to label and isolate surface BBS-DAT. Importantly, Rit2 was recovered from pulldowns with BBS-DAT, but not in control pulldowns from cells expressing WT DAT, demonstrating that Rit2 is recovered specifically following surface DAT pulldown. Additionally, BBS-DAT pulldowns did not recover the Rit2 homolog, Rit1 (Figure II.5C), consistent with a specific association between DAT and Rit2. We further asked whether other proteins required for PKC-mediated brake release are also part of the DAT surface complex. We previously reported that the nonreceptor tyrosine kinase, Ack1 (TNK2) imposes the PKC-sensitive endocytic brake, and that PKC-mediated Ack1 inactivation is required for PKC-stimulated DAT internalization (Wu et al., 2015). However, it is not known whether Ack1 is associated with DAT at the plasma membrane. Following $\alpha$-BTX-b labeling and pulldown, Ack1 was recovered from cells expressing BBS-DAT, but not from control cells expressing WT DAT (Figure II.5D), demonstrating that Ack1 is part of the DAT surface complex. Thus, BBS-DAT has precise utility to interrogate surface DAT and its associated proteins, such as Rit2 and Ack1.

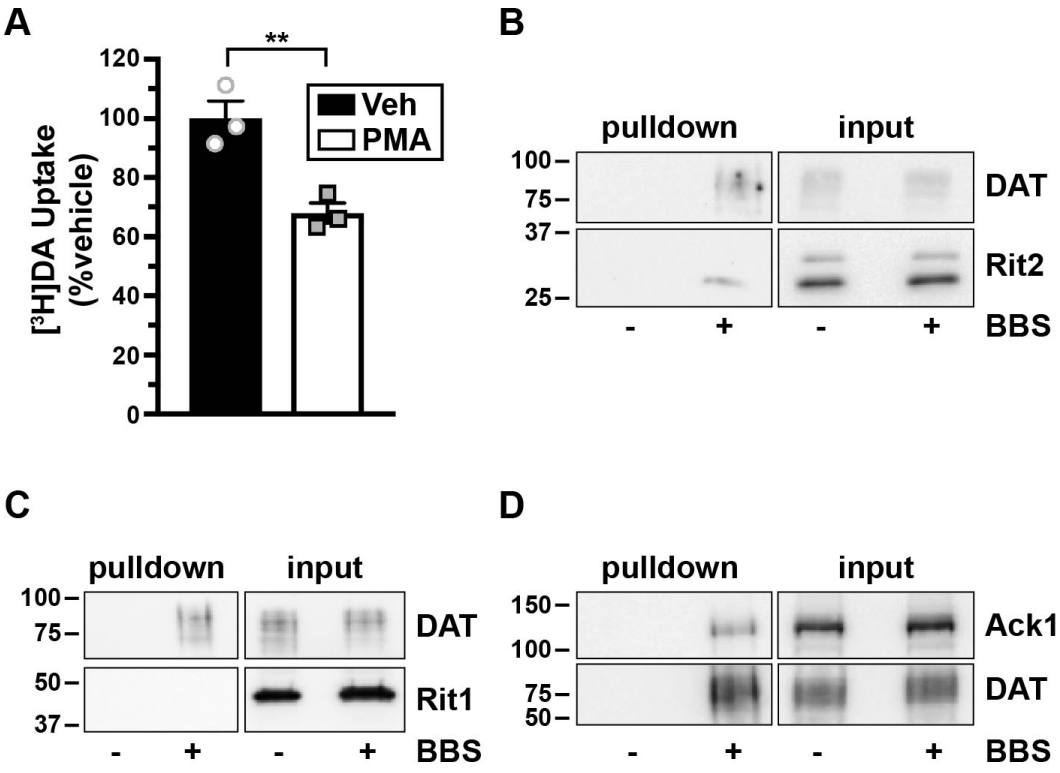


**Figure II.5 Surface DAT associates with Rit2 and Ack1, but not Rit1. A**, [$^3$H]DA uptake assay. SK-N-MC cells expressing BBS-DAT were treated with or without 1 μM PMA for 30 min at 37 °C, and [$^3$H]DA uptake was measured as described under "*Experimental procedures*." Average data are expressed as percentage of vehicle-treated specific [$^3$H]DA uptake ±S.E.M. (error bars). **p=0.009, two-tailed Student's t test, n=3. **B-D**, BBS-DAT pulldowns. HEK293T cells were co-transfected with DAT (with or without BBS tag) and either HA-Rit2 (**B**), GFP-Rit1 (**C**), or Ack1-HA (**D**), and DAT surface complexes were labeled and isolated by streptavidin pulldown as described under "*Experimental procedures*." Representative immunoblots for pull-downs (left panels) and their respective inputs (one-fourth of total input, right panels) are presented (n=3 independent experiments).

Given our previous cellular imaging results (Navaroli et al., 2011), we hypothesized that PKC activation causes DAT and Rit2 to dissociate. Since PKC-stimulated DAT internalization can only occur when the endocytic brake is disengaged, we first leveraged BBS-DAT pulldowns to ask whether PKC-mediated brake release alters the DAT-Rit2 surface association. PKC activation (1μM PMA, 30 min, 37°C) significantly decreased the DAT-Rit2 plasma membrane association (Figure II.6A). Additionally, DAT and Rit2 significantly dissociated when we directly released the DAT endocytic brake, by inactivating Ack1 with AIM-100 (20μM, 30 min, 37°C) (Figure II.6B). DAT and Rit2 may specifically dissociate at the cell surface in response to releasing the PKC-sensitive endocytic brake, or may do so following any stimulus that drives DAT internalization. To discern between these two possibilities, we measured the DAT-Rit2 surface association in response to AMPH treatment, which also accelerates DAT internalization, but is Rho-dependent (Wheeler et al., 2015). In contrast to PKC-stimulated DAT-Rit2 dissociation, AMPH treatment (10μM, 30 min, 37°C) significantly increased the DAT-Rit2 surface association (Figure II.6C). Thus, the DAT-Rit2 surface dissociation occurs specifically when the PKC-sensitive DAT endocytic brake is disengaged, either in response to PKC activation or direct Ack1 inactivation, but is not a general result of accelerated DAT endocytosis.

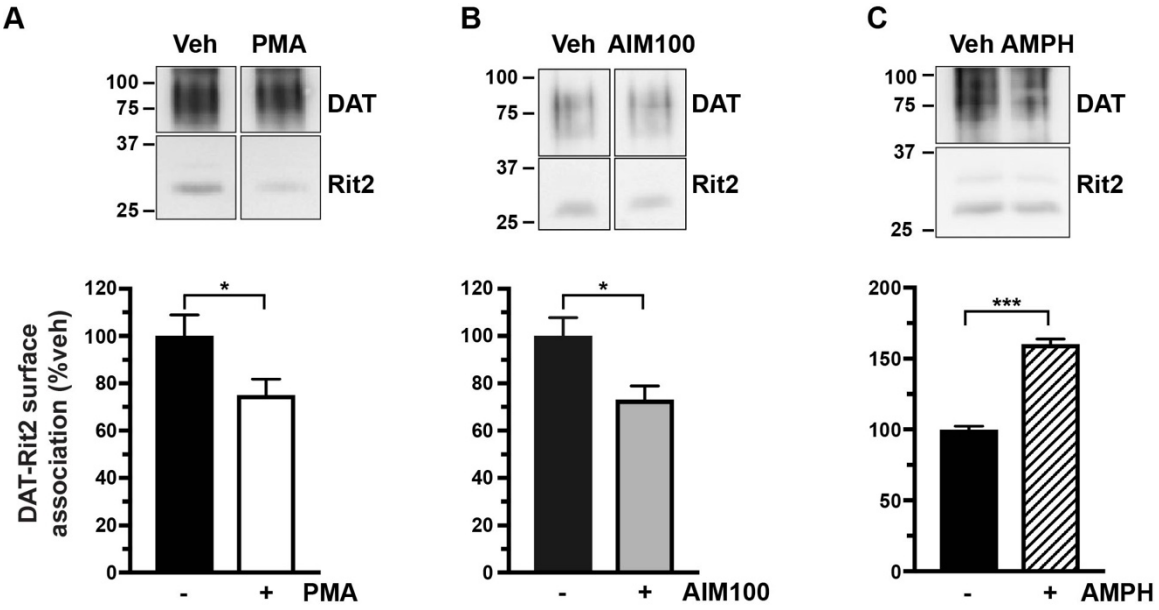


**Figure II.6 PKC-mediated endocytic brake release drives DAT-Rit2 dissociation at the plasma membrane.** For BBS-DAT pull-downs, HEK293T cells were co-transfected with BBS-DAT and HA-Rit2, were treated with or without the indicated drugs for 30 min at 37 °C, and were labeled with α-BTX-b, and DAT surface complexes were isolated as described under "*Experimental procedures*." Top, representative immunoblots. Bottom, average DAT-Rit2 association expressed as percentage of vehicle-treated control ±S.E.M. (error bars), assessed by two-tailed Student's t test. **A**, PKC activation significantly decreased the DAT-Rit2 surface association. *p=0.04, n=6. **B**, Ack1 inactivation with AIM-100 decreased the DAT-Rit2 surface association. *p=0.03, n=4. **C**, AMPH treatment significantly increased DAT-Rit2 surface association. ***p=0.0002, n=3.

*The DAT amino terminus is integral to the DAT-Rit2 interaction and PKC-stimulated dissociation*

The DAT-Rit2 interaction was originally identified in a yeast two-hybrid screen, using DAT C-terminal residues 587-596 (FREKLAYAIA) as bait (Navaroli et al., 2011). However, it is not known which DAT domains are required (or sufficient) for the DAT-Rit2 association in the context of intact DAT protein; nor is it known whether any DAT domains are specifically required for PKC-stimulated DAT-Rit2 dissociation. Rit2 specifically binds DAT, but not SERT (Navaroli et al., 2011); thus, we hypothesized that replacing DAT N- or C-termini with those of SERT may define DAT domains required for Rit2 binding and/or PKC-stimulated DAT-Rit2 dissociation. To test this possibility, we leveraged a series of DAT/SERT chimeras we previously characterized (Sweeney et al., 2017), in which either the DAT N-terminus, C-terminus, or both termini were substituted with those of SERT. HEK293T cells were co-transfected with YFP-Rit2 and CFP-tagged versions of these chimeras, and we performed live FRET imaging to quantify the chimera-Rit2 interactions. As we previously reported, control CFP-DAT and YFP-Rit2 elicited a significant FRET signal as compared with soluble YFP/CFP expression (Figure II.7A). Interestingly, replacing the DAT N-terminus with that of SERT (CFP-N-S/DAT) significantly increased the DAT-Rit2 interaction compared with CFP-DAT, whereas replacing the DAT C-terminus (CFP-DAT/C-S) or both termini (CFP-S/DAT/S) did not affect the DAT-Rit2 interaction (Figure II.7A). We also observed a significant increase in the interaction between YFP-Rit2 and CFP-N-S/DAT using

the donor recovery after photobleaching (DRAP) approach (Figure II.7B), demonstrating that the FRET signal is a *bona fide* interaction between the fluorophores. Using the BBS pulldown approach, Rit2 was likewise recovered with BBS-tagged versions of each DAT/SERT chimera (Figure II.7C). We next asked whether PKC-stimulated DAT-Rit2 dissociation requires either the DAT N- and/or C-termini. Substituting the DAT C-terminus with that of SERT (DAT/C-S) had no significant effect on PKC-stimulated DAT-Rit2 dissociation, as compared with WT DAT controls (Figure II.7D, one-way ANOVA with Dunnett's multiple comparison test, $p=0.69$). However, substituting the DAT N- terminus with that of SERT (N-S/DAT) completely abolished PKC-stimulated DAT/Rit2 dissociation, and there was a strong trend for attenuated DAT/Rit2 dissociation when both DAT N- and C-termini were replaced by SERT (S/DAT/S) (Figure II.7D, $p=0.058$). Taken together, these results indicate that the DAT N-terminus is required for the PKC-stimulated DAT-Rit2 dissociation, and that the SERT N-terminus does not suffice. However, SERT N- and C- termini suffice to maintain the DAT-Rit2 association.

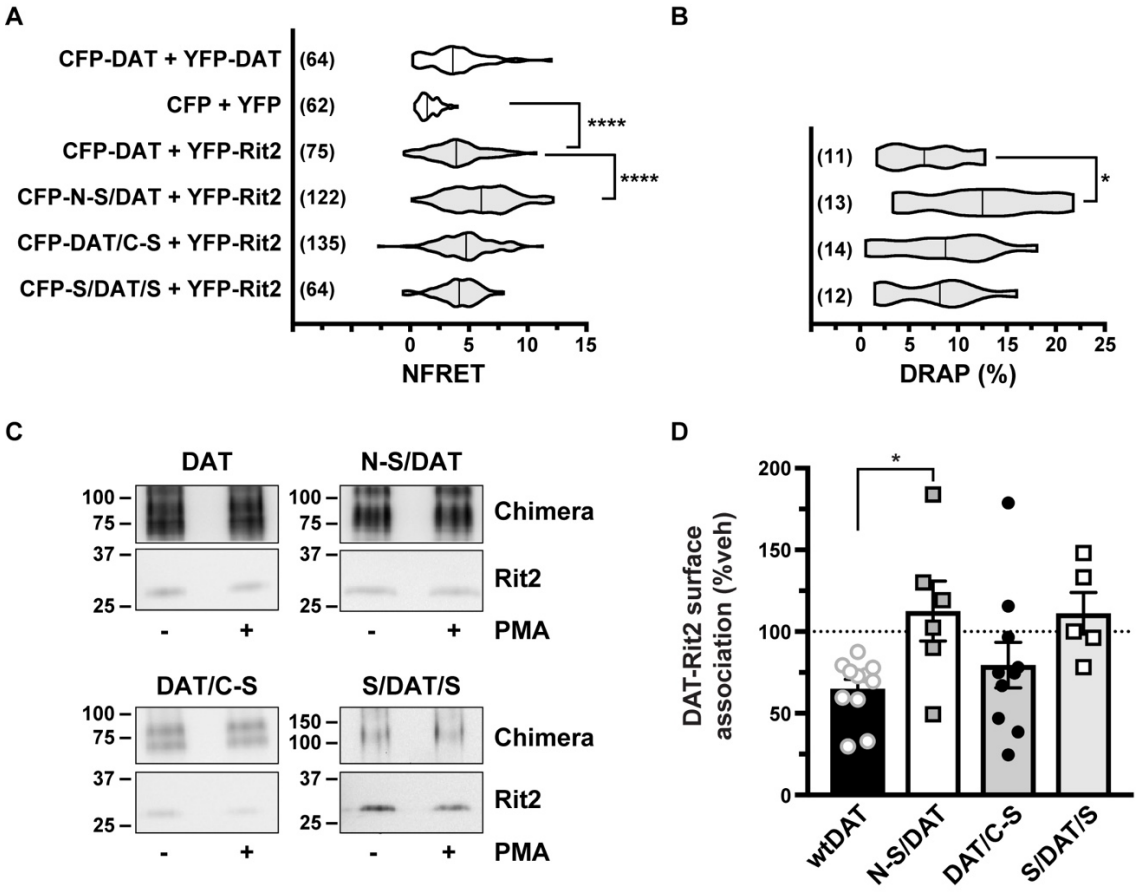


**Figure II.7 The SERT N-terminus promotes the DAT-Rit2 interaction and blocks PKC-stimulated DAT-Rit2 dissociation. A** and **B**, FRET studies. HEK293 cells were transfected with the indicated plasmids, and surface FRET measurements were made 24 h post-transfection, as described under "*Experimental procedures*." Average NFRET values (x100) for the indicated pairs are presented as violin plots, with median lines provided within each violin. n values are provided for each violin. **A**, NFRET values. Asterisks, significant differences between the indicated pairs (Kruskal–Wallis test, p=0.0001 with Dunn's multiple comparisons test: DAT versus N-S/DAT: ****p=0.0001; versus DAT/C-S: p=0.13; versus S/DAT/S: p>0.99; versus CFP/YFP: ****p=0.0001. **B**, DRAP values (one-way ANOVA $F_{(3, 46)} = 3.31$, p=0.028; Dunnett's multiple-comparison test: DAT versus N-S/DAT: *p=0.02; DAT/C-S: p=0.81; versus S/DAT/S: p=0.99). **C** and **D**, BBS-DAT pull-downs. HEK293T cells were co-transfected with HA-Rit2 and the indicated BBS-tagged proteins. Cells were treated with or without 1μM PMA for 30 min at 37 °C and surface-labeled with α-BTX-b, and DAT surface complexes were recovered by streptavidin pulldown as described under "*Experimental procedures*."

**C**, representative immunoblots. **D**, average data presented as percentage of vehicle-treated DAT-Rit2 association for each indicated protein. N-S/DAT significantly blocked PKC-stimulated DAT-Rit2 dissociation (one-way ANOVA $F_{(3, 28)} = 3.44$, $p=0.03$; Dunnett's multiple-comparison test: DAT versus N-S/DAT: *$p=0.03$; versus DAT/C-S: $p=0.69$; versus S/DAT/S: $p=0.06$, n=5-11). Error bars, S.E.M.

*The DAT N-terminus is required for PKC-stimulated DAT internalization*

Because the DAT N-terminus is required for PKC-stimulated DAT-Rit2 dissociation, this raised the possibility that the N-terminus may also be required for stimulated DAT internalization, driven by release of the DAT endocytic brake. To test these possibilities, we measured DAT and DAT/SERT chimera internalization rates in response to either PKC activation or direct Ack1 inactivation (with AIM-100) in stably-transfected SK-N-MC cells, in which we previously characterized both PKC- and AIM-100-stimulated DAT internalization (Gabriel et al., 2013; Wu et al., 2015). PKC activation (1μM PMA, 10 min, 37°C) significantly increased WT DAT internalization, and substituting the DAT C-terminus with the SERT C-terminus (DAT/C-S) did not significantly affect PKC-stimulated internalization (Figure II.8A). However, PKC-stimulated DAT internalization was abolished when either the DAT N-terminus, or both N- and C-termini, were substituted with SERT termini (N-S/DAT and S/DAT/S, Figure II.8A). In contrast, direct Ack1 inactivation (20μM AIM-100, 10 min, 37°C) significantly stimulated WT DAT, N-S/DAT, and DAT/C-S internalization, but had no effect on S/DAT/S internalization (Figure II.8A). We further evaluated the basal endocytic rates of the chimeric DATs, as compared with WT DAT. As presented in Figure II.8B, none of the chimera basal internalization rates differed significantly from WT DAT. To assure that these effects were not due to the lack of Rit2 expression in SK-N-MC cells, we further assessed basal and PKC-stimulated N-S/DAT internalization in stably transfected SK-N-DZ cells, which endogenously express *RIT2* (Table II.1). In SK-N-DZ cells,

N-S/DAT internalized significantly slower than WT DAT under basal conditions (Figure II.8C). Additionally, while PKC activation significantly increased the WT DAT internalization rate, it had no effect on N-S/DAT internalization as compared with its own vehicle control ($p=0.17$, one-way ANOVA with Bonferroni's multiple comparison test, $n=4-7$). These results demonstrate that the DAT N-terminus is required, and that the SERT N-terminus does not suffice, for PKC-stimulated DAT internalization.

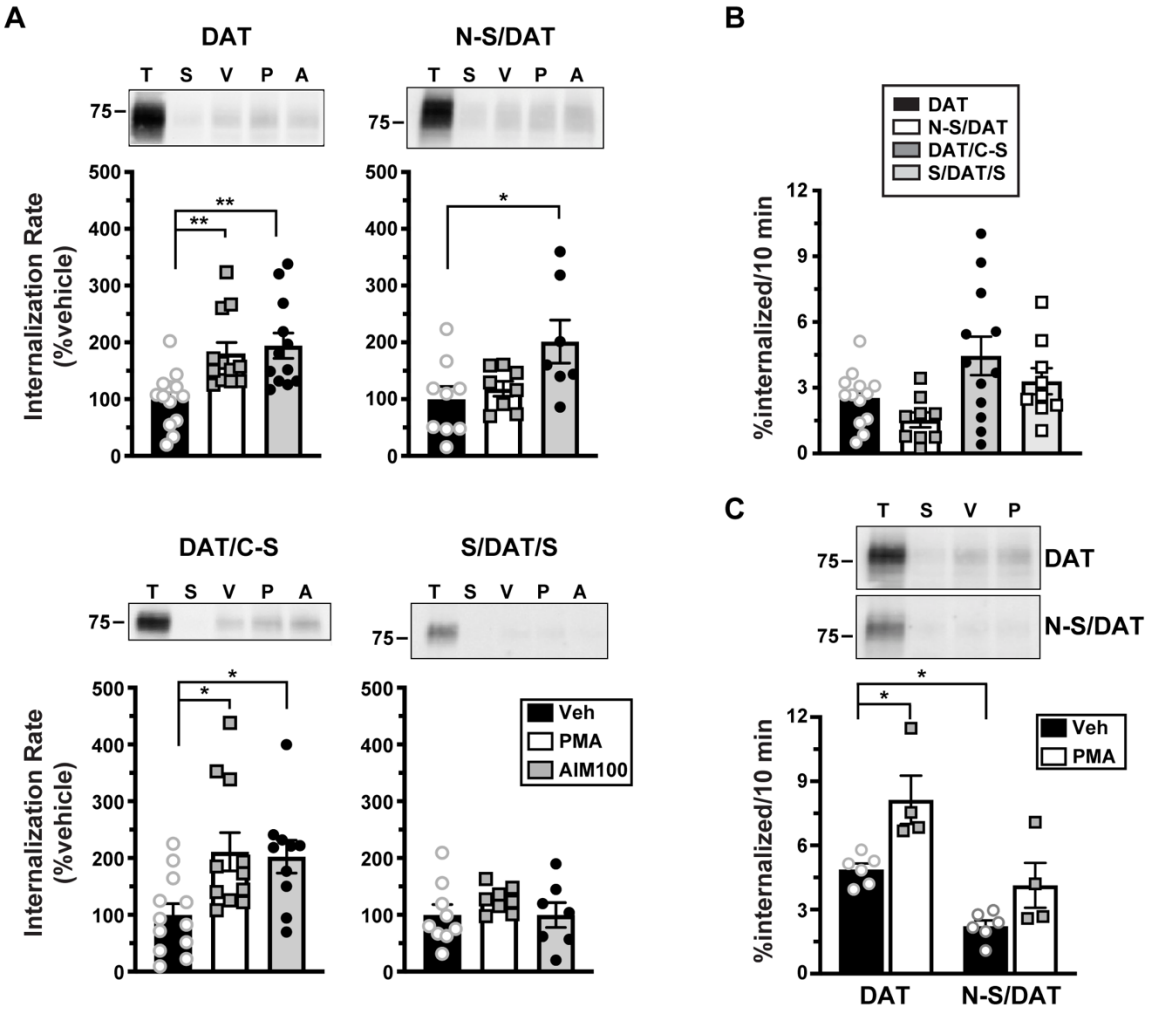


**Figure II.8 The DAT N-terminus is required for PKC-stimulated DAT internalization.** For DAT internalization assays, WT DAT and DAT/SERT chimera internalization rates were measured with or without 1 μM PMA or with or without 20 μM AIM-100 for 10 min at 37 °C, as described under "*Experimental procedures*." Top panels, representative immunoblots showing total surface expression at t=0 (T), strip control (S), and internalized protein during either vehicle (V), PMA (P), or AIM-100 (A) treatments. Bottom panels, averaged data. **A**, stimulated internalization in stable SK-N-MC cell lines. Rates are expressed as percentage of vehicle-treated controls ±S.E.M. (error bars). Asterisks, significant difference from vehicle controls (one-way ANOVA with Dunnett's multiple-comparison test, n=8 - 13; DAT: ANOVA $F_{(2, 34)} = 7.94$, p=0.0015; vehicle versus PMA: **p=0.007; vehicle versus AIM-100: **p=0.002; N-S/DAT: ANOVA $F_{(2, 21)} = 4.38$, p=0.03; vehicle versus PMA: p=0.82; vehicle versus AIM-100: *p=0.02; DAT/C-S: ANOVA $F_{(2, 30)} =$

5.22, p=0.01; vehicle versus PMA: *p=0.01; vehicle versus AIM-100: **p=0.026. S/DAT/S: ANOVA $F_{(2, 21)}$ = 0.84, p=0.44). **B**, basal internalization in stable SK-N-MC cell lines. Chimera basal internalization rates did not significantly differ from WT DAT (one-way ANOVA $F_{(3, 39)}$ = 4.046, p=0.013; Dunnett's multiple comparison test: DAT versus N-S/DAT: p=0.54; versus DAT/C-S: p=0.06; versus S/DAT/S: p=0.72, n=9-12). **C**, DAT and N/S-DAT internalization in stable SK-N-DZ cell lines. Average internalization rates are expressed as percentage of surface protein internalized/10 min ±S.E.M. Asterisks, significant difference from the indicated protein or treatment (two-way ANOVA: interaction: $F_{(1, 16)}$ = 1.06, p=0.32; construct: $F_{(1, 16)}$ =15.6, p=0.001; drug: $F_{(1, 16)}$ = 25.6, p=0.0001; Tukey's multiple-comparison test: DAT(veh) versus DAT(PMA): *p=0.01, DAT(veh) versus N-S/DAT(veh): *p=0.03; N-S/DAT(veh) versus N-S/DAT(PMA): p=0.21, n=4-7).

*Rit2 and Ack1 independently converge on DAT in response to PKC*

We next asked whether there is a mechanistic relationship between Rit2, Ack1, and PKC-mediated DAT endocytic brake release. Rit2 may be either upstream or downstream from Ack1 in the signaling cascade that leads from PKC to DAT. Alternatively, Rit2 and Ack1 may respond independently to PKC activation to stimulate DAT internalization. We first used Rit2-KD in SK-N-DZ cells to ask whether Rit2 was required for PKC-mediated Ack1 inactivation, a requisite step for PKC-mediated release of the endocytic brake and for stimulated DAT internalization (Wu et al., 2015). As we previously reported, in vector-transduced cells, PKC activation significantly reduced pY284-Ack1, to levels comparable with that achieved with the Ack1 inhibitor, AIM-100 (Figure II.9A). In cells transduced with shRit2-107, pY284-pAck1 levels, were also significantly reduced in response to either PKC activation or AIM-100 treatment, and there was no difference in the magnitude change of pY284-pAck1 levels following PKC activation (Figure II.9A). These results indicate that Rit2 is not likely upstream of Ack1 in the signaling pathway that leads from PKC to Ack1 inactivation.

We next asked whether PKC-mediated Ack1 inactivation is required for, and therefore upstream of, PKC-stimulated DAT-Rit2 dissociation. To test this possibility, we measured DAT-Rit2 dissociation in cells co-transfected with DAT, Rit2, and either vector or the PKC-insensitive, constitutively active Ack1 mutant (S445P) which we previously reported blocks PKC-stimulated DAT internalization

(Wu et al., 2015). In control cells, PKC activation drove a significant DAT-Rit2 dissociation (Figure II.9B). In cells co-transfected with S445P-Ack1, PKC activation likewise drove DAT-Rit2 dissociation, at levels indistinguishable from vector controls (Figure II.9B). These results demonstrate that PKC-stimulated DAT-Rit2 dissociation does not require Ack1 inactivation. Moreover, they demonstrate that even in conditions where DAT cannot internalize in response to PKC activation (i.e. because Ack1 is constitutively active), PKC activation still drives DAT and Rit2 to dissociate. Thus, PKC-stimulated DAT-Rit2 dissociation is likely to occur prior to Ack1-mediated release of the DAT endocytic brake.

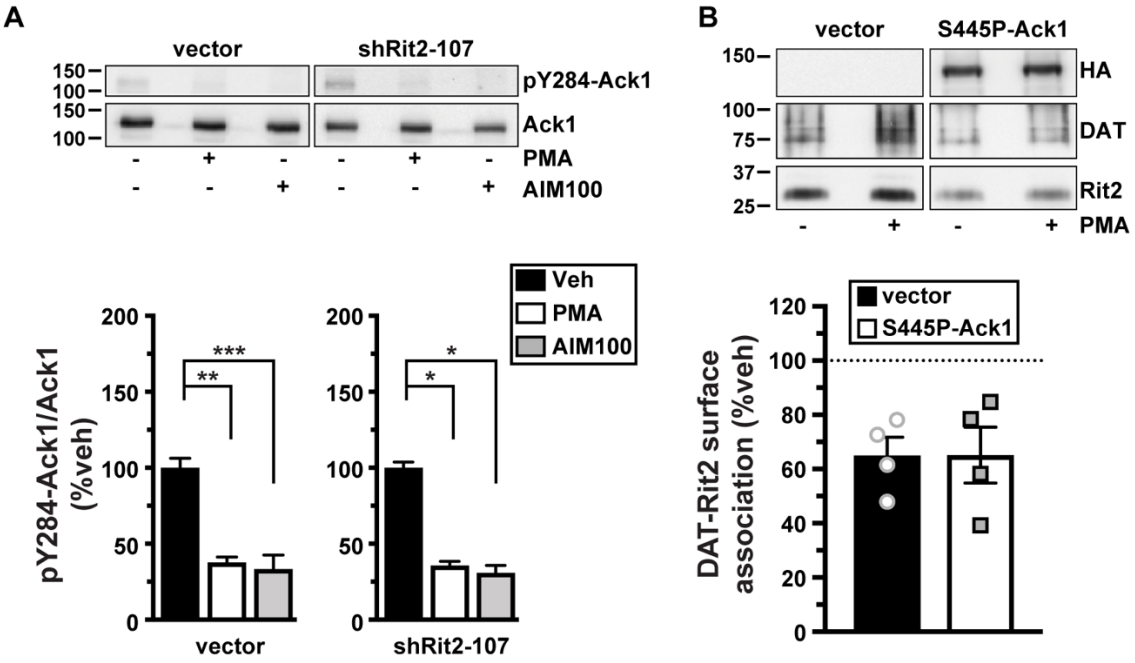


**Figure II.9 Rit2 and Ack1 independently converge on DAT downstream of PKC activation. A**, Effect of Rit2 silencing on PKC-mediated Ack1 inactivation. SK-N-DZ cells were transduced with lentiviral particles expressing either vector (pGIPZ) or shRit2-107 and were treated with or without 1 μM PMA or with or without 20 μM AIM-100 for 10 min at 37 °C. pY284-Ack1 and total Ack1 levels were measured from parallel lysate aliquots by immunoblot. Top, representative immunoblots. Bottom, average pY284-Ack1 levels expressed as percentage of vehicle-treated control cells ±S.E.M. (error bars). Asterisks, significant difference from vehicle-treated controls (one-way ANOVA with Dunnett's multiple-comparison test; vector: ANOVA$F_{(2, 12)}$ = 16.43, p=0.0004; vehicle versus PMA: **p=0.001; versus AIM-100: ***p=0.0004; shRit2-107: ANOVA $F_{(2, 9)}$ = 5.858, p=0.02; vehicle versus PMA: *p=0.03; versus AIM-100: *p=0.03, n=4-5). **B**, PKC-stimulated DAT-Rit2 dissociation. HEK293T cells were triple-transfected with BBS-DAT, HA-Rit2, and either empty vector or S445P-Ack1-HA. Cells were treated with or without 1 μM PMA for 30 min at 37 °C and labeled with α-BTX-b, and DAT complexes were recovered by streptavidin pulldown as described under "*Experimental procedures*." Top, representative immunoblots. Bottom, average DAT-Rit2 association expressed as percentage of vehicle-treated control ±S.E.M. p=0.99, two-tailed Student's t test, n=4.

## II.D Discussion

DAT is stabilized at the cell surface by a PKC-sensitive endocytic brake that requires 1) residues in both the DAT N- and C- termini to engage (Boudanova et al., 2008b; Sorkina et al., 2009), and 2) Ack1 inactivation to be released (Wu et al., 2015). Here, we found that Rit2 is required to release the PKC-sensitive DAT endocytic brake in cell lines and tissues where Rit2 is endogenously expressed, such as SK-N-DZ cells (Figure II.2C) and in VS (Figures II.3 and II.4), respectively. Curiously, over two decades of evidence has demonstrated that PKC activation stimulates DAT internalization in a wide range of cultured cell lines (Pristupa et al., 1998; Daniels and Amara, 1999; Melikian and Buckley, 1999; Sorkina et al., 2003; Sorkina et al., 2006), which our results demonstrate have negligible, if any, *RIT2* expression (Table II.1). Given that Ack1 is ubiquitously expressed, and that Rit2 and Ack1 converge independently on DAT in response to PKC activation (Figure II.9), we conclude that PKC-stimulated Ack1 inactivation can suffice to release the endocytic brake when DAT is heterologously expressed in a context that does not express Rit2. However, when DAT is expressed in its appropriate context (i.e. striatal terminals), Rit2 expression is absolutely required for PKC-stimulated DAT internalization, and PKC-mediated Ack1 inactivation alone does not suffice to release the endocytic brake (Figures II.3 and II.4). These results further suggest that although Rit2 and Ack1 independently converge on DAT in response to PKC activation in cell lines (Figure II.9), there may be an, as of yet, unidentified DAergic-

specific mechanism(s) that facilitates a Rit2/Ack1 interdependence required for endocytic brake release.

Our previous study using total (i.e. not subdissected) striatal slices found that PKC activation decreased DAT surface expression by ~20% (Gabriel et al., 2013). Interestingly, in the current study, PKC activation drove ~35% DAT surface loss in both male and female VS, but had no effect on DAT surface expression in DS from either sex (Figure II.3). These data suggest that the somewhat modest PKC-stimulated DAT surface loss detected in total striatum reflects robust DAT surface loss in VS, diluted by the lack of a net effect in DS. Is DAT endocytosis completely resistant to PKC activation in DS? It is currently unknown which PKC isoform(s) stimulate DAT internalization. We activated PKC with the phorbol ester PMA, which activates all diacylglycerol-sensitive PKC isoforms, including PKC$\alpha$, -$\beta$1, -$\beta$2, -$\gamma$, and -$\delta$. PKC$\beta$ activity is required for DRD2 receptor-mediated DAT insertion into the plasma membrane, and selective PKC$\beta$ activation rapidly delivers DAT to the cell surface in both cell lines and striatal synaptosomes (Chen et al., 2013). Thus, it is possible that in DS, Rit2-dependent, PKC-stimulated DAT internalization may be countered by PKC$\beta$-mediated DAT insertion, resulting in no detectable net change within the 30-min timeframe we tested. In contrast to DS, DAT surface levels in VS were significantly decreased in response to PMA treatment, suggesting that the balance between PKC$\beta$-mediated DAT insertion and Rit2-dependent DAT internalization may differ between DS and VS. A recent study by

Blakely and colleagues (Gowrishankar et al., 2018) further supports this premise, in which they reported that DRD2 activation increased DAT surface expression in the DS, but not VS. Given that few studies, to date, have identified the receptor-mediated signaling pathways that lead to PKC-stimulated DAT internalization, nor the temporal profile of DAT response to PKC activation in DAergic terminals, it remains unclear how DAT insertion and internalization balance may occur. Finally, although our current data indicate that Rit2-KD is required for PKC-stimulated DAT endocytosis in female and male VS, it is important to bear in mind that DAT basal surface expression in both male (Sweeney et al., 2020) and female (Figure II.3B) VS was reduced following DAergic Rit2-KD. Thus, there is a possibility that a general floor effect blocked PKC-mediated DAT internalization, rather than a requirement for Rit2. However, we do not believe that this is likely, as DAT is capable of undergoing additive degrees of internalization when cells are subjected to dual PKC activation and AMPH exposure (Hong and Amara, 2013).

We used an extracellular BBS tag to interrogate surface DAT and its associated protein complex. This approach was previously used successfully by several groups (Sekine-Aizawa and Huganir, 2004; Bogdanov et al., 2006; Wilkins et al., 2008), and has distinct advantages over co-IP approaches, since 1) the $\alpha$-BTX/BBS affinity is significantly higher than that of antibody/antigen interactions, and 2) $\alpha$-BTX/BBS binding is maintained in detergent lysates. Moreover, using an extracellular labeling approach, in general, maintains intracellular protein

complexes that might be disrupted using an intracellularly targeted antibody in lysates/solution. Interestingly, although we observed significant DAT-Rit2 dissociation in response to releasing the PKC-sensitive DAT endocytic brake (Figure II.6), AMPH-stimulated DAT internalization increased the surface DAT-Rit2 population. Surface DAT is distributed among several membrane microdomains (Adkins et al., 2007; Cremona et al., 2011; Navaroli et al., 2011; Butler et al., 2015; Kovtun et al., 2015; Rahbek-Clemmensen et al., 2017; Lebowitz et al., 2019; Thal et al., 2019). Moreover, we previously reported that, 1) PKC activation preferentially depletes DAT from cholera toxin-positive (CTX+) microdomains (Gabriel et al., 2013), and 2) there is significantly more DAT-Rit2 co-localization in CTX+ microdomains (Navaroli et al., 2011). Conversely, AMPH treatment increases DAT localization to CTX+ domains (Butler et al., 2015). Taken together, these results suggest that DAT may dissociate from Rit2 and internalize preferentially from CTX+ microdomains, in response to PKC activation. In contrast, AMPH potentially drives DAT internalization from CTX- domains, in which there is less DAT-Rit2 interaction, thereby leaving an enriched DAT-Rit2 population at the cell surface.

We originally identified the DAT-Rit2 interaction via a yeast two-hybrid screen using the C-terminal DAT domain “FREKLAYAIA” as bait, and FRET studies revealed that Rit2 directly interacts with DAT, but not SERT, at the plasma membrane (Navaroli et al., 2011). However, the domains required for the DAT-Rit2

interaction, and their requirement for either PKC-stimulated DAT internalization or DAT-Rit2 dissociation were not defined. To address these questions, we used a series of DAT/SERT chimeras previously reported by our lab (Sweeney et al., 2017), and found that the DAT N-terminus was required for PKC-stimulated DAT-Rit2 dissociation (Figure II.8). Indeed, under basal conditions, N-S/DAT and Rit2 interacted to a significantly higher degree than DAT-Rit2 controls (Figure II. 6), consistent with a lack of DAT-Rit2 dissociation for the N-S/DAT chimera and higher steady-state interaction. N-S/DAT also basally internalized significantly slower than WT DAT selectively in SK-N-DZ cells, consistent with its inability to disengage the endocytic brake. Moreover, DAT/C-S retained both Rit2 interaction and ability release the endocytic brake in response to PKC activation. This was surprising, given that 1) the DAT C-terminal bait (FREKLAYAIA) used to identify the DAT/Rit2 interaction is highly conserved across the SLC6 gene family (Holton et al., 2005; Boudanova et al., 2008b), and 2) full-length SERT does not interact with Rit2 (Navaroli et al., 2011). So, while the FREKLAYAIA domain is sufficient to interact with Rit2, its context within full-length DAT or SERT appears to dictate ultimate Rit2 binding potential. Interestingly, although N-S/DAT was resistant to PKC-stimulated internalization, it retained AIM-100-dependent internalization, whereas S/DAT/S did not (Figure II.8), indicating that the DAT N-terminus is not required for direct Ack1-dependent endocytic brake release, and further supports the hypothesis that Rit2 and Ack1 converge on DAT independently in response to PKC activation. It should also be noted that we, and others, reported that AIM-100 also

binds noncompetitively to DAT (Wu et al., 2015; Sorkina et al., 2018), and recent reports suggest that AIM-100 can enhance DAT surface oligomerization (Sorkina et al., 2018; Cheng et al., 2019). Since both Ack1-dependent and AIM-100-stimulated internalization are specific for DAT, and not SERT, it is possible that S/DAT/S endocytic resistance to AIM-100 may be because the substituted SERT domains perturb the DAT/AIM-100 interaction. Likewise, it is possible that the ability of N-S/DAT to internalize in response to AIM-100, but not PKC activation, may be due to a direct AIM-100 effect on DAT.

In this study we present one of the first descriptions of region- and sex-dependent differences in DAT trafficking regulation. Furthermore, we greatly extend our knowledge of the mechanisms by which Rit2 governs DAT surface expression in *bona fide* DAergic terminals. Future studies that examine the cell autonomous endogenous signaling events that drive striatal DAT trafficking, and require Rit2, will shed further light on mechanisms that influence DA clearance and DA-dependent behaviors.

## II.E Experimental Procedures

### *Materials*

Phorbol 12-myristate 13-acetate (PMA) was from LC Laboratories (P-1680). GF 109203X (Bisindolylmaleimide I, BIM I) and AIM-100 were from Tocris-Cookson.

All other reagents were from either Sigma-Aldrich or Fisher Scientific, and were of the highest possible grade.

### *Animals*

All studies were conducted in accordance with UMASS Medical School IACUC Protocol A-1506 (H.E.M). *Pitx3*$^{IRES2\text{-}tTA}$ mice on the *C57Bl/6* background were the generous gift of Dr. Huaibin Cai (National Institute on Aging), and were continually backcrossed to *C57Bl/6* mice. Mice were maintained in 12hr light/dark cycle at constant temperature and humidity and food and water were available ad libitum.

### *Antibodies*

Primary antibodies used: mouse anti-Rit2 18G4 (27G2; Sigma), mouse anti-Rit2 4B5 (GTX83711, GeneTex), rat anti-DAT (MAB369), mouse anti-SERT (ST51-2; Mab Technologies), rabbit anti-HA (C29F4; Cell Signaling Technology), mouse anti-GFP (Roche), mouse anti-Ack1 (A-11; sc-28336), and rabbit anti-pY284-Ack1 (Millipore). Horseradish peroxidase-conjugated secondary antibodies: goat anti-rat, goat anti-mouse and goat anti-rabbit were from Jackson ImmunoResearch.

### *Plasmids and cloning*

N-S/DAT (SERT1-78/DAT60-620), DAT/C-S (DAT1-583/SERT601-630), and S/DAT/S (SERT1-78/DAT60-583/SERT601-630) plasmids, in which either the DAT N-terminus (N-S/DAT), C-terminus (DAT/C-S), or both termini (S/DAT/S)

were substituted with those of SERT, were generated as previously described (Sweeney et al., 2017) using PCR-ligation-PCR approach to clone the DAT or SERT terminal domains onto the hSERT or hDAT-pCDNA3.1(+) backbone. CFP-tagged chimeras were generated by cloning their cDNAs into the pECFP-C1 vector using HindIII/XbaI (N-S/DAT), HindIII (DAT/C-S), and HindIII/SalI (S/DAT/S). Bungarotoxin binding site (BBS)-tagged hDAT and DAT chimera constructs were generated using the extracellular tagging strategy as previously described (Wu et al., 2017) with the following amino acid sequence inserted into extracellular loop 2 of hDAT and DAT chimera constructs: GSSGSSGWRYYESSLEPYPDGSSGSSG. The underlined BBS is flanked by linker sequences. All plasmids were verified by Sanger sequencing (Genewiz). Human constitutively active Ack1 mutant (S445P-Ack1-HA) was generated as previously described (Wu et al., 2015).

***AAV production and stereotaxic viral delivery***

pscAAV-TRE-eGFP and pscAAV-TREmiR33-shRit2-eGFP plasmids were generated as previously described (Sweeney et al., 2020), and AAV particles (AAV9 serotype) were produced, purified, and titers determined by the University of Massachusetts Medical School Viral Vector Core, as previously described (Mueller et al., 2012). For intracranial stereotaxic AAV injections, male and female mice (minimum 3 weeks age) were anesthetized with 100mg/kg ketamine/10mg/kg xylazine (I.P.), and 20% mannitol was administered (I.P.) 15 minutes prior to viral delivery, to increase viral spread (Burger et al., 2005). Mouse heads were shaved,

placed in the stereotaxic frame, and bilateral 0.8mm holes were drilled into the skull at the indicated stereotaxic coordinates. 1µl of the indicated viruses were infused bilaterally into the VTA (Bregma: anterior/posterior: -3.08mm, medial/lateral: ±0.5mm, dorsal/ventral: -4.5mm) at a rate of 0.2µL/min. Syringes were left in place for a minimum of 5 minutes post-infusion prior to removal. Mice were housed for a minimum of four weeks before experiments were performed. Viral expression in each animal was confirmed by visualizing GFP expression in 0.3mm coronal ventral midbrain slices.

***Ex vivo slice biotinylation***

*Ex vivo* striatal slices were prepared 4-5 weeks following viral injection in *Pitx3*$^{IRES2\text{-}tTA/+}$ mice (for Rit2 KD studies), or from 5-7 week old C57Bl/6J (for PKC specificity studies). Mice were sacrificed by cervical dislocation and rapid decapitation and heads were immediately submerged in ice cold, oxygenated cutting solution, pH 7.4 (in mM: 20 HEPES, 2.5 KCl, 1.25, $NaH_2PO_4$, 30 $NaHCO_3$, 25 glucose, 0.5 $CaCl_2{\cdot}4H_2O$, 10 $MgSO_4{\cdot}7H_2O$, 92 N-methyl-D-glucamine (NMDG), 2.0 thiourea, 5.0 $Na^+$-ascorbate, 3.0 $Na^+$-pyruvate) for 1 min. Brains were removed and 300µm coronal slices were prepared with a VT1200 Vibroslicer (Leica) in ice-cold, oxygenated cutting solution. Slices were hemisected along the midline, and were recovered in ACSF, pH 7.4 (in mM: 125 NaCl, 2.5 KCl, 1.24, $NaH_2PO_4$, 26 $NaHCO_3$, 11 glucose, 2.4 $CaCl_2{\cdot}4H_2O$, and 1.2 $MgCl_2{\cdot}6H_2O$) 40 min, 31°C. Hemi-slices were treated ±1µM PMA in ACSF, 30min, 37°C with constant oxygenation,

using their contralateral hemi-slice as a vehicle-treated control. Following drug treatment, slices were moved to ice and surface DAT was labeled by biotinylation as previously described (Gabriel et al., 2013; Wu et al., 2015; Sweeney et al., 2020). Briefly, slices were biotinylated with membrane-impermeant sulfo-NHS-SS-biotin (1mg/ml), 45min, 4°C. Residual biotin was quenched 2x 20 min washes of ice-cold ACSF supplemented with 100mM glycine, and were washed with ice-cold ACSF. Hemi-slices were enriched for dorsal and ventral striatum, by sub-dissecting in a line from the anterior commissure to the lateral olfactory tract.

Sub-dissected slices were lysed in RIPA buffer containing protease inhibitors, and tissue was disrupted by triturating sequentially through a 200µL pipet tip, 22G and 26G tech-tips. Samples rotated 30min at 4°C to complete lysis, insoluble material was removed by centrifugation, and protein concentrations were determined using the BCA protein assay. Biotinylated proteins were isolated by batch streptavidin chromatography, overnight with rotation, 4°C, at a ratio of 20µg striatal lysate to 30µL streptavidin agarose beads, which was empirically determined to recover all biotinylated DAT. Recovered proteins were washed with RIPA buffer and eluted from beads in 2X SDS-PAGE sample buffer, 30min, room temperature with rotation. Eluted (surface) proteins and their respective lysate inputs were resolved by SDS-PAGE, and DAT was detected by immunoblotting as described above. %DAT at the cell surface was calculated by normalizing surface signals to the corresponding total DAT input signal in a given hemi-slice, detected in parallel.

Note that all slice data for Rit2-KD experiments in the current study were acquired during the course of our previous study, in which we first achieved AAV-mediated Rit2 KD (Sweeney et al., 2020). Basal DAT surface levels in vehicle-treated male slices were compared and reported in that study, and thus were not re-analyzed for the current study. However, the DAT surface levels from vehicle-treated male hemislices were reused in the current study as controls to determine whether PMA treatment affected DAT surface levels in contralateral hemi-slices. Rit2 knockdown in females was confirmed by RT-qPCR (Figure S1c of previous study (Sweeney et al., 2020)). For males, successful viral expression (AAV9-eGFP and AAV9-eGFP-shRit2) was confirmed by visual detection of GFP reporter immunofluorescence in midbrain slices from each experimental animal. For PKC specificity studies, data were reported as %change in DAT surface levels in drug-treated hemislices, normalized to their vehicle-treated, contralateral hemi-slices.

***Cell Culture and transfection***

Cells were maintained at 37°C, 5% CO2. SK-N-MC cells were grown in MEM (Sigma), and HEK293T, HEK293 (FRET studies) and N2a cells were grown in DMEM (CellGro/Corning), each supplemented with 10% fetal bovine serum, 2mM glutamine, and 100 units/mL penicillin-streptomycin. SK-N-DZ cells were grown in DMEM (ATCC #30-2002) supplemented with 10%FBS, 1X non-essential amino acids (Gibco) and 100u/mL penicillin-streptomycin. HEK293T cells were transfected using Lipofectamine 2000 (Invitrogen) according to manufacturer's

instructions with the following modifications: For biochemical and RT-qPCR studies, cells were seeded into 6-well plates at a density of $1x10^6$ (SK-N-MC), $5x10^5$ (HEK293T), or $2.5x10^5$ (N2a) cells/well one day prior to transfection, and were transfected with 3µg (SK-N-MC) or 2µg (HEK293T and N2a) plasmid DNA/well using a lipid:DNA ratio of 2:1 (SK-N-MC and HEK293T) or 4:1 (N2a). Stable cell lines were generated by selecting cells starting 48 hrs following transfection, with 0.5 mg/mL (SK-N-MC) or 0.8 mg/L (SK-N-DZ) G418 (Geneticin, Invitrogen/Life Technologies). Stably transfected cells were pooled and cell lines were maintained under selective pressure using 0.2 mg/mL or 0.32 mg/mL G418 for SK-N-MC and SK-N-DZ cells, respectively. For FRET imaging studies, HEK293 cells were seeded into an 8-well chambered coverslip (ibidi) at a density of $2x10^4$ cells/well one day prior to transfection, and were transfected with the indicated plasmids using JetPRIME (Polyplus-transfection) according to the manufacturer's protocol. FRET studies were performed 24 hrs post-transfection.

***shRNA, Lentiviral production and cell transduction***

GIPZ lentiviral shRNA constructs targeted to Rit2, and empty pGIPZ vector control, were obtained from Dharmacon. Tested shRNA clone ID's and mature antisense sequences were as follows:

shRit2-104: V3LHS_380104; CTTCTTCTTCAAAGAACCT

shRit2-105: V3LHS_380105; TTGTTACCCACCAGCACCA

shRit2-107: V3LHS_380107; CTTCTTCTTCAAAGAACCT

Lentiviral particles were produced in HEK293T cells as previously described (Wu et al., 2015). For cell transduction, $1x10^6$ cells DAT-SK-N-DZ cells were seeded onto 6-well plates and were transduced with 3.0mL of lentiviral supernatant, supplemented with 0.8µg/mL polybrene, 16-24 hours post-seeding. Cells were selected for transduction beginning 24 hours post-infection (72 hrs total) with SK-N-DZ media supplemented with 1.25µg/mL puromycin. Assays were conducted 96 hrs post-transduction.

***FRET***

FRET was measured using an iMIC inverted microscope (TILL Photonics GmbH). Samples were focused using a 60X (N.A. 1.49) oil objective (Olympus). Fluorescence was excited using a 100 W Xenon Lamp (Polychrome, Till Photonics GmbH). Excitation light was filtered through either a 436/20 nm (CFP) or 514/10 nm (YFP) excitation filter (Semrock) and directed to the sample via a 442/514 dual line dichroic mirror (Semrock). Emitted fluorescence light was filtered through a 480/40 nm - 570/80 nm dual emission filter (Semrock) and directed to a beamsplitter unit (Dichrotom, Till Photonics). Briefly the emission light was separated spatially according to the fluorescence wavelength using a 515 nm dichroic mirror (Semrock). The resultant two channels (<515 nm & >515 nm) were projected next to each other onto an EMCCD chip (iXon Ultra 897Andor) and recorded using Live Acquisition software (version 2.5.0.21; TILL Photonics GmbH). To guarantee the best signal to noise ratio and dynamic range, the camera

was operated in 16-bit mode with a readout speed of 1 MHz. According to manufactories recommendation; an EM-Gain of 16 was applied to overcome the noise floor. To analyze FRET (see below) two images were taken per set (Donor excitation -> Donor Emission / Acceptor Emission and Acceptor Excitation -> Acceptor Emission respectively). Per condition ten sets were recorded each experimental day; the images were then analyzed using Offline Analysis software (version 2.5.0.2; TILL Photonics GmbH). One region of interest (part of the plasma membrane) per cell was selected in the CFP channel. Background fluorescence was subtracted from each image and the average intensity of each region of interest was used for calculations. Spectral bleed through (BT) for donor (0.57) and acceptor (0.04) was determined using HEK293 cells expressing a CFP or YFP signal only. Normalized FRET (NFRET) was calculated as follows:

$$\mathrm{NFRET} = \frac{I_{FRET} - (BT_{Donor} \times I_{Donor}) - (BT_{Acceptor} \times I_{Acceptor})}{\sqrt{I_{Donor} \times I_{Acceptor}}}\, x\, 100$$

A fused CFP-YFP construct (CYFP) was included as positive control, resulting in maximum FRET. Non-fused donor and acceptor fluorophores were included as a negative control. To confirm that the calculated NFRET values reflect bona fide FRET, donor (CFP) recovery after acceptor (YFP) photobleaching (DRAP) experiments were included to support the conclusion that the fluorophore-tagged proteins directly interact at the site of the photobleaching. Average acceptor photobleaching was 85±4% (mean ±SD).

***RNA extraction & RT-qPCR***

RNA was isolated from cell lines and rodent midbrain using RNAqueous®-Micro Kit RNA Isolation (Thermo Fisher Scientific). For ventral midbrain samples, 1.0 mm bilateral tissue punches, encompassing both the ventral tegmental area and substantia nigra par compacta, were taken from 300µm acute mouse and rat midbrain slices. Reverse transcription was performed using RETROscript® Reverse Transcription Kit (Thermo Fisher Scientific). Quantitative PCR was performed and analyzed using the Applied Biosystems® 7500 Real-Time PCR System Machine and Software, using Taqman® Gene Expression Assays for human Rit2 (Hs01046673_m1), Rit1 (Hs00608424_m1), and GAPDH (Hs99999905_m1), mouse Rit2 (Mm01702749_mH), and GAPDH (Mm99999915_g1), and rat Rit2 (Rn01760884_m1) and GAPDH (Rn01775763_g1).

***[$^3$H]DA uptake assay***

SK-N-MC cells stably expressing BBS-DAT were seeded onto 96-well plates at a density of 7.5x10$^4$/well 24 hrs prior to assay. Cells were washed twice with Krebs-Ringer-HEPES buffer (120mM NaCl, 4.7mM KCl, 2.2mM $CaCl_2$, 1.2mM $MgSO_4$, 1.2mM $KH_2PO_4$, and 10mM HEPES, pH 7.4) and pre-incubated in KRH supplemented with 0.18% glucose ±1µM PMA, 30 min, 37°C. 100nM desipramine was included in all samples to eliminate uptake contribution of endogenous norepinephrine transporter. DA uptake was initiated by addition of 1µM [$^3$H]DA

(Perkin Elmer: Dihydroxyphenylethylamine (Dopamine), 3,4-[Ring-2,5,6-$^{3}$H]) in KRH supplemented with 0.18% glucose, 10μM pargyline, and 10μM ascorbic acid. Assays proceeded for 10min, 37°C, and were terminated by three rapid washes with ice-cold KRH buffer. Cells were solubilized in scintillation fluid, and accumulated radioactivity was determined by liquid scintillation counting in a Wallac MicroBeta scintillation plate counter. Non-specific DA uptake was defined in the presence of 10μM GBR12909.

***Internalization Assays and Immunoblotting***

Relative internalization rates over 10 minutes were measured by reversible biotinylation as previously described (Loder and Melikian, 2003; Holton et al., 2005; Wu et al., 2015). Briefly, the indicated stably transfected cells were seeded into 6-well plates at 1.5x$10^{6}$ cells/well one day prior to analysis. Cells incubated twice with 2.5 mg/mL sulfo-NHS-SS-biotin (15 min, 4°C) and quenched twice with $PBS^{2+}$ (PBS, pH 7.4, 1.0mM $MgCl_2$, 0.1mM $CaCl_2$) supplemented with 100mM glycine (15 min, 4°C). Internalization was initiated by rapidly warming cells in prewarmed $PBS^{2+}$ supplemented with 0.18% glucose, 0.2% protease-/IgG-free bovine serum albumin, and proceeded for 10min, 37°C in the presence of the indicated drugs. Parallel surface-labeled controls remained at 4°C. Cells were rapidly cooled by washing thrice with ice-cold NT buffer (150mM NaCl, 20mM Tris, pH 8.6, 1.0mM EDTA, pH 8.0, 0.2% protease-/IgG-free bovine serum albumin) and remaining surface biotin was stripped by reducing in 100mM TCEP in NT buffer

twice (25 min, 4°C). Cells were rinsed rapidly in $PBS^{2+}$, and were lysed in RIPA buffer (10mM Tris, pH 7.4, 150mM NaCl, 1.0mM EDTA, 0.1% SDS, 1% Triton-X-100, 1% sodium deoxycholate) containing protease inhibitors (1.0mM PMSF and 1.0g/mL each leupeptin, aprotinin, and pepstatin). Lysates were cleared by centrifugation and protein concentrations were determined with the BCA protein assay (Thermo Fisher) using BSA as a standard. Biotinylated proteins were recovered by streptavidin batch chromatography from equivalent amounts of cell lysate, and were eluted in 2X Laemmli sample buffer, 30 min, room temperature with rotation. Eluted proteins were resolved by SDS-PAGE and proteins were detected and quantified by immunoblotting: hDAT and DAT/C-S were detected with amino-directed rat anti-DAT (MAB369, Millipore, 1:2000), and N-S/DAT and S/DAT/S were detected with amino-directed mouse anti-hSERT (MAb Technologies,1:2000). Immunoreactive bands were detected using a VersaDoc imaging station (Bio-Rad), and were in the linear range of detection. Internalization rates were calculated as %surface protein internalized/10 min, as compared to their respective surface signal at t=0 min (controls that were biotinylated and kept at 4°C). Note that for all representative immunoblots shown throughout the study, all brightness/contrast manipulations were made uniformly across any given blot. For presentation purposes, immunoreactive bands were cropped from the same exposure of the same immunoblot.

***BBS-DAT/chimera pulldowns***

HEK293T cells were transiently co-transfected with HA-Rit2, and either BBS-DAT or BBS-DAT chimeras, at a DAT:Rit2 plasmid ratio of 1:4, as described above. Cells were washed thrice with ice cold $PBS^{2+}$ and surface BBS-DAT chimeras were labeled with 120μM biotinylated α-bungarotoxin (α-BTX-b, Thermo Fisher) in $PBS^{2+}$, 2 hrs, 4ºC. For drug treatments, cells were treated with the indicated drugs 30 min, 37°C, prior to labeling with α-BTX-b. Following labeling, α-BTX-b solution was removed, cells were washed thrice with ice cold $PBS^{2+}$, and were lysed in ice-cold co-immunoprecipitation (co-IP) lysis buffer (50mM Tris, pH 7.4, 100mM NaCl, 1% Triton X-100, 10% glycerol, and 1.0mM EDTA) containing protease inhibitors (1.0mM PMSF and 1.0g/mL each leupeptin, aprotinin, and pepstatin) and Phosphatase Inhibitor Cocktail V (EMD Millipore), 30 min, 4°C. Labeled proteins were recovered from equivalent amounts of protein by batch affinity chromatography with streptavidin-coupled M280 Dynabeads (Thermo Fisher), 4°C, overnight with rotation. Lysate/bead ratios were empirically determined to assure quantitative recovery of all labeled proteins in lysates. Beads were gently washed thrice with ice-cold co-IP buffer, with magnetic recovery between washes, and isolated proteins were eluted from beads in an equal volume of co-IP lysis buffer and 2X SDS-PAGE sample buffer (100mM Tris, pH 6.8, 4.4% SDS, glycerol, 100mM DTT, and 0.04% bromophenol-blue). Isolated proteins were resolved by SDS-PAGE, and specific protein bands were detected by immunoblotting with antibodies for rat anti-DAT (1:2000), mouse anti-hSERT (1:2000), and rabbit anti-HA (1:2000) as indicated above. Immunoreactive HA-Rit2 band densities were

normalized to their respective recovered DAT, or chimera, bands in each independent experiment.

### *Statistical Analysis*

All data were analyzed using GraphPad Prism software. Prior to analyses, statistical outliers within data sets were identified using either Grubb's or Rout's outlier test, and were removed from further analysis. Specific statistical tests used are detailed within each figure legend. For comparisons between two groups, a Student's t test was used. For comparison among more than two experimental groups, one-way ANOVA with appropriate post-hoc multiple comparison test was performed, as indicated within each figure legend.

## Preface to Chapter III

## Ric GTPase activity regulates dopaminergic function and sleep quality in a dopamine transporter-dependent manner in *Drosophila melanogaster*

Author Contributions:

Rita R. Fagan, Patrick Emery, Harald H. Sitte, and Haley E. Melikian designed experiments.

Rita R. Fagan and Dino Leuthi performed experiments.

Rita R. Fagan, Patrick Emery, Harald H. Sitte, and Haley E. Melikian analyzed data.

# CHAPTER III

## Ric GTPase activity regulates dopaminergic function and sleep quality in a dopamine transporter-dependent manner in *Drosophila melanogaster*

Rita R. Fagan, Dino Leuthi, Harald Sitte, Patrick Emery, Haley E. Melikian

### III.A Summary

DA is a critical regulator of movement, sleep, reward, and cognition. The presynaptic dopamine transporter (DAT) clears released DA with spatial and temporal precision essential for maintaining DA signaling and homeostasis. Addictive and therapeutic psychostimulants, including MPH (Ritalin), cocaine, and AMPH, are competitive DAT inhibitors (MPH, cocaine) and substrates (AMPH) that enhance extracellular DA. DAT genetic ablation in mice and invertebrates leads to hyperactivity, reduced sleep, and blunted psychostimulant responses, highlighting DAT's essential role in maintaining DA homeostasis. DAT plasma membrane is tightly regulated by intrinsic mechanisms, including PKC activation. However, the physiological impact of disrupted DAT trafficking remains unknown. Our group found that Rit2, a neuronal GTPase that binds to DAT, is required in mice for PKC-stimulated DAT downregulation in *ex vivo* striatal slices. DAergic Rit2 expression is also required for the acute locomotor response to cocaine injection in male mice. Here, we leveraged the model organism, *Drosophila melanogaster*, to genetically

test whether Rit2 impacts DAT function. We found that, similar to mammalian DAT and Rit2, dDAT and Ric (the *Drosophila* Rit2 homolog) directly interact. Moreover, constitutively active Ric increased dDAT function in cell culture and *ex vivo Drosophila* brain preparations. Importantly, constitutively active Ric expressed in DA neurons impacted sleep consolidation in a DAT-dependent manner, but had no effect on overall locomotion or sleep. These studies are among the first to provide evidence that manipulating proteins required for regulated DAT endocytosis alter a DA-dependent behavior via its actions at DAT.

## III.B Introduction

The catecholamine neurotransmitter DA mediates a variety of behaviors such as motor function, sleep, learning, and reward (Wise, 2004; Schultz, 2007a). Addiction is also fundamentally linked to plastic changes in DA transmission (Hyman et al., 2006). Moreover, neuropsychiatric diseases including PD, ADHD, ASD, and schizophrenia are associated with aberrant DA signaling (Iversen and Iversen, 2007; Sharma and Couture, 2014; Howes et al., 2017; Eissa et al., 2018; Geibl et al., 2019). The DAT is expressed on presynaptic DA neurons and spatially and temporally controls DA transmission by clearing extracellular DA following release, thereby terminating the DA signal. DAT not only regulates extracellular DA levels, but also critically replenishes vesicular DA stores for future release (Gainetdinov et al., 1998). Psychostimulants such as cocaine, AMPH, and MPH

competitively inhibit DA reuptake through DAT, further emphasizing DAT's role in regulating DA transmission and addiction.

Genetic DAT ablation in vertebrate and invertebrate animal models blocks psychostimulant-induced hyperactivity and reward, and causes hyperactivity and sleep loss (Giros et al., 1996; Wisor et al., 2001; Kume et al., 2005; Pizzo et al., 2013). DAT knock-out (*DAT*$^{-/-}$) mice display alterations in their sleep and waking patterns in which their waking episodes (or bouts) are three times longer than wildtype controls (Wisor et al., 2001). *Drosophila melanogaster* DAT (dDAT)-null fruit flies ("fumin", *fmn*) also sleep significantly less than wildtype flies, with shorter and fewer resting bouts (Kume et al., 2005). Given DAT's fundamental role in regulating DA homeostasis and signaling, mechanisms that modify DAT function or expression at the plasma membrane will likely alter DAergic neurotransmission and behavior.

Decades of research support that acute PKC activation increases the DAT internalization rate and decreases the surface delivery rate, resulting in a net loss of DAT plasma membrane expression, demonstrated *in vitro* and in *ex vivo* striatal slice preparations (Daniels and Amara, 1999; Melikian and Buckley, 1999; Kristensen et al., 2011; Gabriel et al., 2013; Bermingham and Blakely, 2016). However, it remains unknown whether PKC-stimulated DAT trafficking impacts DA-dependent behavior. Our group first discovered that PKC-stimulated DAT

endocytosis requires activity of the GTPase, Rit2, and that DAT also interacts with Rit2 (Navaroli et al., 2011). In a follow-up study, we demonstrated that PKC activation caused DAT and Rit2 to dissociate at the cell surface, and the DAT N-terminus was required (Fagan et al., 2020). Using a conditional and inducible knockdown approach (Rit2-KD), we found that DAergic Rit2 is required for anxiety behavior and acute cocaine locomotor response *in vivo* (Sweeney et al., 2020). Notably, we recently reported that Rit2-KD blocked PKC-stimulated DAT surface loss in DA terminals (Fagan et al., 2020). These data indicate that the Rit2-dependent behavior phenotypes may occur due to the loss of PKC-stimulated DAT internalization, however they do not rule out the possibility that Rit2 acts independently of DAT to regulate DA transmission and behavior.

Apart from regulating DAT surface expression, the neuronal GTPase Rit2 is also required for nerve growth factor-stimulated neurite outgrowth and p38 MAP kinase activation in cultured neuroendocrine cells (Shi et al., 2005). Rit2 can also promote cellular viability of neuronal SH-SY5Y cells by maintaining phosphorylated ERK levels (Uenaka et al., 2018). Of note, SNPs and copy number variations in Rit2 have been identified in multiple GWAS studies investigating neuropsychiatric diseases and disorders, including PD (Daneshmandpour et al., 2018), schizophrenia (Glessner et al., 2010; Emamalizadeh et al., 2017), and ASD (Liu et al., 2016; Hamedani et al., 2017). Additionally, Rit2 expression is restricted to neurons and is suggested to be enriched in DA neurons (Zhou et al., 2011). Thus,

whether the behavioral phenotypes caused by Rit2-KD are a result of Rit2's actions at DAT, or are DAT-independent, remains unknown. *Drosophila* may be a powerful model system to address this question, however it is completely unknown whether dDAT interacts with Ric, the invertebrate Rit2 homolog, or if dDAT is subject to similar surface or functional regulation as its mammalian counterparts.

In this study we used cell type-specific RNAi and mutant overexpression to test whether dDAT and Ric interact, and may serve as invertebrate model for the DAT-Rit2 interaction. We further target Ric to examine the *in vivo* consequence of disrupted DAT function (Wes et al., 1996; Shi et al., 2013). The DA system is highly conserved between flies and mammals, providing a highly tractable and simplified model for studying DA neurotransmission (Martin and Krantz, 2014). Our results indicate that Ric activity modulates dDAT function and surface expression, and expressing constitutively active Ric specifically in DA neurons significantly altered Drosophila sleep architecture in a dDAT-dependent manner.

## III.C Results

*Ric interacts with dDAT*

Our lab discovered that Rit2 is required to stabilize DAT surface expression through its dynamic interaction with DAT at the plasma membrane, and is required for PKC-dependent DAT surface regulation (Navaroli et al., 2011; Fagan et al., 2020). However, it is not known whether Rit2-dependent behavior phenotypes are

due to DAT's reliance on Rit2 for PKC-stimulated internalization, or, alternatively, are DAT-independent. In order to address this question, we utilized the model organism, *Drosophila melanogaster*, which expresses a single Rit2 homolog, Ric. Ric shares ~71% homology with Rit2, however it is expressed ubiquitously in the fruit fly, in contrast to neuron-specific Rit2 (Lee et al., 1996; Wes et al., 1996; Spencer et al., 2002b). The known cellular functions of Ric are limited thus far, though Ric does bind to calmodulin (Wes et al., 1996) and was demonstrated to be important for neurite outgrowth and wing vein formation (Harrison et al., 2005).

We recently discovered that PKC activation causes DAT and Rit2 to dissociate at the plasma membrane, and PKC-mediated DAT-Rit2 dissociation is likely a required step for releasing the DAT endocytic brake (Fagan et al., 2020). Therefore, we first tested whether dDAT and Ric directly interact by live cell fluorescent resonance energy transfer (FRET). HEK293 cells were co-transfected with YFP-tagged DAT (either human or *Drosophila*) and either CFP-Ric or CFP-Rit2, and FRET signals were measured. A significant FRET signal was detected by all FRET pairs compared with CFP+YFP controls (Figure III.1A). As previously reported, hDAT+Rit2 elicited a significant FRET signal. Similarly, dDAT and Ric produced a significant FRET signal as compared with CFP+YFP, and which did not differ from the hDAT+Rit2 signal ($p=0.92$). Interestingly, pairing either hDAT and Ric or dDAT and Rit2 also yielded significant FRET signals, as compared with CFP+YFP controls, suggesting that DAT and Rit2 interacting domains may be

conserved across species. This result was intriguing, and prompted us to examine whether hDAT and Ric associate at the plasma membrane when measured using a labeling and pulldown approach previously described by our lab. Specifically, we engineered a bungarotoxin (BTX) binding site (BBS) into the second extracellular loop of human DAT (hDAT), which allowed specific examination of the surface hDAT protein complex, and confirmed the DAT-Rit2 surface interaction (Fagan et al., 2020). To evaluate whether a surface association could occur between Ric and dDAT, we co-transfected HEK293T cells with HA-tagged Ric and BBS-hDAT, labeled with $\alpha$-BTX-b, and protein complexes were isolated by streptavidin pulldown. BBS-hDAT recovered HA-Ric (Figure III.1B), indicating that hDAT and Ric can form a complex in heterologous cells, and lending further support to the hypothesis that the DAT and Rit2 interacting domains are conserved.

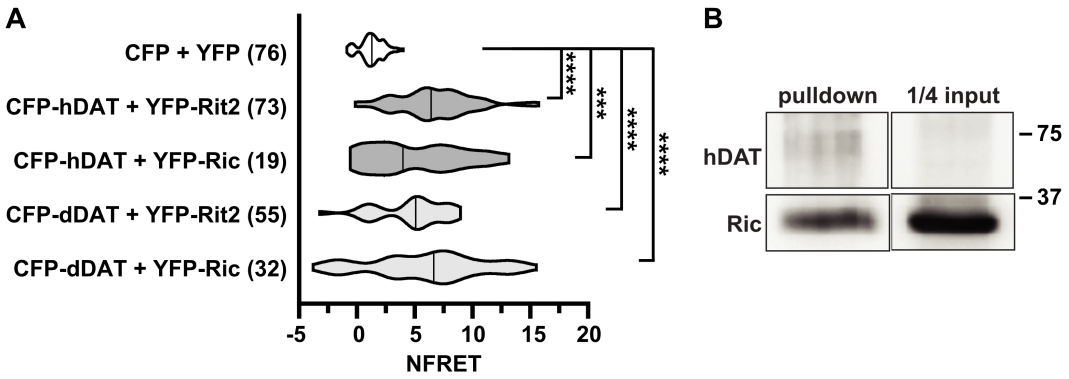


**Figure III.1: Ric interacts with dDAT. A.** *FRET microscopy*. HEK293 cells were transfected with YFP-tagged hDAT or dDAT and CFP-tagged Rit2 or Ric constructs. FRET microscopy was performed in live cells as described in *Experimental Procedures*. A significant FRET signal was detected by Kruskal-Wallis test ($p<0.0001$, n=19-76 cells) compared to CFP+YFP controls in all FRET pairs (Dunn's multiple comparisons test): hDAT+Rit2 (****$p<0.0001$), hDAT+Ric (***$p=0.0002$), dDAT+Rit2 (****$p<0.0001$), and dDAT+Ric (****$p<0.0001$). hDAT+Rit2 FRET signal did not differ from dDAT+Ric ($p=0.9128$). **B.** *BBS-DAT pulldown*. HEK293T cells were transfected with BBS-hDAT and HA-Ric. Cells were labeled with biotinylated bungarotoxin and BBS-hDAT was pulled down as described in *Experimental Procedures*. BBS-hDAT associated with HA-Ric (representative blots of three individual experiments shown.

*Constitutively active Ric increases dDAT function and surface levels*

Next, we asked whether Ric activity is required for dDAT function. DA transport kinetics were measured in HEK293T cells transfected with dDAT and either vector, wildtype (Ric-WT) constitutively active (CA) Ric (RicQ117L), or dominant negative (DN) Ric (RicS73N). dDAT took up DA with a $K_m$ of 5.49 ± 1.79μM, consistent with previously reported values (Porzgen et al., 2001) (Figure III.2A), and co-expression of WT or mutant Ric did not significantly affect dDAT DA affinity (Figure III.2B). DN-RicS73N had no effect on the Vmax of dDAT compared with Ric-WT, however, RicQ117L expression significantly increased DA uptake velocity (Figure III.2B). An increase in Vmax could be a result of either increased dDAT surface expression or enhanced substrate turnover rates. To distinguish between these two possibilities, we used surface biotinylation to directly test whether RicQ117L increased dDAT surface levels. Compared with cells transfected with Ric-WT, RicQ117L overexpression significantly increased dDAT surface expression (Figure III.2C), indicating that RicQ117L-dependent increased dDAT function likely resulted from enhanced dDAT surface levels.

*DAergic RicQ117L expression increases DA uptake ex vivo*

Given that Ric activity regulates dDAT function and expression in mammalian heterologous cell models, we tested whether this regulation occurs in DA terminals where these proteins are endogenously expressed. To ask this question, we employed an *ex vivo Drosophila* whole brain uptake assay (Cartier et al., 2015)

and asked whether RicQ117L similarly increases DA uptake *in situ*. *TH-GAL4* flies were crossed to wildtype or *UAS-HA-RicQ117L* flies to drive RicQ117L expression selectively in DA neurons (Friggi-Grelin et al., 2003), and DA uptake was measured in male progeny (*TH-GAL/UAS-RicQ117L*). Control *TH-GAL4/+* flies took up 2.36 ± 0.63μM fmol/min/brain, and RicQ117L overexpression significantly increased uptake to 3.94 ± 0.03μM fmol/min/brain (Figure III.2D). Together, these data demonstrate that Ric GTPase activity regulates dDAT function in intact fly brains, and suggest that dDAT is subject to similar mechanistic control as its mammalian homolog.

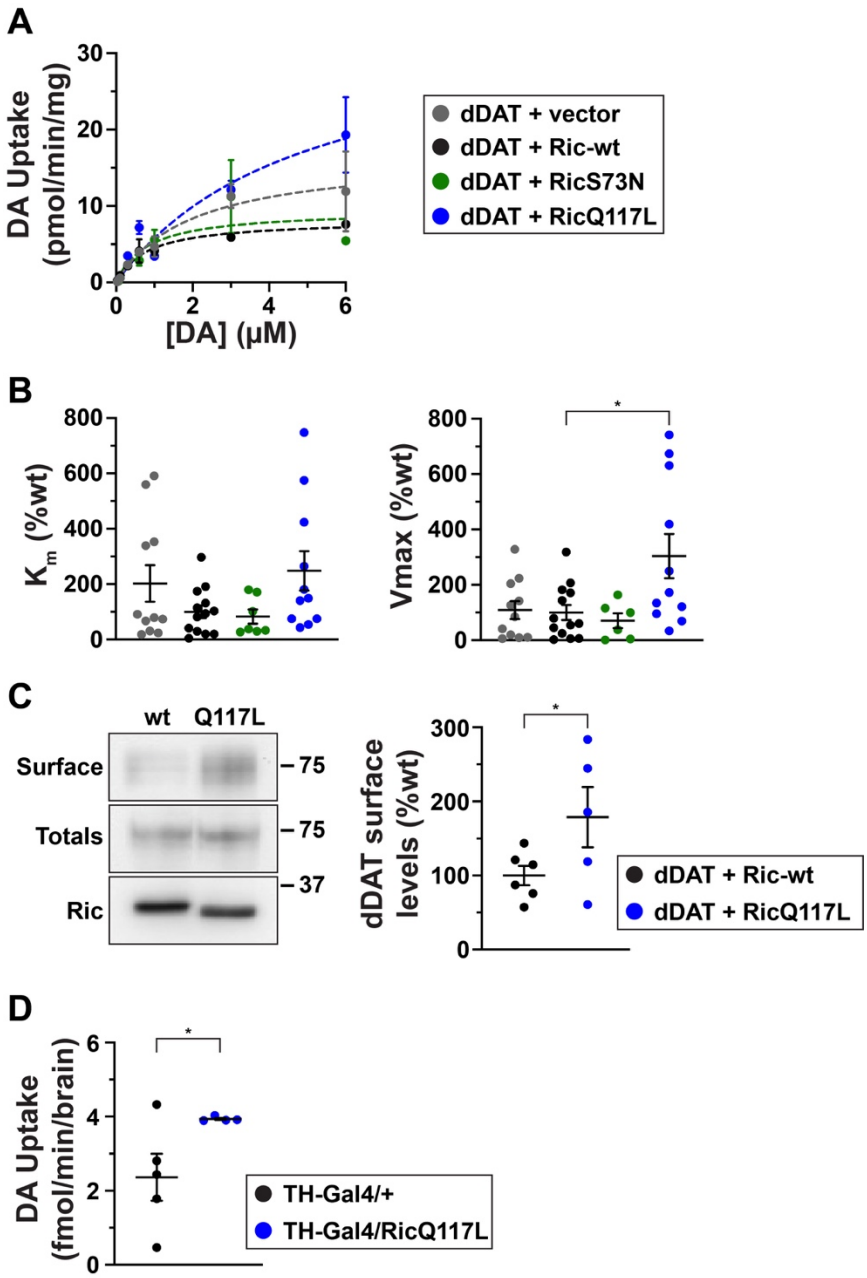


**Figure III.2 Ric activity increases dDAT function and surface expression.** *DA uptake kinetics*. HEK-293T cells were transfected with HA-dDAT and pcDNA3.1(+) (vector), HA-Ric-WT, HA-RicQ117L, or HA-RicS73N and [$^3$H]DA uptake kinetics were measured as described in *Experimental Procedures*. **A.** Representative kinetic curves. **B.** Average $K_m$ (left) and average Vmax are presented as a percentage of Ric-WT overexpression. HA-RicQ117L significantly increased dDAT Vmax (one-way ANOVA: $F_{(3, 37)} = 4.52$, p=0.008; Dunnett's multiple comparisons

test *p=0.01, n=7-13). Ric activity had no effect on DA affinity (one-way ANOVA: $F_{(3, 38)} = 2.141$, p=0.11). **C**. *Surface biotinylation*. HEK293T cells were transfected with HA-dDAT and vector or HA-RicQ117L constructs and dDAT surface expression was measured as described in *Experimental Procedures*. Representative blots (left). RicQ117L significantly increased dDAT surface levels compared to vector-transfected controls (one-tailed student's *t* test: *p=0.038, n=5). **D.** *Ex vivo whole brain [$^3$H]DA uptake*. *TH-Gal4* flies were crossed to +/+ (*TH-Gal4/+*) or *UAS-RicQ117L* (*TH-Gal4/UAS-RicQ117L*) flies. Crosses were maintained and dissected from male progeny as described in *Experimental Procedures*. DA uptake was measured in 4 brains per condition, and nonspecific uptake was defined with 10μM nisoxetine. *TH-Gal4/UAS-RicQ117L* flies had significantly more DA uptake than *TH-Gal4/+* controls (one-tailed student's *t* test: *p=0.034, n=4-5).

*DAergic Ric activity does not impact locomotor activity or total sleep*

DA controls locomotion and regulates sleep in *Drosophila* (Riemensperger et al., 2011; Ueno et al., 2012). Moreover, flies lacking dDAT are hyperactive and sleep significantly less than wildtype and do not recover following sleep deprivation, indicating that dDAT is also required for total sleep and homeostatic sleep regulation (Kume et al., 2005; Ueno and Kume, 2014). Given that RicQ117L increases dDAT transport velocity in whole brain preparations, we tested whether DAergic Ric activity is required for sleep or locomotion. We hypothesized that if dDAT function increases, there will be less extracellular DA, which could reduce locomotor activity. Using the *TH-GAL4* driver, we overexpressed Ric-WT (*TH-GAL4/UAS-Ric-WT*), DN RicS73N (*TH-GAL4/UAS-RicS73N*), or CA RicQ117L (*TH-GAL4/UAS-RicQ117L*) in DA neurons. Male progeny 0-3dpe were placed in the *Drosophila* Activity Monitor (DAM) system, and sleep and locomotor behavior were assessed at 12hr light/dark cycle following entrainment. Data were analyzed using the sleep and circadian analysis MATLAB program (SCAMP), and sleep was defined as 5 consecutive minutes of inactivity (Donelson et al., 2012). DAergic expression of Ric-WT, RicS73N, and RicQ117L had no effect on total locomotor activity as measured by beam breaks at any time (24h bin, day (12h), or night (12h) (Figure III.3). Total time spent asleep was likewise unaffected, with the exception of Ric-WT overexpression during the day, which resulted in. small, but significant, decrease in sleep (Figure III.3D).

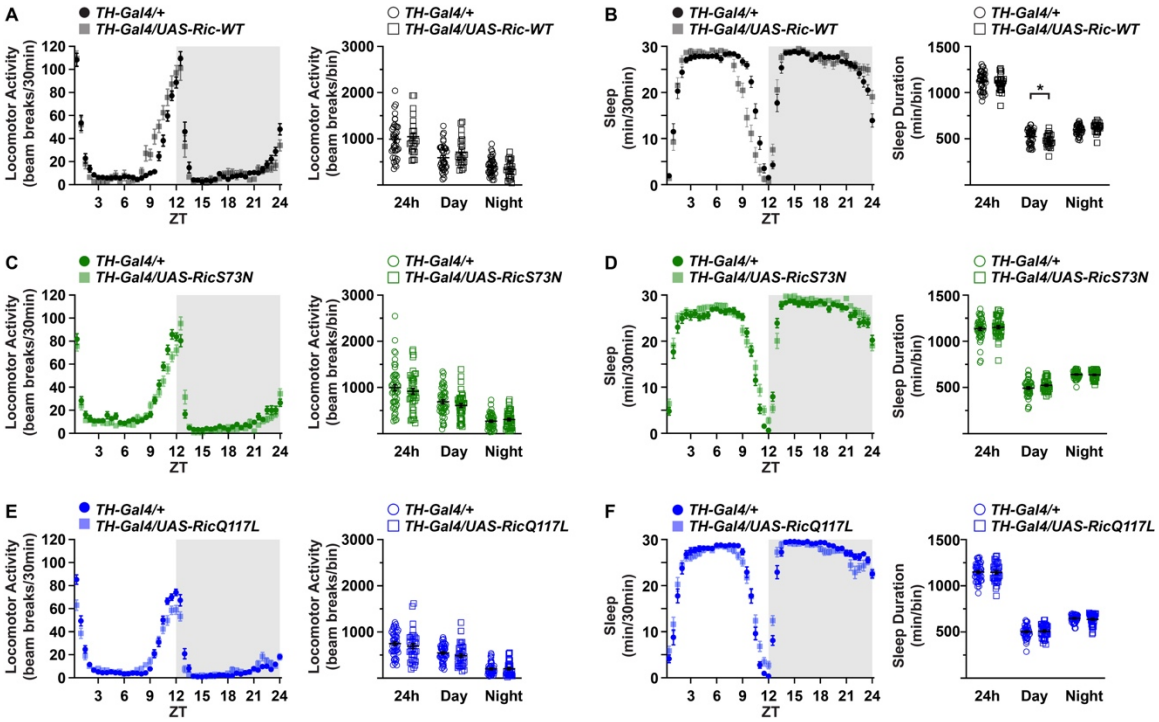


**Figures III.3 Ric activity in DA neurons is not required for baseline locomotor or sleep behavior.** *Locomotor and sleep behavior*. *TH-Gal4* and *UAS-Ric-WT*, *UAS-RicS73N*, or *UAS-RicQ117L* flies were crossed and locomotor activity and sleep were measured in progeny as the total number of beam breaks and minutes spent sleeping during 24h, day (12h lights-on), and night (12h lights-off) bins. Data were analyzed by two-tailed student's *t* test or Welch's correction between *TH-Gal4/+* control and experimental animals. **A, C, E.** *Locomotor activity*. Left: Total locomotor activity counts per 30min averaged over three days at LD. Right: Ric-WT (**A**), RicS73N (**C**), and RicQ117L (**E**) overexpression had no effect on total activity counts during the 24h, day, or night bins (3-6 independent experiments, n=24-47 flies/GT). **B, D, F.** *Sleep*. Left: Minutes spent asleep per 30min averaged over three days at LD. Right: Ric-WT (**B**) significantly decreased total sleep during the day (*p=0.028, n=24-38), but not in the 24h bin or at night. RicS73N (**D**) and RicQ117L (**F**) had no effect on total sleep in the during the 24h, day, or night bins.

*DAergic Ric expression is not required for locomotor activity or sleep*

We next tested whether DAergic Ric expression is required for sleep or locomotor activity. Four distinct *UAS-RicRNAi* lines (Figure III.4A) were crossed to *Elav-GAL4* in order to measure their efficacy for RNAi-mediated Ric knockdown. The pan-neuronal driver was used because Ric is ubiquitously expressed, and therefore DA neuron-specific knockdown would be undetectable. RT-qPCR was performed on dissected fly brains of male progeny, and, indeed, all four RNAi lines significantly reduced Ric mRNA expression as compared to *Elav-Gal4/+* control (Figure III.4B). Locomotor and sleep behavior were measured in male progeny as described above. RicRNAi3 (Figure III.4G-H) and RicRNAi4 (Figure III.4I-J) had no effect on total activity or sleep. RicRNAi1 had the most pronounced effects: significantly increased locomotor activity and decreased sleep during the lights-on period (Figure III.4C-D). Finally, RicRNAi2 showed a subtle decrease in locomotion at night (Figure III.4E), with significantly increased sleep at night and decreased sleep during the day (Figure III.4F). Due to the fact that, 1) none of these phenotypes are consistent across multiple efficacious RNAi lines, and 2) RicRNAi1 is predicted to target two other genes apart from Ric, it is not likely that any of the observed changes in behavior were specifically due to DAergic Ric knockdown.

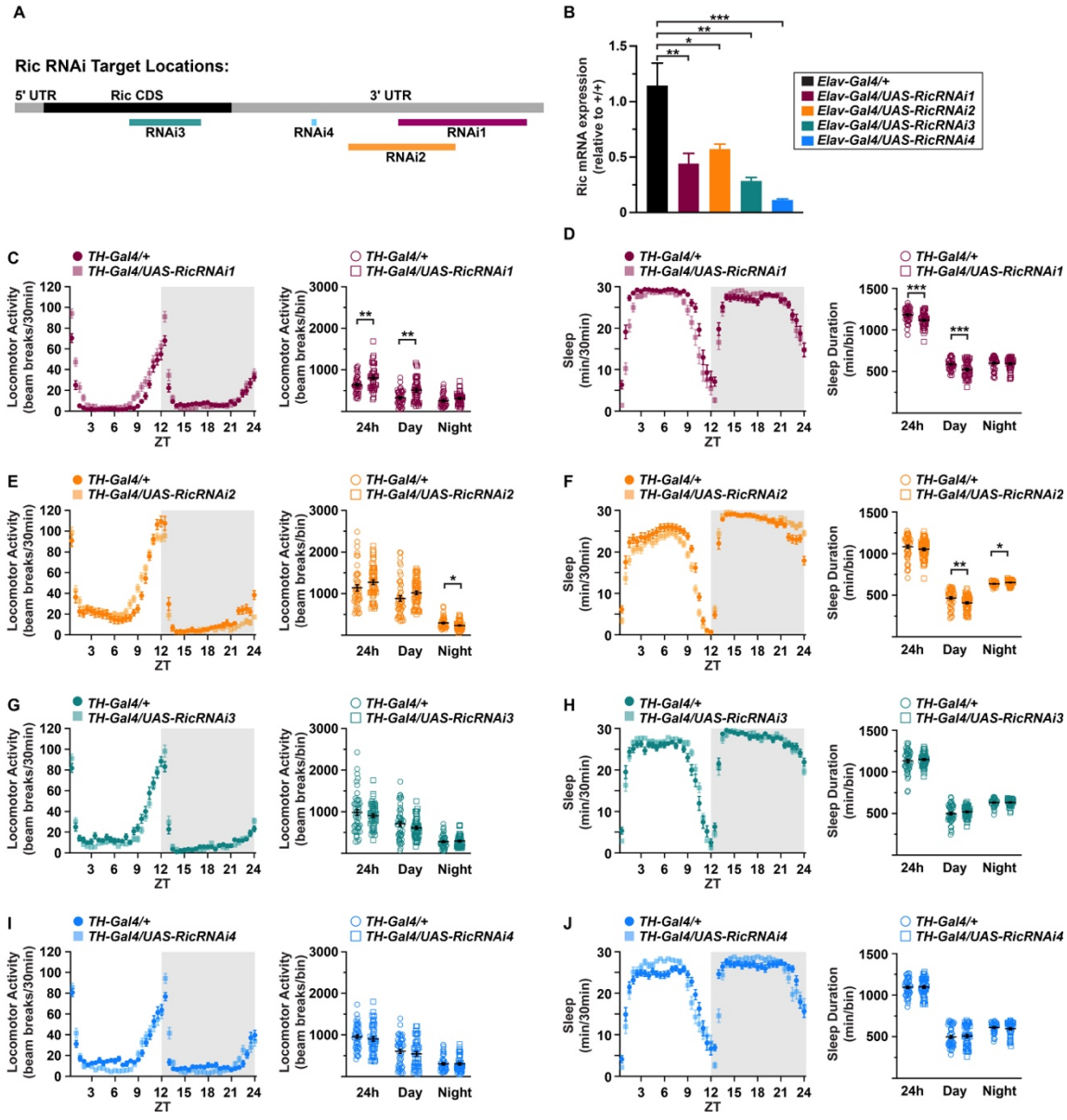


**Figure III.4 Ric expression in DA neurons is not required for locomotor or sleep behavior. A.** Schematic of Ric RNAi target locations. **B.** *RNAi-mediated Ric mRNA knockdown*. *Elav-Gal4* flies were crossed to *UAS-RicRNAi* lines 1-4, RNA was extracted from dissected fly brains from male progeny, and RT-qPCR was performed as described in *Experimental Procedures*. Ric expression was significantly decreased by the *Elav-Gal4* driver in all four RicRNAi lines (one-way ANOVA: $F_{(4, 11)} = 11.20$, p=0.0007; Dunnett's multiple comparisons test versus *Elav-Gal4/+* results: RNAi1: **p=0.006, RNAi2: *p=0.022, RNAi3: **p=0.001, RNAi4: ***p=0.003; n=3-4). **C-J**. *Locomotor and sleep behavior*. *TH-Gal4* and *UAS-RicRNAi* flies were crossed and locomotor activity and sleep were measured

and analyzed in progeny as described above. **C, E, G, I.** *Locomotor activity*. Left: Total locomotor activity counts per 30min averaged over three days at LD. Right: RicRNAi1 (**C**) significantly increased activity counts during the 24h bin (Welch's *t* test **p=0.005, n=38-43) and daytime bin (Welch's *t* test **p=0.001). RicRNAi2 (**E**) significantly decreased activity at night (*p=0.014; n=44-48). RNAi3 (**G**) and RNAi4 (**I**) had no significant effect on total activity. **D, F, H, J.** *Sleep*. Left: Minutes spent asleep per 30min averaged over three days at LD. Right: RicRNAi1 (**D**) significantly decreased total sleep during the 24h bin (***p=0.0008, n=38-43) and daytime bin (Welch's *t* test, ***p=0.0007). RicRNAi2 (**F**) had no effect during the 24h bin, but significantly decreased sleep during the day (**p=0.004, n=44-48), and significantly increased sleep at night (*p=0.012). RNAi3 (**H**) and RNAi4 (**J**) had no significant effect on total sleep.

*DAergic Ric activity decreases sleep bout consolidation*

Sleep and activity bout fragmentation is indicative of reduced sleep consolidation and quality, and can negatively impact health and cognitive function (Koh et al., 2006; Medic et al., 2017), hence we also asked whether DAergic Ric expression or activity is required for typical number of sleep episodes in the same animals used to test total activity and sleep. Again, RicRNAi lines gave inconsistent results. RicRNAi1 (Figure III.5A) and RicRNAi3 (Figure III.5C) had no effect during any time frame. RicRNAi2 significantly increased sleep bout numbers, but only during the day (Figure III.5B), whereas RicRNAi4 decreased sleep bout numbers at all times of the day (Figure III.5D). DAergic Ric-WT overexpression significantly reduced sleep bout numbers during the day (Figure III.5E), and DN RicS73N reduced sleep bouts, but only at night (Figure III.5F). However, CA RicQ117L significantly increased sleep bout numbers during the 24h and daytime bins (Figure III.5G), indicating a specific phenotype for CA Ric overexpression.

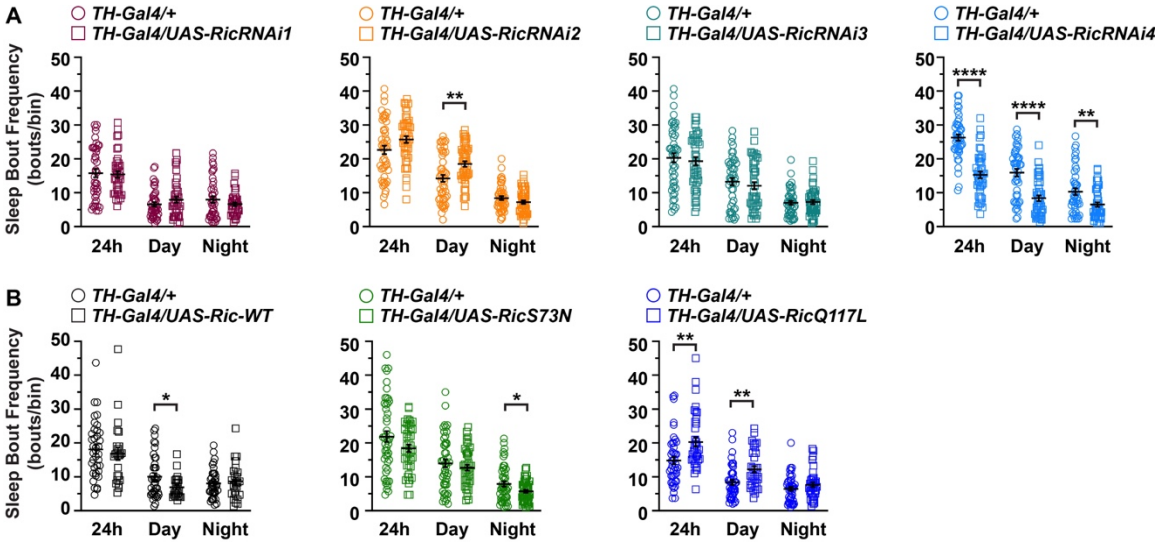


**Figure III.5 DAergic Ric activity modulates sleep bout frequency.** *TH-Gal4* and *UAS-RicRNAi, Ric-WT, UAS-RicS73N,* or *UAS-RicQ117L* flies were crossed and the number of sleep episodes in male progeny were counted for bins of 24h, daytime (12h lights-on), and nighttime (12h lights-off), and data were analyzed as described above. **A-D.** *RicRNAi sleep bout frequency.* RNAi1 (**A**) and RNAi3 (**C**) had no effect on sleep bout frequency at any time. RNAi2 (**B**) did not alter sleep bout frequency in the 24h nighttime bins, but significantly increased episode frequency during the day (**p=0.001, n=44-48). RNAi4 (**D**) significantly decreased sleep bouts at all three bins (24h: ****p<0.0001, n=43-45; day: Welch's *t* test: ****p<0.0001; night: Welch's *t* test: **p=0.002). **E-G.** *Ric activity sleep bout frequency*. Ric-WT (**E**) had no effect on sleep bout number over 24h or at night, but significantly decreased sleep frequency during the daytime (Welch's t test: *p=0.015, n=24-38). RicS73N (**F**) had no effect on sleep bout number over 24h or during the day, but significantly decreased sleep frequency during at night (Welch's *t* test, *p=0.022, n=41-47). RicQ117L significantly increased sleep bouts during the 24h bin (**p=0.003, n=36-44) and during the day (**p = 0.001), but did affect sleep bout numbers at night.

*dDAT is required for the RicQ117L sleep fragmentation phenotype*

The data thus far suggest that the RicQ117L-dependent decreased consolidation of sleep may be a result of the increased rate of DA reuptake caused by overexpression of RicQ117L. However, Ric has other cellular functions, including neurite outgrowth and environmental stress survival (Harrison et al., 2005; Cai et al., 2011). Moreover, although we demonstrated that Rit2 is required for DA-dependent behavior and regulated DAT trafficking (Fagan et al., 2020; Sweeney et al., 2020), we still do not know if the phenotypes are a result of disrupted DAT trafficking or function. Thus, in order to determine whether the RicQ117L-induced phenotype is DAT-dependent, we performed epistasis studies in which both driver (*TH-GAL4*) and responder (*UAS-HA-RicQ117L*) fly strains were crossed onto the dDAT null background (*fmn;TH-GAL4* and *fmn;UAS-RicQ117L*). We predicted that if any of the locomotor phenotypes were mediated by Ric's impact on DAT function, these phenotypes would be lost on the DAT null background (*fmn;TH-GAL4/UAS-RicQ117L*). In fact, we observed that DAergic RicQ117L overexpression in the absence of dDAT had no effect on sleep bout number as compared to control flies (Figure III.6), indicating that the Ric activity-dependent increase in dDAT function and/or surface expression likely drives the increased sleep fragmentation phenotype.

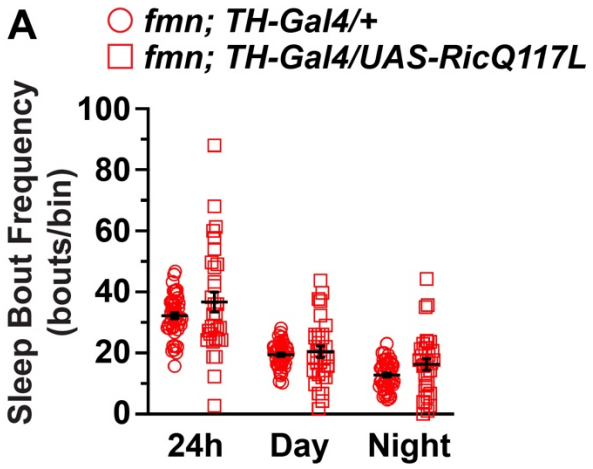


**Figure III.6 RicQ117L-dependent wake and sleep bout fragmentation is dDAT-dependent.** *TH-Gal4* and *UAS-RicQ117L* flies were crossed onto the dDAT-null background (*fmn*). Locomotor activity and sleep were measured in male progeny (*fmn; TH-Gal4/UAS-RicQ117L*) and analyzed as previously described. **A**. *Sleep fragmentation*. RicQ117L expression on the dDAT-null background did not affect the number of sleep episodes (24h: p=0.1935; day: p=0.608; night: p=0.087, n=31-47) compared to *fmn; TH-Gal4/+* controls.

## III.D Discussion

In the present study, we set out to examine the *in vivo* impact of the DAT-Rit2 interaction using *Drosophila* as a model system. We found that the *Drosophila* homologs, dDAT and Ric, do interact (Figure III.1), indicating that the fruit fly is a good model for studying DAT and Rit2. Moreover, DAergic overexpression of the CA Ric mutant, RicQ117L, increased dDAT Vmax and surface expression (Figure III.2), and decreased sleep quality in adult *Drosophila* (Figure III.5). Of note, we demonstrate that dDAT is absolutely required for this phenotype, providing the first indication that indirectly manipulating DAT surface regulation impacts DAergic behaviors DAT-dependently. This is an important distinction because proteins that regulate DAT surface expression or function likely play other critical roles in the cell. Specifically, Ric activity was also demonstrated to stimulate neurite outgrowth in PC6 cells (Harrison et al., 2005). Ric binds to calmodulin (Wes et al., 1996), and *in vivo* overexpression of RicQ117L induced ectopic wing vein growth, which was exacerbated by concurrent null mutations in calmodulin (Harrison et al., 2005). Furthermore, genetic ablation of Ric reduced fly viability in response to environmental stress (Cai et al., 2011). Of yet, the only indication that Ric plays a role within the central nervous system originates from a large genetic screen that utilized pan-neuronal RNAi expression, and identified Ric as a suppressor of olfactory memory formation (Walkinshaw et al., 2015). Thus, the results from the epistasis experiment (Figure III.6) allow us to more confidently interpret that DAergic Ric regulates behavior through its function at DAT. Given that RicRNAi4

has the opposite effect on sleep episode number, and is the most efficacious for silencing Ric expression, it would be interesting to know whether the RicRNAi4 phenotype is also DAT-dependent.

What is the mechanism by which RicQ117L increases dDAT function and surface expression? In the first report characterizing the Rit2 and DAT interaction, our group found that DAT and Rit2 dissociate when DAT internalizes following PKC activation, but that this was blocked by the CA Rit2 mutant (Navaroli et al., 2011). Moreover, we recently demonstrated that the lack of PKC-stimulated DAT and Rit2 dissociation correlates with a loss of PKC-stimulated DAT internalization (Fagan et al., 2020). Together these data suggest that RicQ117L may not dissociate from dDAT, thereby anchoring dDAT to the plasma membrane which, in the presence of ongoing cellular signaling, increases dDAT surface levels over time. However, it remains to be tested whether RicQ117L blocks PKC-stimulated dDAT endocytosis, or, importantly, whether PKC stimulates dDAT trafficking. Due to the lack of dDAT-targeted antibodies, PKC-dependent dDAT surface regulation has not yet been studied. Further, we did not examine whether PKC stimulates Ric dissociation from dDAT, or if Ric mutations block this process. Generating a BBS-DAT construct would aid in addressing these questions. Of note, qualitative microscopy studies suggested that DN Rit2 did not dissociate from DAT in our earlier report (Navaroli et al., 2011), however these experiments were not quantitative, and did not specifically examine the surface DAT population.

Additional experiments will be required to test whether Rit2 or Ric activity is required for PKC-stimulated surface DAT dissociation.

How might an increase in DAT surface expression decrease sleep consolidation? It is tempting to speculate that increased DAT surface expression would lead to decreased extracellular DA concentrations, leading to increased numbers of waking and sleeping episodes. In fact, extracellular DA concentrations are reduced by nearly half in the DAT overexpression mouse model, which expresses ~2.5 times more DAT protein (Salahpour et al., 2008). This hypothesis is also consistent with the fact that *DAT*$^{-/-}$ animals display 1) increased extracellular DA (Gainetdinov et al., 1998; Makos et al., 2009), and 2) decreased sleep bout number (or increased wake episode length) (Wisor et al., 2001; Kume et al., 2005). However, whether DA release or overall DA concentrations in the brain are altered by RicQ117L expression remain to be tested. dDAT is also required for sleep rebound characterized by increased sleep after mechanical sleep deprivation, indicating a role for dDAT in homeostatic sleep regulation (Kume et al., 2005). Given that our genetic Ric manipulations did not appear to affect overall waking or sleeping behavior, but had more subtle effects on specific sleep quality parameters, it is intriguing whether Ric, through dDAT, is required for sleep rebound. Further, DAergic RicQ117L expression increased sleep bout frequency during the light phase of activity, but not at night (Figure III.5), suggesting a possible influence of circadian regulation. Extracellular DA concentrations and rates of DA uptake vary

over the light/dark cycle, and DAT is required for circadian oscillations in DA release (Ferris et al., 2014). However, whether DAT is differentially sensitive to Ric-mediated regulation throughout the day remains unknown.

Our results describe a role for Ric in regulating DAT that impacts behavior and is driven by the majority of DA neurons due to our use of the *TH-GAL4* driver. *TH-GAL4* expressing cells can be subclassified into different groups based on localization (Mao and Davis, 2009). Several labs have isolated individual DA neurons and circuits that drive specific behaviors, such as aggression, memory, and reward, using genetic approaches (Aso et al., 2012; Alekseyenko et al., 2013; Rohwedder et al., 2016). For example, Rohwedder and colleagues demonstrated that four DA neurons in the larval *Drosophila* (i.e. the primary protocerebral anterior medial cluster) are required and sufficient for sucrose reward (Rohwedder et al., 2016). In general, these approaches rely on activating, inactivating, or ablating whole neurons in order to define the *Drosophila* circuits required for distinct DA-driven behaviors. Investigators recently published a genetic toolkit that leveraged GAL4, GAL80, and Split GAL4 lines to delicately control DA neuron activity and gene expression (Xie et al., 2018). Thus, future experiments can test whether DAT regulation is required for different DA-dependent behaviors with very high circuit resolution, and may reveal novel roles for Ric missed by this study given the limitations of our driver line.

We previously reported that the mammalian homolog of Ric, Rit2, is required in DA neurons for baseline anxiety behavior, however Rit2-KD had no effect on overall locomotion in mice, consistent with our results testing the role of DAergic Ric silence in *Drosophila* (Figure III.4). Notably, Rit2-KD changed the response to an acute cocaine injection; Rit2-KD increased cocaine sensitivity in male mice, and decreased cocaine sensitivity in females (Sweeney et al., 2020). Although cocaine binding to DAT is required for cocaine-induced reward (Chen et al., 2006), it is unclear whether Rit2-KD alters the cocaine response though DAT. *Drosophila* also exhibit psychostimulant-mediated hyperactivity and preference (Bainton et al., 2000; Andretic et al., 2005; Belovich et al., 2019), and dDAT is required for AMPH-dependent hyperlocomotion (Pizzo et al., 2013). Thus, future experiments should capitalize on the genetic tractability of *Drosophila* to examine whether Ric activity or expression in DA neurons is required for psychostimulant-based behaviors DAT-dependently. Of note, cocaine and AMPH also target the *Drosophila* SERT (dSERT) with similar affinities to dDAT (Porzgen et al., 2001). With the goal of specifically targeting dDAT, we preliminarily investigated dDAT's and dSERT's MPH affinity, with the hypothesis that MPH would preferentially compete for reuptake at dDAT, similar to the mammalian homologs (Han and Gu, 2006). Inhibitor dose-response curves performed in transfected HEK293T cells revealed, surprisingly, that the $IC_{50}$ of MPH for dDAT and dSERT does not significantly differ (dDAT: 43.0 ± 12.6μM vs. dSERT: 38.4 ± 10.6μM, two-tailed student's *t* test, p=0.79, n=5), whereas $IC_{50}$ values for hDAT and hSERT differed, as previously

reported (hDAT: 0.23 ± 0.12μM vs. hSERT: 158 ± 82.2μM, two-tailed student's *t* test, p=0.02, n=3-6). These results indicate that MPH is not selective for dDAT vs dSERT, and thus cannot be used to pharmacologically dissect DAT- vs SERT-selective behaviors. However, these results may help elucidate the specific residues required for MPH binding through conservation analyses.

The experiments presented here took an indirect approach to test whether endocytic DAT regulation impacts behavior. A more direct way of asking this pressing question would be to express trafficking-dysregulated mutants in place of WT DAT. Previous studies have demonstrated the feasibility of this method in *Drosophila*. Importantly, hDAT suffices to rescue hyperactivity and psychostimulant response in *fmn* flies (Hamilton et al., 2013; Pizzo et al., 2013; Hamilton et al., 2014; Pizzo et al., 2014). Using this approach, researchers overexpressed WT or mutant hDAT on the *fmn* background and found that hDAT coding variants identified in ASD patients (R51W and T356M) significantly increase locomotion and block/reduce the psychostimulant-mediated locomotor response (Hamilton et al., 2013; Cartier et al., 2015). These mutations do not affect regulated DAT endocytosis, but instead alter baseline DAT function and AMPH-mediated efflux. On the other hand, the ADHD-associated mutation, R615C-DAT, internalizes and recycles significantly faster than WT-DAT at basal states and these rates are no longer sensitive to PKC or AMPH stimulation (Sakrikar et al., 2012; Wu et al., 2015). Hence, this mutation causes a "gain-of-endocytic-function"

phenotype. Our group recently characterized a DAT/SERT chimera, in which the DAT N-terminus was replaced with the N-terminus (N-S/DAT). N-S/DAT constitutively internalizes significantly slower than WT-DAT and also does not undergo PKC-stimulated endocytosis, representing a “loss-of-endocytic-function” DAT mutant (Fagan et al., 2020). Together, these transporters provide important and novel tools for future experiments testing whether perturbing DAT trafficking directly impacts DA-dependent behaviors.

This study investigates a conserved role for DAT regulation in invertebrates that was previously undescribed. We demonstrate that dDAT is subject to regulation in a similar fashion as its mammalian counterparts in heterologous and intact DA neuron models. Furthermore, we found that disrupting this regulation through genetic tools perturbs DA-mediated behavior DAT-dependently. Future experiments that capitalize on DAT trafficking-dysfunctional mutants will further our understanding of how regulated DAT endocytosis influences DA transmission and behavior.

## III.E Experimental Procedures

### *Fly stocks*

All fly stocks were maintained on low yeast medium (g/L: 6.5 agar, 23.5 brewer’s yeast, 60 cornmeal; 60ml/L molasses, 4mL/L acid mix, 0.13% tegosept) at 25°C, 60% humidity, and on a 12-hour light/dark cycle. Isogenic $w^{1118}$ fly strain

(VDRC60000) was a gift from Dr. Patrick Emery (UMass Medical School), and was used as the wildtype (WT) control. Transgenic strains *TH-GAL4* and *fmn* were gifts from Dr. Heinrich Matthies (University of Alabama, Birmingham). Upstream activation sequence (UAS) stocks *UAS-HA-Ric*, *UAS-HA-RicQ117L*, and *UAS-HA-RicS73N* were generated using phiC31-mediated insertion at BestGene Inc. UAS-Ric RNAi stocks were from BDSC or VDRC (as indicated below, exact location within Ric gene indicated in Figure III.4). All fly strains were backcrossed to the $w^{1118}$ wildtype (+/+) strain for at least six generations and balanced prior to behavioral analysis. Transgenes were verified by eye color, or PCR, as necessary.

***RicRNAi target sequences***

*RNAi1 (VDRC 104782)*:

CGAAACAACATGGACACGACACATTGCTTTGAACATCTAGTTCCCAAGCCTT
TTCTCTTAAAACGTACTTTTTAATCGCTTAACTTTCGCGGCGAAAGCAATTCT
ATTATATTTCTACCCGCATTTGATTCGTTTTCGTGTTGGAGCTGTTGTTTTTC
TTTTTTTCGTCAGTCGATCTGTTTGGTTCGAACGGTTGCAGGATTCGCAATA
ACAATTAATTATTAGTAATTATGGGTAGTCCATTCAACTGTTTTTTGGGATCA
TGTAACAAACAGAGTAATTAAAGCCGTGTTAGTATTTTGTTTCCGGTGATGC
AGTTAACATTGATGAGAGGAACTCATGGTGATTGCTTAGAGAACGTGATGTG
TGGTTTCTTGTGGTAAAAGTAATCAACAGATTTCGTTAAACTAATAATAAATA
AACTTAGGCGTAACACGTGTGTCCTTAACAATATAAACAATAGACTTTTCTCA

AACTTAAACAACAAATGCATCGGCTGTCGTGGACTTAAATTATCAATTTGGG
CTTGGATCTGAAATGAA

*RNAi2 (BDSC 27520)*:

AGGGCAGAGAATTGGAGGATTTTTAAACTTATGTATGTACGTATTTACCCAG
AATACACGCACATGACATACGTTACACGAGCCACACATTTAACTAATCGAAT
AAATGTTGAATTTAATGTATACTAATATTATAAATCGATCGATCGACCTAAGA
AGTATGTAAAACGCGGGAACATTGCAAATTATGAAATATGAATGAGAATGTG
CGTTCATTTCAGATCCAAGCCCAAATTGATAATTTAAGTCCACGACAGCCGA
TGCATTTGTTGTTTAAGTTTGAGAAAAGTCTATTGTTTATATTGTTAAGGACA
CACGTGTTACGCCTAAGTTTATTTATTATTAGTTTAACGAAATCTGTTGATTA
CTTTTACCACAAGAAACCACACATCACGTTCTCTAAGCAATCACCATGAGTT
CCTCTCATCAATGTTAACTGCATCACCGGAAACA

*RNAi3 (VDRC 32929/CyO)*:

GGCCATGCGGGACCAATACATGCGTTGCGGCGAAGGTTTCATCATATGCTA
CTCGGTCACCGACCGCCACAGCTTCCAGGAGGCCTCCGAGTACAGGAAAC
TAATAACCCGTGTCCGCCTGTCCGAGGACATTCCGCTGGTTCTGATTGCCA
ACAAGGTGGACCTGGAGTCGCAGCGACGCGTGACCACCGAGGAGGGCCG
GAATCTCGCCAACCAGTTCGGCTGCCCGTTTTTTGAGACATCGGCTGCACT
GCGTCATTACATCGACGAGGCATTCTACACGTTGGTCCGCGAGATTCGACG

*RNAi4 (BDSC 41819)*:

TAGACGAGAGCGATTAAGCAA

***cDNA Constructs***

dDAT construct was purchased from Addgene Vector Database, cloned into pcDNA3.1(+), and HA-tagged on the N-terminus. Wildtype Ric construct was a gift from Dr. Douglas Harrison (University of Kentucky). Ric was cloned into pcDNA3.1(+) and tagged on the N-terminus with HA. Site-directed mutagenesis was performed using the QuikChange II kit in order to generate Ric activity mutants S73N and Q117L. dDAT and Ric were tagged by cutting with HindIII/XbaI and subcloned into pEYFP-C1 and cECFP-C1 vectors, respectively, for FRET microscopy experiments. HA-Ric constructs were cloned into 5XUAS-pUASTattB vector (gift from Dr. Marc Freeman (Vollum Institute – Oregon Health and Science University) for phiC31-mediated insertion by BestGene Inc. All sequences (including genomic DNA isolated from generated fly stocks) were verified by sanger sequencing (GeneWiz).

***Locomotor/sleep behavior***

Male progeny 0-3dpe were placed in the *Drosophila* Activity Monitor (DAM) system, and sleep and locomotor behavior were assessed at 25°C, 60% humidity, and 12hr light/dark (LD) cycle for 3 days, following 3 days of entrainment under the same conditions. At least 3 independent experiments with multiple flies were

performed for each genetic manipulation, and data from 3 days of LD were averaged from each experiment. Data were analyzed using the sleep and circadian analysis MATLAB program (SCAMP) (Donelson et al., 2012). Sleep was defined as 5 consecutive minutes of inactivity.

***Materials***

Nisoxetine was purchased from Tocris-Cookson and rabbit anti-HA antibody used was clone C29F4 from Cell Signaling Technology. All other reagents were from either Sigma-Aldrich or Fisher Scientific, and were of the highest possible grade.

***Cell culture and transfections***

HEK293T cell culture maintenance and transfections were done as described in *Chapter II: Experimental Procedures.*

***FRET***

FRET experiments were performed as described in *Chapter II: Experimental Procedures*.

***RNA extraction and RT-qPCR***

Male flies 0-5dpe were dissected in 1X PBS and RNA extraction, reverse transcription, and qPCR were done as described in *Chapter II: Experimental*

*Procedures*. TaqMan® Gene Expression Assays used are as follows: Ric (Dm01842764_g1), dGAPDH (Dm0184188_g1).

### *[$^3$H]DA uptake assay*

*Kinetics*

HEK293T cells were transfected with indicated constructs and [$^3$H]DA uptake was measured as described previously (Sweeney et al., 2017). Nonspecific uptake was defined using 10μM nisoxetine, a highly potent dDAT competitive inhibitor. HA-Ric construct expression was confirmed for each experiment via immunoblot, probing for HA tag.

*Ex vivo uptake*

Whole brain uptake assays were performed as described previously, with slight alterations (Cartier et al., 2015). Brains from male progeny 0-3dpe were dissected in hemolymph-like solution (70mM NaCl, 5mM KCl, 1.5mM $Ca^{2+}$ acetate, 10mM $MgSO_4$, 5mM HEPES, supplemented daily with fresh 115mM sucrose, 5mM trehalose, 10mM $NaHCO_3$, 10μM sodium ascorbate, 10μM pargyline) and incubated in HL3 ±10μM nisoxetine (nonspecific) for 30min at 25°C (4 brains/condition) in cell culture inserts. Uptake was measured using 1μM [$^3$H]DA, applied for 7min at RT (linear phase of uptake). Brains were washed 3x1mL ice cold KRH, transferred to 96-well plate, and solubilized in scintillation fluid. Radioactivity was measured using a Wallac MicroBeta scintillation plate counter.

### *Immunoblotting*

Immunoblotting was performed as described in *Chapter II: Experimental Procedures*.

### *BBS pulldown*

BBS-DAT pulldowns were performed as described in *Chapter II: Experimental Procedures*.

### *Statistical analysis*

All data were analyzed using GraphPad Prism software. Statistical outliers were identified and removed prior to analysis using Grubb's or Rout's outlier tests. Specific statistical tests are described within Figure legends. Student's *t* test was used to compare between two groups, unless the standard deviations were significantly different from each other (significant Bartlett's test). In these cases, a Welch's correction test was used. To compare among more than two experimental groups, a one-way ANOVA was used, with appropriate post-hoc multiple comparisons test(s), as described within each figure legend.

# CHAPTER IV

## Discussion and Future Directions

DA neurotransmission is a critical regulator of several behaviors and cognitive functions, including movement, sleep, reward, and cognition (Wise, 2004; Schultz, 2007a; Sulzer, 2011). Extracellular DA is cleared via reuptake through the presynaptic DAT; thus, DAT temporally and spatially controls DA signaling events. In the absence of DAT, or when DAT is competitively inhibited by either therapeutic or addictive psychostimulants, drastic disruptions occur in DA homeostasis and DA-dependent behaviors, such as locomotion (Giros et al., 1996; Kume et al., 2005; Ueno and Kume, 2014). DAT surface expression is therefore crucial to its primary function in maintaining DA homeostasis. Further, mutations in DAT found in patients with neuropsychiatric diseases and disorders, namely ADHD, ASD, BPD, and DTDS, disrupt DAT function and surface expression (Table I.1), further highlighting DAT's importance regulating typical DA neurotransmission. The molecular mechanisms underlying DAT surface expression regulation have been well-characterized over the past few decades (Kristensen et al., 2011; Bermingham and Blakely, 2016), however, the impact of regulated DAT endocytosis on behavior remains unexplored. In this thesis, I describe the specific mechanism by which Rit2 controls DAT internalization, and demonstrate a requirement for Rit2 in regulated DAT trafficking *in vivo*, with surprising region-specific differences (Chapter II). Additionally, I leveraged the *Drosophila* model

system to examine the physiological impact of regulated DAT endocytosis on DA-dependent behavior (Chapter III).

### IV.A Rit2 is required for PKC-stimulated DAT endocytosis

Acute PKC activation decreases DAT surface expression by increasing DAT internalization and reducing DAT recycling rates. Our lab previously reported that the neuronal GTPase Rit2 binds to DAT and is required for PKC-stimulated DAT internalization (Navaroli et al., 2011). However, there were several contradictions in this study that only truly came to light a few years after publishing this manuscript. First, Rit2 mRNA is limited to neuronal tissues, as demonstrated by multiple groups (Lee et al., 1996; Wes et al., 1996), yet we detected equivalent Rit2 immunoreactivity with the seemingly specific anti-Rit2 antibody across all cell lines examined (including non-neuronal HEK293T, HeLa, COS-1, CHO, and IMCD3 cells), suggesting Rit2 may be more ubiquitous than previously thought. Second, colocalization experiments performed in PC12 cells with overexpressed DAT and Rit2 constructs demonstrated that PKC activation by phorbol ester PMA induces DAT-Rit2 dissociation, but in co-IP experiments that relied on endogenous Rit2 expression, PKC activation increased the DAT-Rit2 association (Navaroli et al., 2011).

A study published two years later examined Rit2 mRNA in SK-N-MC and HEK293 cells, along with other human neuronal cell lines. Using human brain RNA as a

positive control, they found that SK-N-DZ cells express Rit2 mRNA, but SK-N-MC, HEK293T, and SK-N-AS cells express little to no Rit2 (Zhang et al., 2013). These new findings prompted me to re-evaluate Rit2 expression and potentially reinterpret our previous findings, especially since we presumably used shRNA to knockdown Rit2 in SK-N-MC cells to determine whether Rit2 is required for PKC-stimulated DAT functional downregulation (Navaroli et al., 2011). Indeed, using RT-qPCR probes specifically targeting Rit2, I did not detect substantial Rit2 mRNA in HEK293T, SK-N-MC, or PC12 cells, despite ample expression in mouse and rat midbrain lysates (Table II.1). These results were confirmed using a newly-available antibody (anti-Rit2 clone 4B5), which does not detect an artifactual ~20kDa immunoreactive band in HEK293T cells, whereas the original Rit2 antibody, clone 27G2, does (Figure II.1). Given this new insight into Rit2 expression patterns, I set out to ask, 1) whether Rit2 is, in fact, required for PKC-stimulated DAT internalization in heterologous cells and intact DA terminals, 2) how, or if, PKC activation alters the DAT-Rit2 interaction and what are the DAT domains involved in this process, and 3) whether Ack1 and Rit2 coordinate to facilitate PKC-stimulated DAT trafficking.

Using a reversible biotinylation assay to measure DAT endocytosis, I found that Rit2-KD in DAT-SK-N-DZ cells significantly reduced PKC-stimulated DAT internalization rates (Figure II.2), indicating that in cells with measurable Rit2 mRNA, Rit2 is required for PKC-dependent DAT endocytosis. One caveat to this

result is that I was never able to detect Rit2 protein in SK-N-DZ cells by either immunohistochemistry or immunoblotting. However, the anti-Rit2 4B5 antibody detects an immunoreactive band in mouse striatal and ventral midbrain tissues (albeit with low avidity), and conditional Rit2 silencing by viral delivery of Rit2 shRNA to mouse DA neurons also significantly blocked PKC-stimulated DAT surface loss in VS (Figure II.3). Taken together, these results indicate that, indeed, Rit2 is required for PKC-stimulated DAT internalization. Notably, we found that PKC does not stimulate DAT surface loss in DS in male or female mice (Figure II.3-4), providing the first evidence for 1) PKC-stimulated DAT trafficking in female mice and 2) region-specific PKC-dependent DAT surface loss. Previous experiments measuring DAT surface expression in acute striatal slices following PKC activation were done in coronal slices containing the whole striatum from male mice (Gabriel et al., 2013). Other groups have also identified dissimilarities between VS and DS in DAT function and trafficking; however, the underlying mechanisms remain unknown (Zhu et al., 2015; Gowrishankar et al., 2018). Possibly, DAT's intrinsic ability to undergo endocytosis differs in VS compared to DS. Alternatively, the proteins required for, or driving, trafficking events (PKC, Rit2, DRD2, etc.) are differentially expressed, or couple to different downstream signaling cascades. These data highlight that DAT surface regulation is context-dependent, and future experiments investigating the regional specificity of DAT trafficking will further elucidate the mechanisms controlling DAT surface dynamics.

*Endogenous PKC activation*

We demonstrated that PMA-mediated DAT endocytosis in VS requires PKC (Figure II.4). However, the specific isoform required is still not known, although conventional isoforms PKC$\alpha$, $\beta$I, $\delta$, or $\varepsilon$ are likely candidates (discussed in further detail in "Chapter I: *PKC-stimulated DAT trafficking*"). PKC activation occurs downstream of Gq-coupled GPCR activation, nevertheless the endogenous Gq-coupled receptors that putatively lead to PKC activation and DAT trafficking within DA terminals are largely unknown. Moreover, PMA treatment activates PKC in all cells within the striatum, and thus DAT surface changes could be due to PKC activation in nearby cells that feeds back onto DA terminals. One possible candidate Gq-coupled GPCR is the metabotropic glutamate receptor, mGluR5, which was demonstrated by Page and colleagues to stimulate DAT functional loss in a PKC-dependent manner (Page et al., 2001). Indeed, unpublished data from our lab indicate that mGluR5 activation by agonist (*RS*)-3,5-Dihydroxyphenylglycine (DHPG) initiates a biphasic DAT trafficking event in which DAT is initially delivered to the cell surface (within 5 minutes of DHPG application), followed by a subsequent DAT internalization event that re-establishes baseline DAT surface levels by 10 or 30 minutes in the VS and DS, respectively (Kearney and Melikian, unpublished data). Of note, mGluR5-mediated insertion requires DA release, DRD2 activation, and Vps35 expression, whereas the DAT endocytosis requires PKC activation and DAergic Rit2 expression. Future experiments will continue to explore this mechanism, specifically testing, via a conditional gene

knockout strategy, whether mGluR5 expression in DA terminals is required for biphasic DAT trafficking. Further, activating a chemogenetic Gq-GPCR (hM3Dq DREADD) expressed exclusively on DA terminals elicits the same biphasic DAT trafficking response, confirming that cell-autonomous PKC activation drives DAT internalization (Kearney and Melikian, unpublished data). Taken together, DAT undergoes phorbol ester- and receptor-mediated endocytosis in intact DA terminals, and Rit2 is a required component for both modes of stimulated DAT endocytosis.

*Is Rit2 required for AMPH's actions at DAT?*

Data from Chapter II support that Rit2 is required for PKC-stimulated DAT endocytosis, but whether Rit2 is required for other types of stimulated endocytosis, including AMPH-mediated DAT internalization, is unknown. In argument against a role for Rit2 in the mechanism underlying AMPH-stimulated trafficking, AMPH treatment increased the DAT-Rit2 surface association (Figure II.6), whereas I observed DAT and Rit2 dissociation following PKC-stimulated DAT endocytic brake release. This is consistent with previous studies indicating that AMPH- and PKC-stimulated DAT trafficking require distinct cellular mechanisms (Boudanova et al., 2008a; Hong and Amara, 2013; Wheeler et al., 2015), and differentially alter DAT microdomain localization (Navaroli et al., 2011; Butler et al., 2015). However, this interpretation must be considered more carefully, as Wheeler and colleagues did not examine whether RhoA GTPase (required for AMPH-stimulated

internalization) was similarly required for PKC-stimulated trafficking. Likewise, I did not examine whether AMPH-stimulated internalization requires Rit2. Interestingly, Hoshino and colleagues found that Rit2 associates with other Rho GTPase family members, Rac and Cdc42, and, in PC12 cells, Rit2 can activate RhoA (Hoshino and Nakamura, 2003; Hoshino et al., 2005). Thus, it is possible that AMPH-dependent DAT endocytosis also requires Rit2.

Is Rit2 required for AMPH-stimulated DA efflux via its potential role in DAT membrane localization? Our lab previously demonstrated that DAT and Rit2 colocalize significantly more in CTX+ microdomains (Navaroli et al., 2011). AMPH drives DAT into CTX+ domains (Butler et al., 2015) and increases DAT's association with Rit2 (Chapter II). Importantly, AMPH-stimulated efflux depends on DAT membrane localization in so far as depleting cholesterol redistributes DAT out of microdomains and reduces AMPH-dependent efflux (Cremona et al., 2011; Jones et al., 2012). Together these data suggest two possibilities: 1) AMPH-dependent increase in DAT-Rit2 association is simply a consequence of a change in DAT membrane localization, or 2) Rit2 is required for proper DAT lateral mobility and sublocalization. If the latter is true, I predict that Rit2-KD would block AMPH's ability to increase the DAT-CTX+ colocalization and, therefore, DA efflux. Moreover, Rit2 interacts significantly more with the N-S/DAT chimera, indicating that N-S/DAT may be mis-localized into primarily CTX+ domains. If this is the case, then N-S/DAT would not increase its association with Rit2 by AMPH treatment, or

exhibit AMPH-stimulated efflux. In further support of this prediction, previous studies have expertly demonstrated that AMPH-stimulated efflux requires phosphorylation of the DAT amino terminus, mediated by CaMKII$\alpha$, which binds to DAT's carboxyl terminus (Khoshbouei et al., 2004; Fog et al., 2006; Pizzo et al., 2014; Steinkellner et al., 2014). Thus, it is not necessarily unusual that Rit2 binding, also at the DAT C-terminus (Navaroli et al., 2011), could be influenced by the DAT N-terminus, or that Rit2 is one of the multiple DAT interacting proteins, (e.g. Flotillin-1 and $\alpha$-synuclein), that facilitates DAT membrane localization and psychostimulant response (Cremona et al., 2011; Lebowitz et al., 2019).

### IV.B Rit2-dependent DAT endocytic mechanism

In our previous study, we identified Rit2 as a novel protein bound to the DAT C-terminal endocytic domain, FREKLAYAIA, which negatively regulates basal DAT endocytosis and is required for PKC-stimulated internalization (Holton et al., 2005; Boudanova et al., 2008b; Navaroli et al., 2011). We further characterized the DAT-Rit2 interaction using live cell FRET microscopy with overexpressed constructs and discovered that Rit2 interacts with DAT, but not highly-related SERT or GAT1 (Navaroli et al., 2011), despite high sequence similarity within this domain among these transporters (Holton et al., 2005). Thus, other domains likely contribute to the DAT-Rit2 interaction. Given that SERT does not interact with Rit2, we used DAT/SERT chimeric transporters to examine whether the DAT N- and/or C-terminus is required for the interaction. These chimeras were described previously

by our lab to efficiently transport DA and express on the plasma membrane, although DAT/C-S and S/DAT/S express significantly less than WT-DAT or N-S/DAT (Sweeney et al., 2017). Again, we used live-cell FRET microscopy to test if the amino or carboxyl DAT terminus is required for the interaction with Rit2. To our surprise, Rit2 interacted with all four transporters, and N-S/DAT significantly increased the Rit2 interaction compared with WT-DAT (Figure II.7). Additionally, I found that PKC activation significantly reduced the DAT-Rit2 association at the cell surface (Figure II.6) and this effect was lost in the N-S/DAT chimera, and trended towards a loss in S/DAT/S (Figure II.7). These results correlated with data indicating that the N-S/DAT does not undergo PKC-stimulated internalization (Figure II.8). Altogether, these experiments indicate that Rit2 functions to stabilize DAT surface expression, must dissociate from DAT in order for PKC to stimulate DAT surface loss, and requires the DAT N-terminus for dissociation.

One limitation to this interpretation is that the loss of PKC-stimulated DAT-Rit2 dissociation only correlates with the loss of PKC-stimulated DAT internalization, exemplified by the N-S/DAT chimera. An approach to strengthen this conclusion could be to identify a Rit2 mutant that does not dissociate from DAT (e.g. Rit2-Q78L and Rit2-S34N constitutively active and dominant negative mutants, respectively). These mutants do not dissociate from DAT, as measured by colocalization analysis, and Rit2-S34N also blocks PKC-stimulated DAT internalization (Navaroli et al., 2011). I would therefore predict that, using the BBS-

DAT pulldown approach, PKC activation would no longer cause dissociation between mutant Rit2 and DAT. Nevertheless, even if the results of this experiment support the hypothesis, they still only provide correlative evidence that the dissociation is required for internalization. A more direct way to test this could be to use highly sensitive microscopy approaches used to visualize and measure membrane dynamics and protein-protein interactions at the cell surface in real time. Live TIRF microscopy, for example, permits simultaneous measurement of the DAT endocytic rate and the association between two tagged proteins, as was demonstrated by Lebowitz and colleagues (Lebowitz et al., 2019). This could also enable distinction between two possibilities: 1) PKC reduces the DAT-Rit2 association because only DATs bound to Rit2 can undergo stimulated internalization, and therefore the DATs remaining are less-likely to be associated with Rit2, or 2) PKC redistributes DAT away from Rit2-containing membrane microdomains, thereby indirectly reducing the DAT-Rit2 association, and subsequently causes DAT endocytosis from all microdomains indiscriminately. Given that DAT and Rit2 colocalize significantly more in CTX+ microdomains (Navaroli et al., 2011), and PKC preferentially targets DATs colocalized with CTX for internalization (Gabriel et al., 2013), I predict that PKC stimulates both DAT-Rit2 dissociation and DAT internalization from CTX+ domains, in support of the first hypothesis.

*Rit2 and Ack1 independently facilitate PKC-stimulated DAT internalization*

Multiple lines of evidence support the interpretation that Rit2 and Ack1 act independently to mediate DAT internalization following PKC activation. First, Rit2-KD in SK-N-DZ cells had no effect on PKC-dependent Ack1 inactivation (Figure II.9), indicating that Rit2 is not upstream of Ack1. Second, while Ack1 inactivation is required for PKC-stimulated internalization (Wu et al., 2015), it is not required for the PKC-dependent Rit2 dissociation from DAT, as evidenced by the result that CA Ack1 (S445P-Ack1) did not block PKC-stimulated Rit2 dissociation (Figure II.9). Third, while N-S/DAT did not undergo PKC-stimulated internalization, direct Ack1 inactivation by AIM100 significantly increased N-S/DAT endocytosis rates (Figure II.8). Given that Rit2 is not required for Ack1 inactivation, this result indicates that the DAT N-terminus is not required for Ack1-dependent endocytic brake release. Although I did not examine whether DAT N- and C-termini contribute to Rit2 dissociation by AIM100 treatment, I predict that if Rit2 dissociation is indeed requisite for endocytic brake release, then AIM100 would cause dissociation of Rit2 from DAT, N-S/DAT, and DAT/C-S, but not S/DAT/S as S/DAT/S does not exhibit AIM100-stimulated internalization. However, we must also consider that AIM100 binds noncompetitively to DAT and contributes to its oligomerization, and thus could bypass Rit2-dependent mechanisms to induce DAT endocytosis (Wu et al., 2015; Sorkina et al., 2018; Cheng et al., 2019). Together, my data support the conclusion that Rit2 and Ack1 independently converge on DAT for PKC-mediated internalization.

*Ack1 inactivation*

As discussed above, I initially hypothesized that Rit2 is required downstream of PKC for Ack1 inactivation, however Rit2-KD in SK-N-DZ cells did not block PKC-stimulated Ack1 inactivation (Figure II.9). This could reflect a possible role for Rit2 in regulating baseline Ack1 activity through Cdc42 activity, supported by experiments from one group that demonstrated Rit2-mediated Cdc42 activation (Hoshino and Nakamura, 2003). However, Rit2-KD in SK-N-DZ cells had no effect on steady-state Ack1 phosphorylation (data not shown), indicating that Rit2 is not required for Ack1 activation, and further supports that Rit2 functions independently from Ack1 to regulate DAT endocytosis. Therefore, the question still remains: what inactivates Ack1 downstream of PKC? A potential candidate is the E3 ubiquitin ligase, Nedd4-2. Nedd4-2 interacts with and downregulates Ack1 expression via ubiquitination (Chan et al., 2009), and was also identified in an RNAi-mediated screen for proteins required for PKC-stimulated DAT trafficking and DAT ubiquitination (Sorkina et al., 2006). Nedd4-2 associates with DAT and negatively regulates DAT endocytosis, supporting the hypothesis that these proteins are in close proximity to one another and could potentially work together to regulate DAT trafficking. Future experiments could take fairly straight-forward knockdown approaches to ask whether Nedd4-2 is required for PKC-stimulated Ack1 inactivation. Moreover, Nedd4-2 negatively regulates DAT endocytosis supporting the prediction that imposing the Ack1 endocytic brake (S445P-Ack1) would block

enhanced DAT trafficking caused by Nedd4-2 knockdown, further designating Nedd4-2 upstream of Ack1 as part of the DAT endocytic braking mechanism.

### IV.C Applications for the BBS-DAT pulldown approach

I describe a specific labeling approach for measuring DAT protein associations at the plasma membrane using a tagged DAT in Chapter II. Using our BBS-DAT construct I demonstrated a specific association with Rit2 and Ack1, but not Rit2's highly-related protein, Rit1 (Figure II.5). Further, I successfully measured drug-induced associations and dissociations between DAT and Rit2 using the BBS-DAT approach in heterologous cells (Figure II.6). The experimental advantages to utilizing the BBS-DAT labeling method include that it is specific to the surface DAT population, due to the extracellular location of the BBS tag, and circumvents the necessity of using antibodies to isolate DAT. This last factor is crucial, as the highest-affinity DAT antibody targets the DAT intracellular N-terminus and therefore, a) cells and tissue must be lysed prior to pulldown, and b) the antibody undoubtably disrupts associations occurring at the terminal domains, of which there are many (Table I.2). Indeed, I detected a specific DAT-Ack1 association using BBS-DAT, whereas co-IP approaches proved unsuccessful (Sweeney and Melikian, unpublished data). Accordingly, it is exciting to consider adapting BBS-DAT for use *in vivo* to interrogate the nature of the DAT protein complex within the endogenous DA terminal.

Similar methods for tagging DAT were described previously, nevertheless they have not yet been utilized for assessing protein complexes, nor can effectively label DAT in intact DA neurons (Sorkina et al., 2006; Rao et al., 2012; Hong and Amara, 2013; Wu et al., 2017). One group engineered a DAT construct containing an HA-tag inserted into EL2 in order to measure DAT internalization via an antibody feeding approach and DAT cellular localization in DA terminals (Sorkina et al., 2006; Rao et al., 2012; Block et al., 2015). This transporter takes up DA similar to WT-DAT and is localized to the cell surface in cultured DA neurons of HA-DAT knock-in mice (Rao et al., 2012). However, when researchers attempted high-resolution microscopy approaches to further probe DAT trafficking in intact DA neurons, they detected very little DAT signal on the membranes or in intracellular compartments (Block et al., 2015). This is likely due to the techniques employed (see “Chapter I: *Constitutive DAT trafficking*”), and HA-DAT may yet be of use to visualize endogenous DAT expression in DA terminals. In addition, Hong and Amara reported use of another BBS-tagged DAT to track internalized DAT (Hong and Amara, 2013). This tag is inserted at the same location in DAT EL2 as our construct, though it does not contain flanked linker sequences. Whether this BBS-tagged DAT could be employed to measure protein-protein associations biochemically remains untested. Finally, our group engineered a ligase acceptor protein (LAP) into DAT EL2 (LAP-DAT) in order to covalently couple a fluorophore to DAT and investigate DAT’s post-endocytic itinerary without using large antibodies or tags that could potentially mistarget DAT (Wu et al., 2017). This

approach was very effective for examining DAT recycling and endocytic compartment localization, but did not allow for *ex vivo* labeling in acute striatal slices, likely due to the inability of the large LpIA enzyme to infiltrate the slice and facilitate the fluorophore coupling reaction.

These examples highlight the challenges in the field surrounding tracking and isolating DAT in striatal slice preparations, uncovering a need for a different approach to characterize the DAT interactome with limited disruption. Future experiments can employ viral-mediated delivery of BBS-DAT specifically to mouse midbrain DA neurons where the endogenous DAT is concurrently removed by Cre-mediated excision. Thus, we can identify novel DAT interactors, test what domains are necessary and sufficient for specific interactions, measure drug- and stimulation-dependent changes, and examine whether the DAT complex is distinct between DS and VS. Despite that there are already greater than twenty unique DAT interacting proteins (Table I.2), many of these (including Rit2 and Ack1) have not been investigated in endogenous contexts where the proteins are not overexpressed. Furthermore, DAT mutants identified in patients, such as A559V- and R615C-DAT, may display defects in their protein-protein interactions, and tagging these mutants with BBS and expressing them in DA terminals provides a physiologically relevant way to address this question. Specifically, R615C-DAT interacts significantly more with CaMKII$\alpha$ and Flot1 in cells (Sakrikar et al., 2012), and A559V-DAT is differentially affected by DRD2-dependent signaling in the DS

but not VS (Gowrishankar et al., 2018). Nonetheless, whether these changes in interactions occur in the context of intact DA neurons, or if the disruptions in DAT function or expression results from altered interactions, remains unexplored. Altogether, BBS-DAT opens the door for studying the DAT interactome in its endogenous context in a minimally-disruptive manner.

### IV.D *In vivo* impact of regulated DAT endocytosis

Despite decades of research defining the numerous mechanisms underlying DAT surface regulation, across multiple models and systems (Eriksen et al., 2010a; Kristensen et al., 2011; Bermingham and Blakely, 2016), the physiological relevance of DAT trafficking is still not known. In Chapter III, I aimed to ask whether regulated DAT endocytosis is required for DA-dependent behavior using *Drosophila melanogaster* as the model organism. The fruit fly has been employed successfully to study neurotransmitter systems and the effects of psychostimulants on neurotransmission and behavior (Martin and Krantz, 2014). Further, DAT is conserved in *Drosophila*, and is required for typical locomotion, sleep, and psychostimulant response, as it is in mammals (Kume et al., 2005; Ueno and Kume, 2014). By targeting the *Drosophila* homolog of Rit2, Ric, I tested whether *Drosophila* provides a model system for investigating the DAT-Rit2 interaction and its impact on behavior. Through genetic manipulation of Ric, specifically in DA neurons, I tested whether Ric activity alters sleep and locomotor behavior in a DAT-dependent manner. I further examined whether Ric activity influences dDAT

function and surface expression in heterologous expression systems and intact *Drosophila* whole brain preparations. We found that dDAT and Ric interact to a similar degree as the mammalian homologs (Figure III.1). My results further indicate that constitutive Ric activity increases dDAT function (Figure III.2), but does not influence overall sleep or activity (Figure III.3). In addition, Ric knockdown by RNAi did not consistently alter locomotor or sleep (Figure III.4). However, DAergic expression of constitutively active Ric significantly increased the number of sleep episodes and, through an epistasis experiment, I discovered that this phenotype was dDAT-dependent (Figure III.5-6). These data are the first demonstrating that a protein that regulates DAT surface expression and function requires DAT in order to enact behavioral changes.

These findings are consistent with our previously published results in mice: DA neuron-specific Rit2-KD did not alter baseline locomotor activity (Sweeney et al., 2020). Instead, we only observed Rit2-dependent changes during behavioral challenges, such as anxiety paradigms and acute cocaine injection, although we do not know if this is due to Rit2's actions at DAT. This is a fairly straight-forward question to answer using the *Drosophila* model and epistasis approaches, as psychostimulants alter fruit fly behavior and DA transmission DAT-dependently (Makos et al., 2009; Pizzo et al., 2013). In preliminary studies, however, I found the behavioral response to oral cocaine administration in flies to be highly inconsistent (data not shown). In fact, previous studies exposed flies to volatilized

cocaine in order to elicit acute behavioral responses (McClung and Hirsh, 1998; Bainton et al., 2000). In one of the only available reports of cocaine feeding in adult fruit flies, researchers fed a low dose of cocaine mixed into food for 5-7 days, modeling chronic cocaine exposure (Chang et al., 2006). However, chronic cocaine feeding in flies causes morphological defects and reduces lifespan (Willard et al., 2006), further limiting the ability of cocaine to model acute psychostimulant exposure. Notably, cocaine also acts as a local anesthetic and causes arrhythmia via blockade of voltage-gated sodium and potassium channels (Schwartz et al., 2010). Given that I exposed flies to cocaine-containing food for 24 hours (longer exposures at higher doses ≥10mM were lethal, data not shown), and only sometimes saw hyperactivity, indicates that cocaine's actions at ion channels likely confounded my ability to detect hyperactivity. This is likely not the case for other psychostimulants, such as AMPH, which can be administered orally to adult and larval *Drosophila* to significantly increase locomotion (Andretic et al., 2005; Hamilton et al., 2013; Pizzo et al., 2013; Hamilton et al., 2014; Pizzo et al., 2014; Cartier et al., 2015; Belovich et al., 2019). Thus, future experiments using AMPH as the psychostimulant challenge, or volatilized cocaine, will ostensibly produce more interpretable results and allow us to ask whether DAergic Ric is required for psychostimulant behavior through its actions at DAT.

*Trafficking-dysregulated DAT mutants*

A limitation to our studies targeting Rit2 or Ric to perturb regulated DAT endocytosis is that this method indirectly affects DAT trafficking and likely has multiple off-target affects. One alternative approach to asking whether DAT trafficking influences *in vivo* behavior is to replace endogenous DAT with a trafficking-dysregulated DAT mutant, thereby eliminating any non-specific effects of knocking down a gene involved in multiple cellular processes. In order to test whether PKC-mediated trafficking is required for DA-dependent behavior, I propose using the N-S/DAT chimera. As described in Chapter II, N-S/DAT does not undergo PKC-mediated trafficking, and is more stable in the plasma membrane than WT-DAT, as evidenced by its decreased constitutive internalization rate (Figure II.8). Thus, N-S/DAT can be classified as a “loss-of-endocytic-function” transporter, and I predict N-S/DAT will replicate Rit2- and Ric-dependent phenotypes when expressed in place of WT-DAT, if Rit2 and Ric regulate behavior solely through DAT. Oppositely, the disease-associated DAT mutant, R615C-DAT, can be used to ask whether the DAT endocytic brake is required for DA-dependent behavior. R615C-DAT internalizes and recycles more rapidly than WT-DAT, and is insensitive to enhanced endocytosis by PKC or AMPH (Sakrikar et al., 2012), classifying it is a “gain-of-endocytic-function” transporter. R615C-DAT was identified in an ADHD patient proband; hence, I predict that it will increase locomotor activity when expressed *in vivo*. Additionally, R615C-DAT animals may be insensitive to AMPH-stimulated locomotion, given that R615C-DAT lacks

AMPH-mediated internalization. Whether AMPH stimulates N-S/DAT remains to be tested, however I predict that it does not, and therefore N-S/DAT-expressing animals would also lose AMPH-dependent behavior *in vivo*. Finally, our group demonstrated that imposing the Ack1 endocytic brake (S445P-Ack1) on R615C-DAT restored WT-DAT levels of constitutive internalization (Wu et al., 2015), thus it would be fascinating to test if S445P-Ack1 would likewise rescue behaviors specific to R615C-DAT expression.

Expressing mammalian DATs in *Drosophila* to examine the behavioral consequences of dysfunctional DAT mutants has been successfully demonstrated by multiple groups (Hamilton et al., 2013; Pizzo et al., 2013; Hamilton et al., 2014; Pizzo et al., 2014; Cartier et al., 2015; Asjad et al., 2017). In these studies, researchers used the dDAT null (*fmn*) genetic background and drove wildtype and mutant hDAT specifically in DA neurons using the DAergic *TH-GAL4* driver, thereby generating solely hDAT-expressing flies. Importantly, this strategy further demonstrated that hDAT is sufficient to significantly reduce the inherent hyperactivity of *fmn* flies (Hamilton et al., 2013). Over the course of my studies, I used the FlyC31 system through BestGene Inc. to insert human constructs expressing WT-DAT, R615C-DAT, and N-S/DAT into the fly genome, backcrossed the stocks, and recombined the flies onto the *fmn* background. However, I was unable to reduce hyperactivity of these flies compared to *fmn;TH-GAL4/+* controls (data not shown). I also did not detect hDAT protein expressed in the WT-DAT or

R615C-DAT flies with the highly specific DAT antibody (MAB369). However, I tagged N-S/DAT with HA given that MAB369 targets the DAT N-terminus, and I did detect specific HA signal in TH(+) cells in whole-mounted fly brains (data not shown), indicating that, for this transgene at least, DAT was expressed. The discrepancy between my results and those previously published is likely a result of the upstream activation sequence (UAS) vector I used to generate my constructs. We chose a UAS vector with only five repeats of the UAS cassette with the rationale that too much DAT expression may impede its ability to undergo regulated trafficking (Wu and Melikian, unpublished data). However, previous reports likely used the standard 10-repeat UAS vector (Hamilton et al., 2013; Pizzo et al., 2013), indicating that five UAS repeats is not sufficient to rescue *fmn*-mediated hyperactivity. Current experiments in our laboratory are underway using a molecular replacement strategy in mice to substitute mouse DAT with HA-tagged WT-DAT, R615C-DAT, and N-S/DAT specifically in DA neurons, in conjunction with Cre-mediated excision of the endogenous DAT gene. Using these mice, we can directly examine the behavioral and DA signaling consequences of dysregulated DAT endocytosis. This approach also avoids potential confounds due to expressing mutant DAT throughout development, since the replacement can be performed in juvenile and adult animals, after DA neurons and synapses have developed normally, allowing us to specifically investigate the impact of DAT trafficking defects.

*Drosophila DAT and SERT MPH affinity*

I proposed that another way to increase the specificity of my experiments would be to treat flies with a drug that specifically targets the DAergic system without the confound of 5-HT signaling. Cocaine is equipotent at DAT, SERT and NET in mammals, and in *Drosophila*, cocaine actually inhibits dSERT with an entire order of magnitude greater potency than dDAT (Porzgen et al., 2001). On the other hand, mammalian DAT and NET transporters are much higher affinity for MPH than SERT, allowing better specificity for dissecting the catecholamine system underlying psychostimulant-based behavior (Han and Gu, 2006; Hasenhuetl et al., 2015). This rationale, along with the fact that 1) *Drosophila* larvae exhibit hyperactivity following MPH exposure in a DAT-dependent manner (Pizzo et al., 2013), and 2) fruit flies do not express NET, prompted me to hypothesize that feeding flies MPH would allow us to better decipher whether Ric-dependent behaviors occur through changes specific to DAT. Moreover, oral MPH administration may be more efficacious than cocaine. First, however, I wanted to test whether MPH is similarly less efficacious at dSERT than dDAT. Surprisingly, I found that dDAT and dSERT exhibit comparable, yet fairly low, affinities for MPH (Chapter III, $IC_{50}$: ~40μM), indicating that, although MPH is selective for mammalian DATs over SERTs, it is not selective for dDAT over dSERT. This serendipitous finding may aid in uncovering the residues required for MPH binding. Previous reports describe the importance of residues L104, F105, and A109 in MPH and cocaine affinity for mouse DAT (Wu and Gu, 2003; Chen et al., 2005).

These residues are identical in hDAT, however dDAT contains a methionine at position 105, potentially contributing to its decreased MPH affinity. In fact, Wu and colleagues compared cocaine-dependent transport inhibition between dDAT, mDAT, and mDAT-F105M. They determined that mutating phenylalanine to methionine decreased mDAT cocaine inhibition compared to wildtype mDAT, although cocaine remained still more potent at mDAT-F105M than dDAT (Wu and Gu, 2003). Taken together, these data support the hypothesis that methionine 105 in dDAT contributes to MPH affinity as well, and I predict that mutating dDAT M105 to phenylalanine would increase MPH potency at dDAT. In conclusion, MPH likely does not distinguish between DA- and 5-HT-mediated phenotypes in *Drosophila*.

### IV.E Rit2 GTPase function and expression

The data presented in this thesis add to our growing knowledge of Rit2's intrinsic function in DA neurons. However, very little is known about Rit2 as a Ras-like GTPase "molecular switch", nor its activators (GAPs), exchange factors (GEFs), or effectors. Rit2 binds to GTP in its active form and requires a GAP to undergo GTP hydrolysis in order to switch to the inactive, GDP-bound form. The inactive state is reversed by a GEF, which activates GTPases by exchanging GDP for GTP (Wennerberg et al., 2005). Previous reports demonstrated that Rit2 can bind to certain Ras GEFs and effectors, however these experiments relied on truncated Rit2 constructs and *in vitro* binding assays (Shao et al., 1999; Hoshino and Nakamura, 2002; Hoshino et al., 2005), hence the endogenous mechanisms

underlying Rit2 activation and its downstream effectors in neurons remain completely unknown. Further, whether Rit2 binds to DAT in its active or inactive form, or both, is not known. In fact, Rit2 GTP-GDP exchange may be an important step in its dissociation from DAT at the plasma membrane. In our previous study, neither DN- nor CA-Rit2 dissociated from DAT when DAT internalized from the membrane, as measured by immunocytochemistry in transfected PC12 cells (Navaroli et al., 2011). Though qualitative, this result suggests that Rit2 GTPase switching may be a necessary component of PKC-mediated dissociation, and supports the prediction that Rit2 activity is likewise required for PKC-stimulated DAT internalization, as was already demonstrated for DN-Rit2 by our lab. Interestingly, the Klip group determined that PKC activates a GAP required for glutamate transporter 4 trafficking (Thong et al., 2007), indicating that PKC itself may activate a GAP upstream of Rit2, thereby facilitating Rit2 GTPase activity and DAT dissociation. Finally, an intriguing possibility is that undiscovered Rit2 effectors specifically facilitate PKC-dependent Rit2 dissociation and/or DAT internalization.

*DA neuron-independent Rit2 function*

Apart from regulating DAT surface expression, Rit2 is required for ERK and p38 MAP kinase activation, NGF-dependent neurite outgrowth, and cell viability in heterologous cell models (Hoshino and Nakamura, 2003; Shi et al., 2005; Uenaka et al., 2018). Cai and colleagues demonstrated a requirement for Ric in

survivability *in vivo* using null (*Ric*$^{-/-}$) fruit flies. They found that these flies are more susceptible to environmental stressors and display reduced p38 activation in response to *in vivo* heat-shock treatment compared to wildtype controls (Cai et al., 2011). Another indication of DA neuron-independent Rit2 function is that while Rit2 mRNA is enriched in DA neurons, it is also expressed in other neuronal tissues, including the hippocampus, amygdala, and retina (Lee et al., 1996; Wes et al., 1996; Zhou et al., 2011; Zhang et al., 2013). Nevertheless, Rit2's role in these brain regions remains uninvestigated. Finally, a role for neuronal Ric expression in cognitive function was unearthed in a screen for modulators of olfactory memory wherein pan-neuronal Ric knockdown with the driver, *Nsyb-GAL4*, significantly increased performance in a 3-hour memory task (Walkinshaw et al., 2015). However, the specific cell types or populations driving this phenotype were not examined. Thus, Rit2 in non-DAergic neurons remains unexplored, and future studies that follow this line of investigation will aid in our overall understanding of the mechanisms underlying Rit2's intrinsic cellular functions.

*DAT-independent Rit2 function*

Data from our laboratory indicate that Rit2 contributes to DAT expression, function, and trafficking. However, we cannot yet rule-out other potential Rit2 functions within the DA neuron that could influence DAergic signaling. In our previous study, we found that Rit2-KD in DA neurons significantly reduced TH and DAT mRNA in the ventral midbrain of male mice, however TH protein the striatum was unaffected

(Sweeney et al., 2020). This result could reflect the stability of TH protein in DA terminals, or indicate possible early stages of cell loss that had not yet impacted TH protein in the DA terminals. The consequences of long-term (>4 weeks) Rit2-KD on gene or protein expression have not yet been examined. Moreover, whether Rit2 modulates TH activity is completely unknown. To determine the impact of DAergic Rit2-KD on striatal signaling, we measured spontaneous excitatory postsynaptic potentials (sEPSPs) in DRD1(+) and DRD2(+) MSNs. Overall, Rit2-KD decreased baseline sEPSP frequency in DRD1(+) MSNs, but not DRD2(+), in male mice (Sweeney et al., 2020). This change in MSN physiology is indicative of changes in glutamatergic input onto MSNs occurring indirectly via alterations in DAergic signaling. Nevertheless, it remains unknown whether changes in DAT expression or function are solely responsible for these changes in DA transmission, if Rit2-KD increases or decreases DA release, or if Rit2 influences DA neuron firing rates. Future experiments will investigate Rit2's specific role across multiple DA neuron physiological properties.

*Rit2 sexual dimorphisms in DA signaling and behavior*

Rit2-KD differentially impacted male and female mice. As described above, Rit2-KD decreased TH and DAT mRNA in the ventral midbrain in male mice, but had no effect on either gene in females. Additionally, whereas Rit2-KD decreased overall DAT protein levels in the striatum of males, it had no effect on total DAT protein in female mice (Sweeney et al., 2020). Instead, we demonstrated in

Chapter II that Rit2-KD in females significantly decreased the surface:intracellular DAT ratio in VS. Rit2-KD-dependent MSN physiology changes also diverged in females: female DRD1(+) MSNs were unaffected by Rit2-KD, however Rit2-KD significantly decreased baseline sEPSP frequency in DRD2(+) MSNs. Furthermore, Rit2-KD affected the acute locomotor response in male and female mice differently: male mice responded to a sub-threshold cocaine dose following Rit2-KD, whereas females became less sensitive to cocaine, and displayed significantly reduced cocaine-dependent locomotion compared to controls (Sweeney et al., 2020). The mechanisms underlying these differences in Rit2-dependent DA neuron properties remain unexplored. Interestingly, a recent study from Calipari and colleagues identified a specific role for estradiol in driving enhanced DA neuron firing rates, DA release, and cocaine preference in oestrous females compared to males and dioestrous females (Calipari et al., 2017). Whether Rit2 contributes to the cellular processes underlying estrogen-dependent DA signaling and regulation is not known. Therefore, future experiments exploring this possibility will help us to better understand the sexual dimorphic mechanisms of DA neurotransmission, and will shed light on how Rit2 impacts DA neuron function and behavior.

*Rit2 in PD and neuronal viability*

Rit2 genetic variations have been identified in patients with various neurological diseases and disorders that are DAergic in nature (Table I.3). In particular, SNPs

in Rit2 have been identified in PD patients across multiple populations (Daneshmandpour et al., 2018), however whether Rit2 genetic anomalies contribute to disease progression remains unknown. Bossers and colleagues demonstrated a ~65% decrease in Rit2 expression in the SNc of PD patients, even after controlling for overall DA neuron death (Bossers et al., 2009). Nevertheless, it is unclear whether this reduction was caused by polymorphisms within the Rit2 gene, or if Rit2 loss-of-expression is responsible for reduced DA neuron viability. Since Rit2 activity likely contributes to neurite outgrowth (Shi et al., 2013; Uenaka et al., 2018), it stands to reason that introducing patient SNPs (Table I.3) into the Rit2 gene could trigger DA cell death, or reduce neuronal viability throughout aging. Moreover, it will be fascinating to examine whether this effect is specific to DA neurons, or if Rit2 contributes to neuron survival generally. DAergic Rit2-KD experiments performed in our laboratory thus far have not extended past 4 weeks of shRNA-mediated gene silencing. Hence, future experiments employing long-term Rit2-KD using our conditional and inducible model will bolster the field's understanding of how Rit2 impacts DA neuron viability, and may substantiate Rit2 as a PD risk factor.

## IV.F Concluding remarks

Throughout the course of this thesis research, our understanding of the mechanisms underlying DAT trafficking increased substantially. With the development of novel tools, we can now examine DAT-protein interactions and

surface regulation in endogenous contexts with minimal disruption and mis-targeting. Our lab and others have further characterized a multitude of mechanisms regulating DAT surface stability and trafficking, and have begun investigating the *in vivo* impact of disrupted DAT function. My studies shed light on the PKC-stimulated DAT internalization mechanism, and leveraged a new conditional and inducible DAergic knockdown approach to examine this mechanism for the first time in intact DA terminals. I also demonstrate that indirectly perturbing this process in *Drosophila* alters certain DA-driven behaviors in a DAT-dependent manner, providing some of the first evidence that DAT surface regulation influences behavior. Many salient questions still remain, including whether DAT trafficking directly impacts behavior, and defining the molecular mechanisms of Rit2 GTPase-dependent signaling. I expect that by continuing to study the mechanisms fundamental to regulated DAT trafficking we will greatly increase our understanding of typical DA neurotransmission and homeostasis, as well as the aberrant signaling states present in patients with neuropsychiatric diseases and disorders.

## Bibliography

Adkins EM, Samuvel DJ, Fog JU, Eriksen J, Jayanthi LD, Vaegter CB, Ramamoorthy S, Gether U (2007) Membrane mobility and microdomain association of the dopamine transporter studied with fluorescence correlation spectroscopy and fluorescence recovery after photobleaching. Biochemistry 46:10484-10497.

Alekseyenko OV, Chan YB, Li R, Kravitz EA (2013) Single dopaminergic neurons that modulate aggression in Drosophila. Proc Natl Acad Sci U S A 110:6151-6156.

Andretic R, van Swinderen B, Greenspan RJ (2005) Dopaminergic modulation of arousal in Drosophila. Curr Biol 15:1165-1175.

Anzalone A, Lizardi-Ortiz JE, Ramos M, De Mei C, Hopf FW, Iaccarino C, Halbout B, Jacobsen J, Kinoshita C, Welter M, Caron MG, Bonci A, Sulzer D, Borrelli E (2012) Dual control of dopamine synthesis and release by presynaptic and postsynaptic dopamine D2 receptors. J Neurosci 32:9023-9034.

Ashok AH, Marques TR, Jauhar S, Nour MM, Goodwin GM, Young AH, Howes OD (2017) The dopamine hypothesis of bipolar affective disorder: the state of the art and implications for treatment. Mol Psychiatry 22:666-679.

Asjad HMM, Kasture A, El-Kasaby A, Sackel M, Hummel T, Freissmuth M, Sucic S (2017) Pharmacochaperoning in a Drosophila model system rescues human dopamine transporter variants associated with infantile/juvenile parkinsonism. J Biol Chem 292:19250-19265.

Aso Y, Herb A, Ogueta M, Siwanowicz I, Templier T, Friedrich AB, Ito K, Scholz H, Tanimoto H (2012) Three dopamine pathways induce aversive odor memories with different stability. PLoS Genet 8:e1002768.

Axelrod J (2003) Journey of a late blooming biochemical neuroscientist. J Biol Chem 278:1-13.

Axelrod J, Tomchick R (1958) Enzymatic O-methylation of epinephrine and other catechols. J Biol Chem 233:702-705.

Bainton RJ, Tsai LT, Singh CM, Moore MS, Neckameyer WS, Heberlein U (2000) Dopamine modulates acute responses to cocaine, nicotine and ethanol in Drosophila. Curr Biol 10:187-194.

Barlowe C (1994) COPII: A membrane coat formed by Sec proteins that drive vesicle budding from the endoplasmic reticulum. Cell 77:895-907.

Bauman AL, Apparsundaram S, Ramamoorthy S, Wadzinski BE, Vaughan RA, Blakely RD (2000) Cocaine and antidepressant-sensitive biogenic amine transporters exist in regulated complexes with protein phosphatase 2A. J Neurosci 20:7571-7578.

Beaulieu JM, Gainetdinov RR (2011) The physiology, signaling, and pharmacology of dopamine receptors. Pharmacol Rev 63:182-217.

Beckman ML, Bernstein EM, Quick MW (1998) Protein Kinase C Regulates the Interaction between a GABA Transporter and Syntaxin 1A. J Neurosci 18:6103-6112.

Belovich AN, Aguilar JI, Mabry SJ, Cheng MH, Zanella D, Hamilton PJ, Stanislowski DJ, Shekar A, Foster JD, Bahar I, Matthies HJG, Galli A (2019) A network of phosphatidylinositol (4,5)-bisphosphate (PIP2) binding sites on the dopamine transporter regulates amphetamine behavior in Drosophila Melanogaster. Mol Psychiatry.

Bendor J, Lizardi-Ortiz JE, Westphalen RI, Brandstetter M, Hemmings HC, Jr., Sulzer D, Flajolet M, Greengard P (2010) AGAP1/AP-3-dependent endocytic recycling of M5 muscarinic receptors promotes dopamine release. EMBO J 29:2813-2826.

Bermingham DP, Blakely RD (2016) Kinase-dependent Regulation of Monoamine Neurotransmitter Transporters. Pharmacol Rev 68:888-953.

Bertran-Gonzalez J, Herve D, Girault JA, Valjent E (2010) What is the Degree of Segregation between Striatonigral and Striatopallidal Projections? Front Neuroanat 4.

Biermann B, Sokoll S, Klueva J, Missler M, Wiegert JS, Sibarita JB, Heine M (2014) Imaging of molecular surface dynamics in brain slices using single-particle tracking. Nat Commun 5:3024.

Binda F, Dipace C, Bowton E, Robertson SD, Lute BJ, Fog JU, Zhang M, Sen N, Colbran RJ, Gnegy ME, Gether U, Javitch JA, Erreger K, Galli A (2008) Syntaxin 1A interaction with the dopamine transporter promotes amphetamine-induced dopamine efflux. Mol Pharmacol 74:1101-1108.

Bjerggaard C, Fog JU, Hastrup H, Madsen K, Loland CJ, Javitch JA, Gether U (2004) Surface targeting of the dopamine transporter involves discrete epitopes in the distal C terminus but does not require canonical PDZ domain interactions. J Neurosci 24:7024-7036.

Blackburn KJ, French PC, Merrills RJ (1967) 5-hydroxytryptamine uptake by rat brain. Life Sciences 6:1653-1663.

Blakely RD, Berson HE, Fremeau RT, Jr., Caron MG, Peek MM, Prince HK, Bradley CC (1991) Cloning and expression of a functional serotonin transporter from rat brain. Nature 354:66-70.

Blaschko H (1952) Amine oxidase and amine metabolism. Pharmacol Rev 4:415-458.

Block ER, Nuttle J, Balcita-Pedicino JJ, Caltagarone J, Watkins SC, Sesack SR, Sorkin A (2015) Brain Region-Specific Trafficking of the Dopamine Transporter. J Neurosci 35:12845-12858.

Bogdanov Y, Michels G, Armstrong-Gold C, Haydon PG, Lindstrom J, Pangalos M, Moss SJ (2006) Synaptic GABAA receptors are directly recruited from their extrasynaptic counterparts. EMBO J 25:4381-4389.

Bolam JP, Hanley JJ, Booth PA, Bevan MD (2000) Synaptic organisation of the basal ganglia. J Anat 196 ( Pt 4):527-542.

Bolan EA, Kivell B, Jaligam V, Oz M, Jayanthi LD, Han Y, Sen N, Urizar E, Gomes I, Devi LA, Ramamoorthy S, Javitch JA, Zapata A, Shippenberg TS (2007) D2 receptors regulate dopamine transporter function via an extracellular

signal-regulated kinases 1 and 2-dependent and phosphoinositide 3 kinase-independent mechanism. Mol Pharmacol 71:1222-1232.
Bossers K, Meerhoff G, Balesar R, van Dongen JW, Kruse CG, Swaab DF, Verhaagen J (2009) Analysis of gene expression in Parkinson's disease: possible involvement of neurotrophic support and axon guidance in dopaminergic cell death. Brain Pathol 19:91-107.
Boudanova E, Navaroli DM, Melikian HE (2008a) Amphetamine-induced decreases in dopamine transporter surface expression are protein kinase C-independent. Neuropharmacology 54:605-612.
Boudanova E, Navaroli DM, Stevens Z, Melikian HE (2008b) Dopamine transporter endocytic determinants: carboxy terminal residues critical for basal and PKC-stimulated internalization. Mol Cell Neurosci 39:211-217.
Bouquillon S, Andrieux J, Landais E, Duban-Bedu B, Boidein F, Lenne B, Vallee L, Leal T, Doco-Fenzy M, Delobel B (2011) A 5.3Mb deletion in chromosome 18q12.3 as the smallest region of overlap in two patients with expressive speech delay. Eur J Med Genet 54:194-197.
Bowton E, Saunders C, Reddy IA, Campbell NG, Hamilton PJ, Henry LK, Coon H, Sakrikar D, Veenstra-VanderWeele JM, Blakely RD, Sutcliffe J, Matthies HJ, Erreger K, Galli A (2014) SLC6A3 coding variant Ala559Val found in two autism probands alters dopamine transporter function and trafficking. Transl Psychiatry 4:e464.
Brüss M, Pörzgen P, Bryan-Lluka LJ, Bönisch H (1997) The rat norepinephrine transporter: molecular cloning from PC12 cells and functional expression. Molecular Brain Research 52:257-262.
Burger C, Nguyen FN, Deng J, Mandel RJ (2005) Systemic mannitol-induced hyperosmolality amplifies rAAV2-mediated striatal transduction to a greater extent than local co-infusion. Mol Ther 11:327-331.
Burke DA, Rotstein HG, Alvarez VA (2017) Striatal Local Circuitry: A New Framework for Lateral Inhibition. Neuron 96:267-284.
Butler B, Saha K, Rana T, Becker JP, Sambo D, Davari P, Goodwin JS, Khoshbouei H (2015) Dopamine Transporter Activity Is Modulated by alpha-Synuclein. J Biol Chem 290:29542-29554.
Cachope R, Mateo Y, Mathur BN, Irving J, Wang HL, Morales M, Lovinger DM, Cheer JF (2012) Selective activation of cholinergic interneurons enhances accumbal phasic dopamine release: setting the tone for reward processing. Cell Rep 2:33-41.
Cai W, Rudolph JL, Harrison SM, Jin L, Frantz AL, Harrison DA, Andres DA (2011) An evolutionarily conserved Rit GTPase-p38 MAPK signaling pathway mediates oxidative stress resistance. Mol Biol Cell 22:3231-3241.
Calipari ES, Juarez B, Morel C, Walker DM, Cahill ME, Ribeiro E, Roman-Ortiz C, Ramakrishnan C, Deisseroth K, Han MH, Nestler EJ (2017) Dopaminergic dynamics underlying sex-specific cocaine reward. Nat Commun 8:13877.
Cargill M, Altshuler D, Ireland J, Sklar P, Ardlie K, Patil N, Lane CR, Lim EP, Kalyanaraman N, Nemesh J, Ziaugra L, Friedland L, Rolfe A, Warrington J,

Lipshutz R, Daley GQ, Lander ES (1999) Characterization of single-nucleotide polymorphisms in coding regions of human genes. Nature Genetics 22:231-238.

Carlsson A (1959) The occurrence, distribution and physiological role of catecholamines in the nervous system. Pharmacol Rev 11:490-493.

Carlsson A (2002) Treatment of Parkinson's with L-DOPA. The early discovery phase, and a comment on current problems. J Neural Transm (Vienna) 109:777-787.

Carlsson A, Lindqvist M, Magnusson T (1957) 3,4-Dihydroxyphenylalanine and 5-hydroxytryptophan as reserpine antagonists. Nature 180:1200.

Carlsson A, Lindqvist M, Magnusson T, Waldeck B (1958) On the presence of 3-hydroxytyramine in brain. Science 127:471.

Carneiro AM, Ingram SL, Beaulieu JM, Sweeney A, Amara SG, Thomas SM, Caron MG, Torres GE (2002) The multiple LIM domain-containing adaptor protein Hic-5 synaptically colocalizes and interacts with the dopamine transporter. J Neurosci 22:7045-7054.

Cartier E, Hamilton PJ, Belovich AN, Shekar A, Campbell NG, Saunders C, Andreassen TF, Gether U, Veenstra-Vanderweele J, Sutcliffe JS, Ulery-Reynolds PG, Erreger K, Matthies HJ, Galli A (2015) Rare autism-associated variants implicate syntaxin 1 (STX1 R26Q) phosphorylation and the dopamine transporter (hDAT R51W) in dopamine neurotransmission and behaviors. EBioMedicine 2:135-146.

Carvelli L, Moron JA, Kahlig KM, Ferrer JV, Sen N, Lechleiter JD, Leeb-Lundberg LM, Merrill G, Lafer EM, Ballou LM, Shippenberg TS, Javitch JA, Lin RZ, Galli A (2002) PI 3-kinase regulation of dopamine uptake. J Neurochem 81:859-869.

Cervinski MA, Foster JD, Vaughan RA (2005) Psychoactive substrates stimulate dopamine transporter phosphorylation and down-regulation by cocaine-sensitive and protein kinase C-dependent mechanisms. J Biol Chem 280:40442-40449.

Cervinski MA, Foster JD, Vaughan RA (2010) Syntaxin 1A regulates dopamine transporter activity, phosphorylation and surface expression. Neuroscience 170:408-416.

Chan G, White CC, Winn PA, Cimpean M, Replogle JM, Glick LR, Cuerdon NE, Ryan KJ, Johnson KA, Schneider JA, Bennett DA, Chibnik LB, Sperling RA, De Jager PL, Bradshaw EM (2016) Trans-pQTL study identifies immune crosstalk between Parkinson and Alzheimer loci. Neurol Genet 2:e90.

Chan W, Tian R, Lee YF, Sit ST, Lim L, Manser E (2009) Down-regulation of active ACK1 is mediated by association with the E3 ubiquitin ligase Nedd4-2. J Biol Chem 284:8185-8194.

Chang D, Nalls MA, Hallgrímsdóttir IB, Hunkapiller J, van der Brug M, Cai F, Kerchner GA, Ayalon G, Bingol B, Sheng M, Hinds D, Behrens TW, Singleton AB, Bhangale TR, Graham RR (2017) A meta-analysis of

genome-wide association studies identifies 17 new Parkinson's disease risk loci. Nature Genetics 49:1511-1516.

Chang HY, Grygoruk A, Brooks ES, Ackerson LC, Maidment NT, Bainton RJ, Krantz DE (2006) Overexpression of the Drosophila vesicular monoamine transporter increases motor activity and courtship but decreases the behavioral response to cocaine. Mol Psychiatry 11:99-113.

Chen H, Fre S, Slepnev VI, Capua MR, Takei K, Butler MH, Di Fiore PP, De Camilli P (1998) Epsin is an EH-domain-binding protein implicated in clathrin-mediated endocytosis. Nature 394:793-797.

Chen R, Han DD, Gu HH (2005) A triple mutation in the second transmembrane domain of mouse dopamine transporter markedly decreases sensitivity to cocaine and methylphenidate. J Neurochem 94:352-359.

Chen R, Daining CP, Sun H, Fraser R, Stokes SL, Leitges M, Gnegy ME (2013) Protein kinase Cbeta is a modulator of the dopamine D2 autoreceptor-activated trafficking of the dopamine transporter. J Neurochem 125:663-672.

Chen R, Tilley MR, Wei H, Zhou F, Zhou FM, Ching S, Quan N, Stephens RL, Hill ER, Nottoli T, Han DD, Gu HH (2006) Abolished cocaine reward in mice with a cocaine-insensitive dopamine transporter. Proc Natl Acad Sci U S A 103:9333-9338.

Cheng MH, Ponzoni L, Sorkina T, Lee JY, Zhang S, Sorkin A, Bahar I (2019) Trimerization of dopamine transporter triggered by AIM-100 binding: Molecular mechanism and effect of mutations. Neuropharmacology:107676.

Chi L, Reith ME (2003) Substrate-induced trafficking of the dopamine transporter in heterologously expressing cells and in rat striatal synaptosomal preparations. J Pharmacol Exp Ther 307:729-736.

Colicelli J (2004) Human RAS superfamily proteins and related GTPases. Sci STKE 2004:RE13.

Cotzias GC, Van Woert MH, Schiffer LM (1967) Aromatic amino acids and modification of parkinsonism. N Engl J Med 276:374-379.

Cragg SJ, Baufreton J, Xue Y, Bolam JP, Bevan MD (2004) Synaptic release of dopamine in the subthalamic nucleus. Eur J Neurosci 20:1788-1802.

Cremona ML, Matthies HJ, Pau K, Bowton E, Speed N, Lute BJ, Anderson M, Sen N, Robertson SD, Vaughan RA, Rothman JE, Galli A, Javitch JA, Yamamoto A (2011) Flotillin-1 is essential for PKC-triggered endocytosis and membrane microdomain localization of DAT. Nat Neurosci 14:469-477.

Daneshmandpour Y, Darvish H, Emamalizadeh B (2018) RIT2: responsible and susceptible gene for neurological and psychiatric disorders. Mol Genet Genomics 293:785-792.

Daniels GM, Amara SG (1999) Regulated trafficking of the human dopamine transporter. Clathrin-mediated internalization and lysosomal degradation in response to phorbol esters. J Biol Chem 274:35794-35801.

De Gois S, Slama P, Pietrancosta N, Erdozain AM, Louis F, Bouvrais-Veret C, Daviet L, Giros B (2015) Ctr9, a Protein in the Transcription Complex Paf1, Regulates Dopamine Transporter Activity at the Plasma Membrane. J Biol Chem 290:17848-17862.

Demchyshyn LL, Pristupa ZB, Sugamori KS, Barker EL, Blakely RD, Wolfgang WJ, Forte MA, Niznik HB (1994) Cloning, expression, and localization of a chloride-facilitated, cocaine-sensitive serotonin transporter from Drosophila melanogaster. Proc Natl Acad Sci U S A 91:5158-5162.

Di Chiara G, Imperato A (1988) Drugs abused by humans preferentially increase synaptic dopamine concentrations in the mesolimbic system of freely moving rats. Proc Natl Acad Sci U S A 85:5274-5278.

DiCarlo GE, Aguilar JI, Matthies HJ, Harrison FE, Bundschuh KE, West A, Hashemi P, Herborg F, Rickhag M, Chen H, Gether U, Wallace MT, Galli A (2019) Autism-linked dopamine transporter mutation alters striatal dopamine neurotransmission and dopamine-dependent behaviors. J Clin Invest 130.

Donelson NC, Kim EZ, Slawson JB, Vecsey CG, Huber R, Griffith LC (2012) High-resolution positional tracking for long-term analysis of Drosophila sleep and locomotion using the "tracker" program. PLoS One 7:e37250.

Doolen S, Zahniser NR (2001) Protein tyrosine kinase inhibitors alter human dopamine transporter activity in Xenopus oocytes. J Pharmacol Exp Ther 296:931-938.

Egana LA, Cuevas RA, Baust TB, Parra LA, Leak RK, Hochendoner S, Pena K, Quiroz M, Hong WC, Dorostkar MM, Janz R, Sitte HH, Torres GE (2009) Physical and functional interaction between the dopamine transporter and the synaptic vesicle protein synaptogyrin-3. J Neurosci 29:4592-4604.

Eissa N, Al-Houqani M, Sadeq A, Ojha SK, Sasse A, Sadek B (2018) Current Enlightenment About Etiology and Pharmacological Treatment of Autism Spectrum Disorder. Front Neurosci 12:304.

Emamalizadeh B, Movafagh A, Akbari M, Kazeminasab S, Fazeli A, Motallebi M, Shahidi GA, Petramfar P, Mirfakhraie R, Darvish H (2014) RIT2, a susceptibility gene for Parkinson's disease in Iranian population. Neurobiol Aging 35:e27-e28.

Emamalizadeh B et al. (2017) RIT2 Polymorphisms: Is There a Differential Association? Mol Neurobiol 54:2234-2240.

Eriksen J, Jorgensen TN, Gether U (2010a) Regulation of dopamine transporter function by protein-protein interactions: new discoveries and methodological challenges. J Neurochem 113:27-41.

Eriksen J, Bjorn-Yoshimoto WE, Jorgensen TN, Newman AH, Gether U (2010b) Postendocytic sorting of constitutively internalized dopamine transporter in cell lines and dopaminergic neurons. J Biol Chem 285:27289-27301.

Eriksen J, Rasmussen SG, Rasmussen TN, Vaegter CB, Cha JH, Zou MF, Newman AH, Gether U (2009) Visualization of dopamine transporter

trafficking in live neurons by use of fluorescent cocaine analogs. J Neurosci 29:6794-6808.

Fagan RR, Kearney PJ, Sweeney CG, Luethi D, Uiterkamp FES, Schicker K, Alejandro BS, O'Connor LC, Sitte HH, Melikian HE (2020) Dopamine transporter trafficking and Rit2 GTPase: Mechanism of action and in vivo impact. Journal of Biological Chemistry.

Farhan H, Reiterer V, Korkhov VM, Schmid JA, Freissmuth M, Sitte HH (2007) Concentrative export from the endoplasmic reticulum of the gamma-aminobutyric acid transporter 1 requires binding to SEC24D. J Biol Chem 282:7679-7689.

Faure A, Haberland U, Conde F, El Massioui N (2005) Lesion to the nigrostriatal dopamine system disrupts stimulus-response habit formation. J Neurosci 25:2771-2780.

Ferris MJ, Espana RA, Locke JL, Konstantopoulos JK, Rose JH, Chen R, Jones SR (2014) Dopamine transporters govern diurnal variation in extracellular dopamine tone. Proc Natl Acad Sci U S A 111:E2751-2759.

Fischer JF, Cho AK (1979) Chemical release of dopamine from striatal homogenates: evidence for an exchange diffusion model. J Pharmacol Exp Ther 208:203-209.

Fog JU, Khoshbouei H, Holy M, Owens WA, Vaegter CB, Sen N, Nikandrova Y, Bowton E, McMahon DG, Colbran RJ, Daws LC, Sitte HH, Javitch JA, Galli A, Gether U (2006) Calmodulin kinase II interacts with the dopamine transporter C terminus to regulate amphetamine-induced reverse transport. Neuron 51:417-429.

Foo JN et al. (2017) Genome-wide association study of Parkinson's disease in East Asians. Hum Mol Genet 26:226-232.

Foster DJ, Gentry PR, Lizardi-Ortiz JE, Bridges TM, Wood MR, Niswender CM, Sulzer D, Lindsley CW, Xiang Z, Conn PJ (2014) M5 receptor activation produces opposing physiological outcomes in dopamine neurons depending on the receptor's location. J Neurosci 34:3253-3262.

Foster JD, Pananusorn B, Vaughan RA (2002) Dopamine transporters are phosphorylated on N-terminal serines in rat striatum. J Biol Chem 277:25178-25186.

Foster JD, Adkins SD, Lever JR, Vaughan RA (2008) Phorbol ester induced trafficking-independent regulation and enhanced phosphorylation of the dopamine transporter associated with membrane rafts and cholesterol. J Neurochem 105:1683-1699.

Fowler CJ, Benedetti MS (1983) The metabolism of dopamine by both forms of monoamine oxidase in the rat brain and its inhibition by cimoxatone. J Neurochem 40:1534-1541.

Franekova V, Baliova M, Jursky F (2008) Truncation of human dopamine transporter by protease calpain. Neurochem Int 52:1436-1441.

Freyberg Z et al. (2016) Mechanisms of amphetamine action illuminated through optical monitoring of dopamine synaptic vesicles in Drosophila brain. Nat Commun 7:10652.

Friggi-Grelin F, Coulom H, Meller M, Gomez D, Hirsh J, Birman S (2003) Targeted gene expression in Drosophila dopaminergic cells using regulatory sequences from tyrosine hydroxylase. J Neurobiol 54:618-627.

Fuke S, Suo S, Takahashi N, Koike H, Sasagawa N, Ishiura S (2001) The VNTR polymorphism of the human dopamine transporter (DAT1) gene affects gene expression. Pharmacogenomics J 1:152-156.

Furman CA, Lo CB, Stokes S, Esteban JA, Gnegy ME (2009a) Rab 11 regulates constitutive dopamine transporter trafficking and function in N2A neuroblastoma cells. Neurosci Lett 463:78-81.

Furman CA, Chen R, Guptaroy B, Zhang M, Holz RW, Gnegy M (2009b) Dopamine and amphetamine rapidly increase dopamine transporter trafficking to the surface: live-cell imaging using total internal reflection fluorescence microscopy. J Neurosci 29:3328-3336.

Gabriel L, Stevens Z, Melikian H (2009) Measuring plasma membrane protein endocytic rates by reversible biotinylation. J Vis Exp.

Gabriel LR, Wu S, Kearney P, Bellve KD, Standley C, Fogarty KE, Melikian HE (2013) Dopamine transporter endocytic trafficking in striatal dopaminergic neurons: differential dependence on dynamin and the actin cytoskeleton. J Neurosci 33:17836-17846.

Gainetdinov RR, Jones SR, Fumagalli F, Wightman RM, Caron MG (1998) Re-evaluation of the role of the dopamine transporter in dopamine system homeostasis. Brain Res Brain Res Rev 26:148-153.

Garcia BG, Wei Y, Moron JA, Lin RZ, Javitch JA, Galli A (2005) Akt is essential for insulin modulation of amphetamine-induced human dopamine transporter cell-surface redistribution. Mol Pharmacol 68:102-109.

Garcia-Olivares J, Baust T, Harris S, Hamilton P, Galli A, Amara SG, Torres GE (2017) Gbetagamma subunit activation promotes dopamine efflux through the dopamine transporter. Mol Psychiatry 22:1673-1679.

Garcia-Olivares J, Torres-Salazar D, Owens WA, Baust T, Siderovski DP, Amara SG, Zhu J, Daws LC, Torres GE (2013) Inhibition of dopamine transporter activity by G protein betagamma subunits. PLoS One 8:e59788.

Gasbarri A, Sulli A, Packard MG (1997) The dopaminergic mesencephalic projections to the hippocampal formation in the rat. Progress in Neuro-Psychopharmacology and Biological Psychiatry 21:1-22.

Geibl FF, Henrich MT, Oertel WH (2019) Mesencephalic and extramesencephalic dopaminergic systems in Parkinson's disease. J Neural Transm (Vienna).

Gerfen CR, Surmeier DJ (2011) Modulation of striatal projection systems by dopamine. Annu Rev Neurosci 34:441-466.

Gerfen CR, Engber TM, Mahan LC, Susel Z, Chase TN, Monsma FJ, Jr., Sibley DR (1990) D1 and D2 dopamine receptor-regulated gene expression of striatonigral and striatopallidal neurons. Science 250:1429-1432.

Giros B, Jaber M, Jones SR, Wightman RM, Caron MG (1996) Hyperlocomotion and indifference to cocaine and amphetamine in mice lacking the dopamine transporter. Nature 379:606-612.

Giros B, el Mestikawy S, Godinot N, Zheng K, Han H, Yang-Feng T, Caron MG (1992) Cloning, pharmacological characterization, and chromosome assignment of the human dopamine transporter. Mol Pharmacol 42:383-390.

Glessner JT et al. (2010) Strong synaptic transmission impact by copy number variations in schizophrenia. Proc Natl Acad Sci U S A 107:10584-10589.

Gorentla BK, Vaughan RA (2005) Differential effects of dopamine and psychoactive drugs on dopamine transporter phosphorylation and regulation. Neuropharmacology 49:759-768.

Gorentla BK, Moritz AE, Foster JD, Vaughan RA (2009) Proline-directed phosphorylation of the dopamine transporter N-terminal domain. Biochemistry 48:1067-1076.

Gowrishankar R, Gresch PJ, Davis GL, Katamish RM, Riele JR, Stewart AM, Vaughan RA, Hahn MK, Blakely RD (2018) Region-Specific Regulation of Presynaptic Dopamine Homeostasis by D2 Autoreceptors Shapes the In Vivo Impact of the Neuropsychiatric Disease-Associated DAT Variant Val559. J Neurosci 38:5302-5312.

Grace AA (1991) Phasic versus tonic dopamine release and the modulation of dopamine system responsivity: A hypothesis for the etiology of schizophrenia. Neuroscience 41:1-24.

Grace AA, Bunney BS (1984) The control of firing pattern in nigral dopamine neurons: burst firing. The Journal of Neuroscience 4:2877-2890.

Granas C, Ferrer J, Loland CJ, Javitch JA, Gether U (2003) N-terminal truncation of the dopamine transporter abolishes phorbol ester- and substance P receptor-stimulated phosphorylation without impairing transporter internalization. J Biol Chem 278:4990-5000.

Grünhage F, Schulze TG, Müller DJ, Lanczik M, Franzek E, Albus M, Borrmann-Hassenbach M, Knapp M, Cichon S, Maier W, Rietschel M, Propping P, Nöthen MM (2000) Systematic screening for DNA sequence variation in the coding region of the human dopamine transporter gene (DAT1). Molecular Psychiatry 5:275-282.

Gu H, Wall SC, Rudnick G (1994) Stable expression of biogenic amine transporters reveals differences in inhibitor sensitivity, kinetics, and ion dependence. J Biol Chem 269:7124-7130.

Gulley JM, Doolen S, Zahniser NR (2002) Brief, repeated exposure to substrates down-regulates dopamine transporter function in Xenopus oocytes in vitro and rat dorsal striatum in vivo. J Neurochem 83:400-411.

Haase J, Killian AM, Magnani F, Williams C (2001) Regulation of the serotonin transporter by interacting proteins. Biochemical Society Transactions 29:722-728.

Hahn MK, Blakely RD (2007) The functional impact of SLC6 transporter genetic variation. Annu Rev Pharmacol Toxicol 47:401-441.

Hamedani SY, Gharesouran J, Noroozi R, Sayad A, Omrani MD, Mir A, Afjeh SSA, Toghi M, Manoochehrabadi S, Ghafouri-Fard S, Taheri M (2017) Ras-like without CAAX 2 (RIT2): a susceptibility gene for autism spectrum disorder. Metab Brain Dis 32:751-755.

Hamilton PJ, Belovich AN, Khelashvili G, Saunders C, Erreger K, Javitch JA, Sitte HH, Weinstein H, Matthies HJG, Galli A (2014) PIP2 regulates psychostimulant behaviors through its interaction with a membrane protein. Nat Chem Biol 10:582-589.

Hamilton PJ, Campbell NG, Sharma S, Erreger K, Herborg Hansen F, Saunders C, Belovich AN, Consortium NAAS, Sahai MA, Cook EH, Gether U, McHaourab HS, Matthies HJ, Sutcliffe JS, Galli A (2013) De novo mutation in the dopamine transporter gene associates dopamine dysfunction with autism spectrum disorder. Mol Psychiatry 18:1315-1323.

Han DD, Gu HH (2006) Comparison of the monoamine transporters from human and mouse in their sensitivities to psychostimulant drugs. BMC Pharmacol 6:6.

Harrison SM, Rudolph JL, Spencer ML, Wes PD, Montell C, Andres DA, Harrison DA (2005) Activated RIC, a small GTPase, genetically interacts with the Ras pathway and calmodulin during Drosophila development. Dev Dyn 232:817-826.

Hartwig C, Veske A, Krejcova S, Rosenberger G, Finckh U (2005) Plexin B3 promotes neurite outgrowth, interacts homophilically, and interacts with Rin. BMC Neurosci 6:53.

Hasenhuetl PS, Schicker K, Koenig X, Li Y, Sarker S, Stockner T, Sucic S, Sitte HH, Freissmuth M, Sandtner W (2015) Ligand Selectivity among the Dopamine and Serotonin Transporters Specified by the Forward Binding Reaction. Mol Pharmacol 88:12-18.

Heo WD, Inoue T, Park WS, Kim ML, Park BO, Wandless TJ, Meyer T (2006) PI(3,4,5)P3 and PI(4,5)P2 lipids target proteins with polybasic clusters to the plasma membrane. Science 314:1458-1461.

Herborg F, Andreassen TF, Berlin F, Loland CJ, Gether U (2018) Neuropsychiatric disease-associated genetic variants of the dopamine transporter display heterogeneous molecular phenotypes. J Biol Chem 293:7250-7262.

Hersch SM, Yi H, Heilman CJ, Edwards RH, Levey AI (1997) Subcellular localization and molecular topology of the dopamine transporter in the striatum and substantia nigra. The Journal of Comparative Neurology 388:211-227.

Hertting G, Axelrod J (1961) Fate of tritiated noradrenaline at the sympathetic nerve-endings. Nature 192:172-173.

Holton KL, Loder MK, Melikian HE (2005) Nonclassical, distinct endocytic signals dictate constitutive and PKC-regulated neurotransmitter transporter internalization. Nat Neurosci 8:881-888.

Hong WC, Amara SG (2010) Membrane cholesterol modulates the outward facing conformation of the dopamine transporter and alters cocaine binding. J Biol Chem 285:32616-32626.

Hong WC, Amara SG (2013) Differential targeting of the dopamine transporter to recycling or degradative pathways during amphetamine- or PKC-regulated endocytosis in dopamine neurons. FASEB J 27:2995-3007.

Hong WC, Yano H, Hiranita T, Chin FT, McCurdy CR, Su TP, Amara SG, Katz JL (2017) The sigma-1 receptor modulates dopamine transporter conformation and cocaine binding and may thereby potentiate cocaine self-administration in rats. J Biol Chem 292:11250-11261.

Hoover BR, Everett CV, Sorkin A, Zahniser NR (2007) Rapid regulation of dopamine transporters by tyrosine kinases in rat neuronal preparations. J Neurochem 101:1258-1271.

Hoshino M, Nakamura K (2002) The Ras-like small GTP-binding protein Rin is activated by growth factor stimulation. Biochem Biophys Res Commun 295:651-656.

Hoshino M, Nakamura S (2003) Small GTPase Rin induces neurite outgrowth through Rac/Cdc42 and calmodulin in PC12 cells. J Cell Biol 163:1067-1076.

Hoshino M, Yoshimori T, Nakamura S (2005) Small GTPase proteins Rin and Rit Bind to PAR6 GTP-dependently and regulate cell transformation. J Biol Chem 280:22868-22874.

Howes OD, McCutcheon R, Owen MJ, Murray RM (2017) The Role of Genes, Stress, and Dopamine in the Development of Schizophrenia. Biol Psychiatry 81:9-20.

Huff RA, Vaughan RA, Kuhar MJ, Uhl GR (1997) Phorbol esters increase dopamine transporter phosphorylation and decrease transport Vmax. J Neurochem 68:225-232.

Hyman SE, Malenka RC, Nestler EJ (2006) Neural mechanisms of addiction: the role of reward-related learning and memory. Annu Rev Neurosci 29:565-598.

Inglis FM, Moghaddam B (1999) Dopaminergic innervation of the amygdala is highly responsive to stress. J Neurochem 72:1088-1094.

Isomura Y, Takekawa T, Harukuni R, Handa T, Aizawa H, Takada M, Fukai T (2013) Reward-modulated motor information in identified striatum neurons. J Neurosci 33:10209-10220.

Iversen SD, Iversen LL (2007) Dopamine: 50 years in perspective. Trends Neurosci 30:188-193.

Jiang H, Jiang Q, Feng J (2004) Parkin increases dopamine uptake by enhancing the cell surface expression of dopamine transporter. J Biol Chem 279:54380-54386.

Johnson LA, Guptaroy B, Lund D, Shamban S, Gnegy ME (2005a) Regulation of amphetamine-stimulated dopamine efflux by protein kinase C beta. J Biol Chem 280:10914-10919.

Johnson LA, Furman CA, Zhang M, Guptaroy B, Gnegy ME (2005b) Rapid delivery of the dopamine transporter to the plasmalemmal membrane upon amphetamine stimulation. Neuropharmacology 49:750-758.

Jones KT, Zhen J, Reith ME (2012) Importance of cholesterol in dopamine transporter function. J Neurochem 123:700-715.

Jones SR, Gainetdinov RR, Jaber M, Giros B, Wightman RM, Caron MG (1998) Profound neuronal plasticity in response to inactivation of the dopamine transporter. Proc Natl Acad Sci U S A 95:4029-4034.

Kahlig KM, Lute BJ, Wei Y, Loland CJ, Gether U, Javitch JA, Galli A (2006) Regulation of dopamine transporter trafficking by intracellular amphetamine. Mol Pharmacol 70:542-548.

Kantor L, Gnegy ME (1998) Protein kinase C inhibitors block amphetamine-mediated dopamine release in rat striatal slices. J Pharmacol Exp Ther 284:592-598.

Kasture A, El-Kasaby A, Szollosi D, Asjad HMM, Grimm A, Stockner T, Hummel T, Freissmuth M, Sucic S (2016) Functional Rescue of a Misfolded Drosophila melanogaster Dopamine Transporter Mutant Associated with a Sleepless Phenotype by Pharmacological Chaperones. J Biol Chem 291:20876-20890.

Kaun KR, Devineni AV, Heberlein U (2012) Drosophila melanogaster as a model to study drug addiction. Hum Genet 131:959-975.

Kebabian JW, Calne DB (1979) Multiple receptors for dopamine. Nature 277:93-96.

Kebabian JW, Petzold GL, Greengard P (1972) Dopamine-sensitive adenylate cyclase in caudate nucleus of rat brain, and its similarity to the "dopamine receptor". Proc Natl Acad Sci U S A 69:2145-2149.

Kehr W, Carlsson A, Lindqvist M, Magnusson T, Atack C (1972) Evidence for a receptor-mediated feedback control of striatal tyrosine hydroxylase activity. J Pharm Pharmacol 24:744-747.

Keiflin R, Janak PH (2015) Dopamine Prediction Errors in Reward Learning and Addiction: From Theory to Neural Circuitry. Neuron 88:247-263.

Khoshbouei H, Wang H, Lechleiter JD, Javitch JA, Galli A (2003) Amphetamine-induced dopamine efflux. A voltage-sensitive and intracellular Na+-dependent mechanism. J Biol Chem 278:12070-12077.

Khoshbouei H, Sen N, Guptaroy B, Johnson L, Lund D, Gnegy ME, Galli A, Javitch JA (2004) N-terminal phosphorylation of the dopamine transporter is required for amphetamine-induced efflux. PLoS Biol 2:E78.

Kilty JE, Lorang D, Amara SG (1991) Cloning and expression of a cocaine-sensitive rat dopamine transporter. Science 254:578-579.

Kimmel HL, Carroll FI, Kuhar MJ (2000) Dopamine transporter synthesis and degradation rate in rat striatum and nucleus accumbens using RTI-76. Neuropharmacology 39:578-585.

Kivell B, Uzelac Z, Sundaramurthy S, Rajamanickam J, Ewald A, Chefer V, Jaligam V, Bolan E, Simonson B, Annamalai B, Mannangatti P, Prisinzano

TE, Gomes I, Devi LA, Jayanthi LD, Sitte HH, Ramamoorthy S, Shippenberg TS (2014a) Salvinorin A regulates dopamine transporter function via a kappa opioid receptor and ERK1/2-dependent mechanism. Neuropharmacology 86:228-240.

Kivell BM, Ewald AW, Prisinzano TE (2014b) Salvinorin A analogs and other kappa-opioid receptor compounds as treatments for cocaine abuse. Adv Pharmacol 69:481-511.

Kleine-Vehn J, Leitner J, Zwiewka M, Sauer M, Abas L, Luschnig C, Friml J (2008) Differential degradation of PIN2 auxin efflux carrier by retromer-dependent vacuolar targeting. Proc Natl Acad Sci U S A 105:17812-17817.

Koh K, Evans JM, Hendricks JC, Sehgal A (2006) A Drosophila model for age-associated changes in sleep:wake cycles. Proc Natl Acad Sci U S A 103:13843-13847.

Kovtun O, Tomlinson ID, Ferguson RS, Rosenthal SJ (2019) Quantum dots reveal heterogeneous membrane diffusivity and dynamic surface density polarization of dopamine transporter. PLoS One 14:e0225339.

Kovtun O, Sakrikar D, Tomlinson ID, Chang JC, Arzeta-Ferrer X, Blakely RD, Rosenthal SJ (2015) Single-quantum-dot tracking reveals altered membrane dynamics of an attention-deficit/hyperactivity-disorder-derived dopamine transporter coding variant. ACS Chem Neurosci 6:526-534.

Kravitz AV, Kreitzer AC (2012) Striatal mechanisms underlying movement, reinforcement, and punishment. Physiology (Bethesda) 27:167-177.

Kreitzer AC, Malenka RC (2008) Striatal plasticity and basal ganglia circuit function. Neuron 60:543-554.

Kristensen AS, Andersen J, Jorgensen TN, Sorensen L, Eriksen J, Loland CJ, Stromgaard K, Gether U (2011) SLC6 neurotransmitter transporters: structure, function, and regulation. Pharmacol Rev 63:585-640.

Kume K, Kume S, Park SK, Hirsh J, Jackson FR (2005) Dopamine is a regulator of arousal in the fruit fly. J Neurosci 25:7377-7384.

Kurian MA, Zhen J, Cheng SY, Li Y, Mordekar SR, Jardine P, Morgan NV, Meyer E, Tee L, Pasha S, Wassmer E, Heales SJ, Gissen P, Reith ME, Maher ER (2009) Homozygous loss-of-function mutations in the gene encoding the dopamine transporter are associated with infantile parkinsonism-dystonia. J Clin Invest 119:1595-1603.

Kurian MA et al. (2011) Clinical and molecular characterisation of hereditary dopamine transporter deficiency syndrome: an observational cohort and experimental study. The Lancet Neurology 10:54-62.

Latourelle JC, Dumitriu A, Hadzi TC, Beach TG, Myers RH (2012) Evaluation of Parkinson disease risk variants as expression-QTLs. PLoS One 7:e46199.

Lebowitz JJ, Pino JA, Mackie PM, Lin M, Hurst C, Divita K, Collins AT, Koutzoumis DN, Torres GE, Khoshbouei H (2019) Clustered Kv2.1 decreases dopamine transporter activity and internalization. J Biol Chem.

Lee CH, Della NG, Chew CE, Zack DJ (1996) Rin, a neuron-specific and calmodulin-binding small G-protein, and Rit define a novel subfamily of ras proteins. J Neurosci 16:6784-6794.

Lee FJ, Liu F, Pristupa ZB, Niznik HB (2001) Direct binding and functional coupling of alpha-synuclein to the dopamine transporters accelerate dopamine-induced apoptosis. FASEB J 15:916-926.

Lee FJ, Pei L, Moszczynska A, Vukusic B, Fletcher PJ, Liu F (2007) Dopamine transporter cell surface localization facilitated by a direct interaction with the dopamine D2 receptor. EMBO J 26:2127-2136.

Lee KH, Kim MY, Kim DH, Lee YS (2004) Syntaxin 1A and receptor for activated C kinase interact with the N-terminal region of human dopamine transporter. Neurochem Res 29:1405-1409.

Li JY, Zhang JH, Li NN, Wang L, Lu ZJ, Cheng L, Sun XY, Peng R (2017) Genetic association study between RIT2 and Parkinson's disease in a Han Chinese population. Neurol Sci 38:343-347.

Lin CH, Chen ML, Yu CY, Wu RM (2013) RIT2 variant is not associated with Parkinson's disease in a Taiwanese population. Neurobiol Aging 34:2236 e2231-2233.

Lin Z, Uhl GR (2003) Human dopamine transporter gene variation: effects of protein coding variants V55A and V382A on expression and uptake activities. The Pharmacogenomics Journal 3:159-168.

Linseman DA, Heidenreich KA, Fisher SK (2001) Stimulation of M3 muscarinic receptors induces phosphorylation of the Cdc42 effector activated Cdc42Hs-associated kinase-1 via a Fyn tyrosine kinase signaling pathway. J Biol Chem 276:5622-5628.

Littrell OM, Pomerleau F, Huettl P, Surgener S, McGinty JF, Middaugh LD, Granholm AC, Gerhardt GA, Boger HA (2012) Enhanced dopamine transporter activity in middle-aged Gdnf heterozygous mice. Neurobiol Aging 33:427 e421-414.

Liu TW, Wu YR, Chen YC, Fung HC, Chen CM (2019) Association of RIT2 and RAB7L1 with Parkinson's disease: a case-control study in a Taiwanese cohort and a meta-analysis in Asian populations. Neurobiol Aging.

Liu X et al. (2016) Genome-wide Association Study of Autism Spectrum Disorder in the East Asian Populations. Autism Res 9:340-349.

Liu ZH, Guo JF, Wang YQ, Li K, Sun QY, Xu Q, Yan XX, Xu CS, Tang BS (2015) Assessment of RIT2 rs12456492 association with Parkinson's disease in Mainland China. Neurobiol Aging 36:1600 e1609-1611.

Loder MK, Melikian HE (2003) The dopamine transporter constitutively internalizes and recycles in a protein kinase C-regulated manner in stably transfected PC12 cell lines. J Biol Chem 278:22168-22174.

Lu Y, Liu W, Tan K, Peng J, Zhu Y, Wang X (2015) Genetic association of RIT2 rs12456492 polymorphism and Parkinson's disease susceptibility in Asian populations: a meta-analysis. Sci Rep 5:13805.

Luderman KD, Chen R, Ferris MJ, Jones SR, Gnegy ME (2015) Protein kinase C beta regulates the D(2)-like dopamine autoreceptor. Neuropharmacology 89:335-341.

Luk B, Mohammed M, Liu F, Lee FJ (2015) A Physical Interaction between the Dopamine Transporter and DJ-1 Facilitates Increased Dopamine Reuptake. PLoS One 10:e0136641.

Madsen KL, Thorsen TS, Rahbek-Clemmensen T, Eriksen J, Gether U (2012) Protein interacting with C kinase 1 (PICK1) reduces reinsertion rates of interaction partners sorted to Rab11-dependent slow recycling pathway. J Biol Chem 287:12293-12308.

Makos MA, Kim YC, Han KA, Heien ML, Ewing AG (2009) In vivo electrochemical measurements of exogenously applied dopamine in Drosophila melanogaster. Anal Chem 81:1848-1854.

Mao Z, Davis RL (2009) Eight different types of dopaminergic neurons innervate the Drosophila mushroom body neuropil: anatomical and physiological heterogeneity. Front Neural Circuits 3:5.

Marazziti D, Mandillo S, Di Pietro C, Golini E, Matteoni R, Tocchini-Valentini GP (2007) GPR37 associates with the dopamine transporter to modulate dopamine uptake and behavioral responses to dopaminergic drugs. Proc Natl Acad Sci U S A 104:9846-9851.

Marcott PF, Gong S, Donthamsetti P, Grinnell SG, Nelson MN, Newman AH, Birnbaumer L, Martemyanov KA, Javitch JA, Ford CP (2018) Regional Heterogeneity of D2-Receptor Signaling in the Dorsal Striatum and Nucleus Accumbens. Neuron 98:575-587 e574.

Martin CA, Krantz DE (2014) Drosophila melanogaster as a genetic model system to study neurotransmitter transporters. Neurochem Int 73:71-88.

Mayfield RD, Zahniser NR (2001) Dopamine D2 receptor regulation of the dopamine transporter expressed in Xenopus laevis oocytes is voltage-independent. Mol Pharmacol 59:113-121.

Mazei-Robison MS, Blakely RD (2005) Expression studies of naturally occurring human dopamine transporter variants identifies a novel state of transporter inactivation associated with Val382Ala. Neuropharmacology 49:737-749.

Mazei-Robison MS, Couch RS, Shelton RC, Stein MA, Blakely RD (2005) Sequence variation in the human dopamine transporter gene in children with attention deficit hyperactivity disorder. Neuropharmacology 49:724-736.

Mazei-Robison MS, Bowton E, Holy M, Schmudermaier M, Freissmuth M, Sitte HH, Galli A, Blakely RD (2008) Anomalous dopamine release associated with a human dopamine transporter coding variant. J Neurosci 28:7040-7046.

McCall NM, Kotecki L, Dominguez-Lopez S, Marron Fernandez de Velasco E, Carlblom N, Sharpe AL, Beckstead MJ, Wickman K (2016) Selective Ablation of GIRK Channels in Dopamine Neurons Alters Behavioral Effects of Cocaine in Mice. Neuropsychopharmacology 42:707-715.

McClung C, Hirsh J (1998) Stereotypic behavioral responses to free-base cocaine and the development of behavioral sensitization in Drosophila. Curr Biol 8:109-112.

Medic G, Wille M, Hemels ME (2017) Short- and long-term health consequences of sleep disruption. Nat Sci Sleep 9:151-161.

Meiergerd SM, Patterson TA, Schenk JO (1993) D2 receptors may modulate the function of the striatal transporter for dopamine: kinetic evidence from studies in vitro and in vivo. J Neurochem 61:764-767.

Melikian HE (2004) Neurotransmitter transporter trafficking: endocytosis, recycling, and regulation. Pharmacol Ther 104:17-27.

Melikian HE, Buckley KM (1999) Membrane trafficking regulates the activity of the human dopamine transporter. J Neurosci 19:7699-7710.

Mergy MA, Gowrishankar R, Gresch PJ, Gantz SC, Williams J, Davis GL, Wheeler CA, Stanwood GD, Hahn MK, Blakely RD (2014) The rare DAT coding variant Val559 perturbs DA neuron function, changes behavior, and alters in vivo responses to psychostimulants. Proc Natl Acad Sci U S A 111:E4779-4788.

Miller EK, Cohen JD (2001) An integrative theory of prefrontal cortex function. Annu Rev Neurosci 24:167-202.

Miranda M, Dionne KR, Sorkina T, Sorkin A (2007) Three ubiquitin conjugation sites in the amino terminus of the dopamine transporter mediate protein kinase C-dependent endocytosis of the transporter. Mol Biol Cell 18:313-323.

Miranda M, Sorkina T, Grammatopoulos TN, Zawada WM, Sorkin A (2004) Multiple molecular determinants in the carboxyl terminus regulate dopamine transporter export from endoplasmic reticulum. J Biol Chem 279:30760-30770.

Miranda M, Wu CC, Sorkina T, Korstjens DR, Sorkin A (2005) Enhanced ubiquitylation and accelerated degradation of the dopamine transporter mediated by protein kinase C. J Biol Chem 280:35617-35624.

Missale C, Nash SR, Robinson SW, Jaber M, Caron MG (1998) Dopamine receptors: from structure to function. Physiol Rev 78:189-225.

Molas S, Zhao-Shea R, Liu L, DeGroot SR, Gardner PD, Tapper AR (2017) A circuit-based mechanism underlying familiarity signaling and the preference for novelty. Nat Neurosci 20:1260-1268.

Molinoff PB, Axelrod J (1971) Biochemistry of catecholamines. Annu Rev Biochem 40:465-500.

Moore RY, Bloom FE (1978) Central catecholamine neuron systems: anatomy and physiology of the dopamine systems. Annu Rev Neurosci 1:129-169.

Morales M, Margolis EB (2017) Ventral tegmental area: cellular heterogeneity, connectivity and behaviour. Nat Rev Neurosci 18:73-85.

Moritz AE, Rastedt DE, Stanislowski DJ, Shetty M, Smith MA, Vaughan RA, Foster JD (2015) Reciprocal Phosphorylation and Palmitoylation Control Dopamine Transporter Kinetics. J Biol Chem 290:29095-29105.

Moritz AE, Foster JD, Gorentla BK, Mazei-Robison MS, Yang JW, Sitte HH, Blakely RD, Vaughan RA (2013) Phosphorylation of dopamine transporter serine 7 modulates cocaine analog binding. J Biol Chem 288:20-32.

Moszczynska A, Saleh J, Zhang H, Vukusic B, Lee FJ, Liu F (2007) Parkin disrupts the alpha-synuclein/dopamine transporter interaction: consequences toward dopamine-induced toxicity. J Mol Neurosci 32:217-227.

Mueller C, Ratner D, Zhong L, Esteves-Sena M, Gao G (2012) Production and discovery of novel recombinant adeno-associated viral vectors. Curr Protoc Microbiol Chapter 14:Unit14D 11.

Nalls MA et al. (2014) Large-scale meta-analysis of genome-wide association data identifies six new risk loci for Parkinson's disease. Nat Genet 46:989-993.

Narita M, Matsushima Y, Niikura K, Narita M, Takagi S, Nakahara K, Kurahashi K, Abe M, Saeki M, Asato M, Imai S, Ikeda K, Kuzumaki N, Suzuki T (2010) Implication of dopaminergic projection from the ventral tegmental area to the anterior cingulate cortex in mu-opioid-induced place preference. Addict Biol 15:434-447.

Navaroli DM, Melikian HE (2010) Insertion of tetracysteine motifs into dopamine transporter extracellular domains. PLoS One 5:e9113.

Navaroli DM, Stevens ZH, Uzelac Z, Gabriel L, King MJ, Lifshitz LM, Sitte HH, Melikian HE (2011) The plasma membrane-associated GTPase Rin interacts with the dopamine transporter and is required for protein kinase C-regulated dopamine transporter trafficking. J Neurosci 31:13758-13770.

Neale BM et al. (2012) Patterns and rates of exonic de novo mutations in autism spectrum disorders. Nature 485:242-245.

Ng J et al. (2014) Dopamine transporter deficiency syndrome: phenotypic spectrum from infancy to adulthood. Brain 137:1107-1119.

Nie K, Feng SJ, Tang HM, Ma GX, Gan R, Zhao X, Zhao JH, Wang LM, Huang ZH, Huang J, Gao L, Zhang YW, Zhu RM, Duan ZP, Zhang YH, Wang LJ (2015) RIT2 polymorphism is associated with Parkinson's disease in a Han Chinese population. Neurobiol Aging 36:1603 e1615-1607.

Nirenberg MJ, Vaughan RA, Uhl GR, Kuhar MJ, Pickel VM (1996) The dopamine transporter is localized to dendritic and axonal plasma membranes of nigrostriatal dopaminergic neurons. The Journal of Neuroscience 16:436-447.

Owen MJ, Sawa A, Mortensen PB (2016) Schizophrenia. The Lancet 388:86-97.

Owens WA, Williams JM, Saunders C, Avison MJ, Galli A, Daws LC (2012) Rescue of dopamine transporter function in hypoinsulinemic rats by a D2 receptor-ERK-dependent mechanism. J Neurosci 32:2637-2647.

Owens WA, Sevak RJ, Galici R, Chang X, Javors MA, Galli A, France CP, Daws LC (2005) Deficits in dopamine clearance and locomotion in hypoinsulinemic rats unmask novel modulation of dopamine transporters by amphetamine. J Neurochem 94:1402-1410.

Page G, Peeters M, Najimi M, Maloteaux JM, Hermans E (2001) Modulation of the neuronal dopamine transporter activity by the metabotropic glutamate

receptor mGluR5 in rat striatal synaptosomes through phosphorylation mediated processes. J Neurochem 76:1282-1290.
Pankratz N et al. (2012) Meta-analysis of Parkinson's disease: identification of a novel locus, RIT2. Ann Neurol 71:370-384.
Paval D (2017) A Dopamine Hypothesis of Autism Spectrum Disorder. Dev Neurosci 39:355-360.
Penmatsa A, Wang KH, Gouaux E (2013) X-ray structure of dopamine transporter elucidates antidepressant mechanism. Nature 503:85-90.
Pizzo AB, Karam CS, Zhang Y, Ma CL, McCabe BD, Javitch JA (2014) Amphetamine-induced behavior requires CaMKII-dependent dopamine transporter phosphorylation. Mol Psychiatry 19:279-281.
Pizzo AB, Karam CS, Zhang Y, Yano H, Freyberg RJ, Karam DS, Freyberg Z, Yamamoto A, McCabe BD, Javitch JA (2013) The membrane raft protein Flotillin-1 is essential in dopamine neurons for amphetamine-induced behavior in Drosophila. Mol Psychiatry 18:824-833.
Porzgen P, Park SK, Hirsh J, Sonders MS, Amara SG (2001) The antidepressant-sensitive dopamine transporter in Drosophila melanogaster: a primordial carrier for catecholamines. Mol Pharmacol 59:83-95.
Pothos EN, Przedborski S, Davila V, Schmitz Y, Sulzer D (1998) D2-Like Dopamine Autoreceptor Activation Reduces Quantal Size in PC12 Cells. The Journal of Neuroscience 18:5575-5585.
Pramod AB, Foster J, Carvelli L, Henry LK (2013) SLC6 transporters: structure, function, regulation, disease association and therapeutics. Mol Aspects Med 34:197-219.
Pristupa ZB, McConkey F, Liu F, Man HY, Lee FJ, Wang YT, Niznik HB (1998) Protein kinase-mediated bidirectional trafficking and functional regulation of the human dopamine transporter. Synapse 30:79-87.
Rahbek-Clemmensen T, Lycas MD, Erlendsson S, Eriksen J, Apuschkin M, Vilhardt F, Jorgensen TN, Hansen FH, Gether U (2017) Super-resolution microscopy reveals functional organization of dopamine transporters into cholesterol and neuronal activity-dependent nanodomains. Nat Commun 8:740.
Ramamoorthy S, Bauman AL, Moore KR, Han H, Yang-Feng T, Chang AS, Ganapathy V, Blakely RD (1993) Antidepressant- and cocaine-sensitive human serotonin transporter: molecular cloning, expression, and chromosomal localization. Proc Natl Acad Sci U S A 90:2542-2546.
Ramshaw H, Xu X, Jaehne EJ, McCarthy P, Greenberg Z, Saleh E, McClure B, Woodcock J, Kabbara S, Wiszniak S, Wang TY, Parish C, van den Buuse M, Baune BT, Lopez A, Schwarz Q (2013) Locomotor hyperactivity in 14-3-3zeta KO mice is associated with dopamine transporter dysfunction. Transl Psychiatry 3:e327.
Rao A, Simmons D, Sorkin A (2011) Differential subcellular distribution of endosomal compartments and the dopamine transporter in dopaminergic neurons. Mol Cell Neurosci 46:148-158.

Rao A, Richards TL, Simmons D, Zahniser NR, Sorkin A (2012) Epitope-tagged dopamine transporter knock-in mice reveal rapid endocytic trafficking and filopodia targeting of the transporter in dopaminergic axons. FASEB J 26:1921-1933.

Richardson BD, Saha K, Krout D, Cabrera E, Felts B, Henry LK, Swant J, Zou MF, Newman AH, Khoshbouei H (2016) Membrane potential shapes regulation of dopamine transporter trafficking at the plasma membrane. Nat Commun 7:10423.

Rickhag M, Owens WA, Winkler MT, Strandfelt KN, Rathje M, Sorensen G, Andresen B, Madsen KL, Jorgensen TN, Wortwein G, Woldbye DP, Sitte H, Daws LC, Gether U (2013a) Membrane-permeable C-terminal dopamine transporter peptides attenuate amphetamine-evoked dopamine release. J Biol Chem 288:27534-27544.

Rickhag M, Hansen FH, Sorensen G, Strandfelt KN, Andresen B, Gotfryd K, Madsen KL, Vestergaard-Klewe I, Ammendrup-Johnsen I, Eriksen J, Newman AH, Fuchtbauer EM, Gomeza J, Woldbye DP, Wortwein G, Gether U (2013b) A C-terminal PDZ domain-binding sequence is required for striatal distribution of the dopamine transporter. Nat Commun 4:1580.

Riemensperger T, Isabel G, Coulom H, Neuser K, Seugnet L, Kume K, Iche-Torres M, Cassar M, Strauss R, Preat T, Hirsh J, Birman S (2011) Behavioral consequences of dopamine deficiency in the Drosophila central nervous system. Proc Natl Acad Sci U S A 108:834-839.

Rocha BA, Fumagalli F, Gainetdinov RR, Jones SR, Ator R, Giros B, Miller GW, Caron MG (1998) Cocaine self-administration in dopamine-transporter knockout mice. Nat Neurosci 1:132-137.

Rohwedder A, Wenz NL, Stehle B, Huser A, Yamagata N, Zlatic M, Truman JW, Tanimoto H, Saumweber T, Gerber B, Thum AS (2016) Four Individually Identified Paired Dopamine Neurons Signal Reward in Larval Drosophila. Curr Biol 26:661-669.

Rojas R, Kametaka S, Haft CR, Bonifacino JS (2007) Interchangeable but essential functions of SNX1 and SNX2 in the association of retromer with endosomes and the trafficking of mannose 6-phosphate receptors. Mol Cell Biol 27:1112-1124.

Rojas R, van Vlijmen T, Mardones GA, Prabhu Y, Rojas AL, Mohammed S, Heck AJ, Raposo G, van der Sluijs P, Bonifacino JS (2008) Regulation of retromer recruitment to endosomes by sequential action of Rab5 and Rab7. J Cell Biol 183:513-526.

Sakrikar D, Mazei-Robison MS, Mergy MA, Richtand NW, Han Q, Hamilton PJ, Bowton E, Galli A, Veenstra-Vanderweele J, Gill M, Blakely RD (2012) Attention deficit/hyperactivity disorder-derived coding variation in the dopamine transporter disrupts microdomain targeting and trafficking regulation. J Neurosci 32:5385-5397.

Salahpour A, Ramsey AJ, Medvedev IO, Kile B, Sotnikova TD, Holmstrand E, Ghisi V, Nicholls PJ, Wong L, Murphy K, Sesack SR, Wightman RM,

Gainetdinov RR, Caron MG (2008) Increased amphetamine-induced hyperactivity and reward in mice overexpressing the dopamine transporter. Proc Natl Acad Sci U S A 105:4405-4410.

Sambo DO, Lin M, Owens A, Lebowitz JJ, Richardson B, Jagnarine DA, Shetty M, Rodriquez M, Alonge T, Ali M, Katz J, Yan L, Febo M, Henry LK, Bruijnzeel AW, Daws L, Khoshbouei H (2017) The sigma-1 receptor modulates methamphetamine dysregulation of dopamine neurotransmission. Nat Commun 8:2228.

Sandoval V, Riddle EL, Ugarte YV, Hanson GR, Fleckenstein AE (2001) Methamphetamine-Induced Rapid and Reversible Changes in Dopamine Transporter Function: AnIn VitroModel. The Journal of Neuroscience 21:1413-1419.

Saunders C, Ferrer JV, Shi L, Chen J, Merrill G, Lamb ME, Leeb-Lundberg LM, Carvelli L, Javitch JA, Galli A (2000) Amphetamine-induced loss of human dopamine transporter activity: an internalization-dependent and cocaine-sensitive mechanism. Proc Natl Acad Sci U S A 97:6850-6855.

Schmitz Y, Schmauss C, Sulzer D (2002) Altered Dopamine Release and Uptake Kinetics in Mice Lacking D2Receptors. The Journal of Neuroscience 22:8002-8009.

Schmitz Y, Benoit-Marand M, Gonon F, Sulzer D (2003) Presynaptic regulation of dopaminergic neurotransmission. J Neurochem 87:273-289.

Schultz W (2007a) Multiple dopamine functions at different time courses. Annu Rev Neurosci 30:259-288.

Schultz W (2007b) Behavioral dopamine signals. Trends Neurosci 30:203-210.

Schwartz BG, Rezkalla S, Kloner RA (2010) Cardiovascular effects of cocaine. Circulation 122:2558-2569.

Seaman MN (2004) Cargo-selective endosomal sorting for retrieval to the Golgi requires retromer. J Cell Biol 165:111-122.

Seaman MN (2012) The retromer complex - endosomal protein recycling and beyond. J Cell Sci 125:4693-4702.

Seaman MN, McCaffery JM, Emr SD (1998) A membrane coat complex essential for endosome-to-Golgi retrograde transport in yeast. J Cell Biol 142:665-681.

Seaman MN, Marcusson EG, Cereghino JL, Emr SD (1997) Endosome to Golgi retrieval of the vacuolar protein sorting receptor, Vps10p, requires the function of the VPS29, VPS30, and VPS35 gene products. J Cell Biol 137:79-92.

Seaman MN, Harbour ME, Tattersall D, Read E, Bright N (2009) Membrane recruitment of the cargo-selective retromer subcomplex is catalysed by the small GTPase Rab7 and inhibited by the Rab-GAP TBC1D5. J Cell Sci 122:2371-2382.

Sekine-Aizawa Y, Huganir RL (2004) Imaging of receptor trafficking by using alpha-bungarotoxin-binding-site-tagged receptors. Proc Natl Acad Sci U S A 101:17114-17119.

Shao H, Kadono-Okuda K, Finlin BS, Andres DA (1999) Biochemical characterization of the Ras-related GTPases Rit and Rin. Arch Biochem Biophys 371:207-219.

Sharma A, Couture J (2014) A review of the pathophysiology, etiology, and treatment of attention-deficit hyperactivity disorder (ADHD). Ann Pharmacother 48:209-225.

Shi GX, Han J, Andres DA (2005) Rin GTPase couples nerve growth factor signaling to p38 and b-Raf/ERK pathways to promote neuronal differentiation. J Biol Chem 280:37599-37609.

Shi GX, Cai W, Andres DA (2013) Rit subfamily small GTPases: regulators in neuronal differentiation and survival. Cell Signal 25:2060-2068.

Shin JH, Adrover MF, Wess J, Alvarez VA (2015) Muscarinic regulation of dopamine and glutamate transmission in the nucleus accumbens. Proc Natl Acad Sci U S A 112:8124-8129.

Simon JR, Bare DJ, Ghetti B, Richter JA (1997) A possible role for tyrosine kinases in the regulation of the neuronal dopamine transporter in mouse striatum. Neurosci Lett 224:201-205.

Sitte HH, Huck S, Reither H, Boehm S, Singer EA, Pifl C (1998) Carrier-mediated release, transport rates, and charge transfer induced by amphetamine, tyramine, and dopamine in mammalian cells transfected with the human dopamine transporter. J Neurochem 71:1289-1297.

Smith Y, Bevan MD, Shink E, Bolam JP (1998) Microcircuitry of the direct and indirect pathways of the basal ganglia. Neuroscience 86:353-387.

Snyder SH, Coyle JT (1969) Regional differences in H3-norepinephrine and H3-dopamine uptake into rat brain homogenates. J Pharmacol Exp Ther 165.

Sonders MS, Zhu SJ, Zahniser NR, Kavanaugh MP, Amara SG (1997) Multiple ionic conductances of the human dopamine transporter: the actions of dopamine and psychostimulants. J Neurosci 17:960-974.

Sorkina T, Caltagarone J, Sorkin A (2013) Flotillins regulate membrane mobility of the dopamine transporter but are not required for its protein kinase C dependent endocytosis. Traffic 14:709-724.

Sorkina T, Hoover BR, Zahniser NR, Sorkin A (2005) Constitutive and protein kinase C-induced internalization of the dopamine transporter is mediated by a clathrin-dependent mechanism. Traffic 6:157-170.

Sorkina T, Doolen S, Galperin E, Zahniser NR, Sorkin A (2003) Oligomerization of dopamine transporters visualized in living cells by fluorescence resonance energy transfer microscopy. J Biol Chem 278:28274-28283.

Sorkina T, Richards TL, Rao A, Zahniser NR, Sorkin A (2009) Negative regulation of dopamine transporter endocytosis by membrane-proximal N-terminal residues. J Neurosci 29:1361-1374.

Sorkina T, Ma S, Larsen MB, Watkins SC, Sorkin A (2018) Small molecule induced oligomerization, clustering and clathrin-independent endocytosis of the dopamine transporter. Elife 7.

Sorkina T, Miranda M, Dionne KR, Hoover BR, Zahniser NR, Sorkin A (2006) RNA interference screen reveals an essential role of Nedd4-2 in dopamine transporter ubiquitination and endocytosis. J Neurosci 26:8195-8205.

Speed N, Saunders C, Davis AR, Owens WA, Matthies HJ, Saadat S, Kennedy JP, Vaughan RA, Neve RL, Lindsley CW, Russo SJ, Daws LC, Niswender KD, Galli A (2011) Impaired striatal Akt signaling disrupts dopamine homeostasis and increases feeding. PLoS One 6:e25169.

Spencer ML, Shao H, Andres DA (2002a) Induction of neurite extension and survival in pheochromocytoma cells by the Rit GTPase. J Biol Chem 277:20160-20168.

Spencer ML, Shao H, Tucker HM, Andres DA (2002b) Nerve growth factor-dependent activation of the small GTPase Rin. J Biol Chem 277:17605-17615.

Stagkourakis S, Kim H, Lyons DJ, Broberger C (2016) Dopamine Autoreceptor Regulation of a Hypothalamic Dopaminergic Network. Cell Rep 15:735-747.

Steinberg SF (2008) Structural basis of protein kinase C isoform function. Physiol Rev 88:1341-1378.

Steinkellner T, Yang JW, Montgomery TR, Chen WQ, Winkler MT, Sucic S, Lubec G, Freissmuth M, Elgersma Y, Sitte HH, Kudlacek O (2012) Ca(2+)/calmodulin-dependent protein kinase IIalpha (alphaCaMKII) controls the activity of the dopamine transporter: implications for Angelman syndrome. J Biol Chem 287:29627-29635.

Steinkellner T, Mus L, Eisenrauch B, Constantinescu A, Leo D, Konrad L, Rickhag M, Sorensen G, Efimova EV, Kong E, Willeit M, Sotnikova TD, Kudlacek O, Gether U, Freissmuth M, Pollak DD, Gainetdinov RR, Sitte HH (2014) In vivo amphetamine action is contingent on alphaCaMKII. Neuropsychopharmacology 39:2681-2693.

Sucic S, El-Kasaby A, Kudlacek O, Sarker S, Sitte HH, Marin P, Freissmuth M (2011) The serotonin transporter is an exclusive client of the coat protein complex II (COPII) component SEC24C. J Biol Chem 286:16482-16490.

Sucic S, Koban F, El-Kasaby A, Kudlacek O, Stockner T, Sitte HH, Freissmuth M (2013) Switching the clientele: a lysine residing in the C terminus of the serotonin transporter specifies its preference for the coat protein complex II component SEC24C. J Biol Chem 288:5330-5341.

Sulzer D (2011) How addictive drugs disrupt presynaptic dopamine neurotransmission. Neuron 69:628-649.

Sulzer D, Cragg SJ, Rice ME (2016) Striatal dopamine neurotransmission: regulation of release and uptake. Basal Ganglia 6:123-148.

Sulzer D, Sonders MS, Poulsen NW, Galli A (2005) Mechanisms of neurotransmitter release by amphetamines: a review. Prog Neurobiol 75:406-433.

Sung U, Apparsundaram S, Galli A, Kahlig KM, Savchenko V, Schroeter S, Quick MW, Blakely RD (2003) A regulated interaction of syntaxin 1A with the

antidepressant-sensitive norepinephrine transporter establishes catecholamine clearance capacity. J Neurosci 23:1697-1709.

Svingos AL, Chavkin C, Colago EE, Pickel VM (2001) Major coexpression of kappa-opioid receptors and the dopamine transporter in nucleus accumbens axonal profiles. Synapse 42:185-192.

Swanson JM, Kinsbourne M, Nigg J, Lanphear B, Stefanatos GA, Volkow N, Taylor E, Casey BJ, Castellanos FX, Wadhwa PD (2007) Etiologic subtypes of attention-deficit/hyperactivity disorder: brain imaging, molecular genetic and environmental factors and the dopamine hypothesis. Neuropsychol Rev 17:39-59.

Sweeney CG, Tremblay BP, Stockner T, Sitte HH, Melikian HE (2017) Dopamine Transporter Amino and Carboxyl Termini Synergistically Contribute to Substrate and Inhibitor Affinities. J Biol Chem 292:1302-1309.

Sweeney CG, Kearney PJ, Fagan RR, Smith LA, Bolden NC, Zhao-Shea R, Rivera IV, Kolpakova J, Xie J, Gao G, Tapper AR, Martin GE, Melikian HE (2020) Conditional, inducible gene silencing in dopamine neurons reveals a sex-specific role for Rit2 GTPase in acute cocaine response and striatal function. Neuropsychopharmacology 45:384-393.

Temkin P, Lauffer B, Jäger S, Cimermancic P, Krogan NJ, von Zastrow M (2011) SNX27 mediates retromer tubule entry and endosome-to-plasma membrane trafficking of signalling receptors. Nature Cell Biology 13:715-721.

Thal LB, Tomlinson ID, Quinlan MA, Kovtun O, Blakely RD, Rosenthal SJ (2019) Single Quantum Dot Imaging Reveals PKCbeta-Dependent Alterations in Membrane Diffusion and Clustering of an Attention-Deficit Hyperactivity Disorder/Autism/Bipolar Disorder-Associated Dopamine Transporter Variant. ACS Chem Neurosci 10:460-471.

Thomsen M, Han DD, Gu HH, Caine SB (2009) Lack of cocaine self-administration in mice expressing a cocaine-insensitive dopamine transporter. J Pharmacol Exp Ther 331:204-211.

Thong FS, Bilan PJ, Klip A (2007) The Rab GTPase-activating protein AS160 integrates Akt, protein kinase C, and AMP-activated protein kinase signals regulating GLUT4 traffic. Diabetes 56:414-423.

Torres GE, Gainetdinov RR, Caron MG (2003a) Plasma membrane monoamine transporters: structure, regulation and function. Nat Rev Neurosci 4:13-25.

Torres GE, Carneiro A, Seamans K, Fiorentini C, Sweeney A, Yao WD, Caron MG (2003b) Oligomerization and trafficking of the human dopamine transporter. Mutational analysis identifies critical domains important for the functional expression of the transporter. J Biol Chem 278:2731-2739.

Torres GE, Yao W-D, Mohn AR, Quan H, Kim K-M, Levey AI, Staudinger J, Caron MG (2001) Functional Interaction between Monoamine Plasma Membrane Transporters and the Synaptic PDZ Domain–Containing Protein PICK1. Neuron 30:121-134.

Trossbach SV et al. (2016) Misassembly of full-length Disrupted-in-Schizophrenia 1 protein is linked to altered dopamine homeostasis and behavioral deficits. Mol Psychiatry 21:1561-1572.

Tsai HC, Zhang F, Adamantidis A, Stuber GD, Bonci A, de Lecea L, Deisseroth K (2009) Phasic firing in dopaminergic neurons is sufficient for behavioral conditioning. Science 324:1080-1084.

Uenaka T, Satake W, Cha PC, Hayakawa H, Baba K, Jiang S, Kobayashi K, Kanagawa M, Okada Y, Mochizuki H, Toda T (2018) In silico drug screening by using genome-wide association study data repurposed dabrafenib, an anti-melanoma drug, for Parkinson's disease. Hum Mol Genet 27:3974-3985.

Ueno T, Kume K (2014) Functional characterization of dopamine transporter in vivo using Drosophila melanogaster behavioral assays. Front Behav Neurosci 8:303.

Ueno T, Tomita J, Tanimoto H, Endo K, Ito K, Kume S, Kume K (2012) Identification of a dopamine pathway that regulates sleep and arousal in Drosophila. Nat Neurosci 15:1516-1523.

Underhill SM, Hullihen PD, Chen J, Fenollar-Ferrer C, Rizzo MA, Ingram SL, Amara SG (2019) Amphetamines signal through intracellular TAAR1 receptors coupled to Galpha13 and GalphaS in discrete subcellular domains. Mol Psychiatry.

Vallone D, Picetti R, Borrelli E (2000) Structure and function of dopamine receptors. Neuroscience & Biobehavioral Reviews 24:125-132.

Vandenbergh (2000) Human dopamine transporter gene: coding region conservation among normal, Tourette's disorder, alcohol dependence and attention-deficit hyperactivity disorder populations. Molecular Psychiatry.

Vetter IR, Wittinghofer A (2001) The guanine nucleotide-binding switch in three dimensions. Science 294:1299-1304.

Voorn P, Jorritsma-Byham B, Van Dijk C, Buijs RM (1986) The dopaminergic innervation of the ventral striatum in the rat: a light- and electron-microscopical study with antibodies against dopamine. J Comp Neurol 251:84-99.

Vuorenpaa A, Jorgensen TN, Newman AH, Madsen KL, Scheinin M, Gether U (2016) Differential internalization rates and postendocytic sorting of the norepinephrine and dopamine transporters are controlled by structural elements in the N termini. J Biol Chem 291:5634-5651.

Wakayama S, Kiyonaka S, Arai I, Kakegawa W, Matsuda S, Ibata K, Nemoto YL, Kusumi A, Yuzaki M, Hamachi I (2017) Chemical labelling for visualizing native AMPA receptors in live neurons. Nat Commun 8:14850.

Walkinshaw E, Gai Y, Farkas C, Richter D, Nicholas E, Keleman K, Davis RL (2015) Identification of genes that promote or inhibit olfactory memory formation in Drosophila. Genetics 199:1173-1182.

Wang JY, Gong MY, Ye YL, Ye JM, Lin GL, Zhuang QQ, Zhang X, Zhu JH (2015) The RIT2 and STX1B polymorphisms are associated with Parkinson's disease. Parkinsonism Relat Disord 21:300-302.

Wei Y, Williams JM, Dipace C, Sung U, Javitch JA, Galli A, Saunders C (2007) Dopamine transporter activity mediates amphetamine-induced inhibition of Akt through a Ca2+/calmodulin-dependent kinase II-dependent mechanism. Mol Pharmacol 71:835-842.

Wennerberg K, Rossman KL, Der CJ (2005) The Ras superfamily at a glance. J Cell Sci 118:843-846.

Wes PD, Yu M, Montell C (1996) RIC, a calmodulin-binding Ras-like GTPase. EMBO J 15:5839-5848.

Wheeler DS, Underhill SM, Stolz DB, Murdoch GH, Thiels E, Romero G, Amara SG (2015) Amphetamine activates Rho GTPase signaling to mediate dopamine transporter internalization and acute behavioral effects of amphetamine. Proc Natl Acad Sci U S A 112:E7138-7147.

Wilkins ME, Li X, Smart TG (2008) Tracking cell surface GABAB receptors using an alpha-bungarotoxin tag. J Biol Chem 283:34745-34752.

Willard SS, Koss CM, Cronmiller C (2006) Chronic cocaine exposure in Drosophila: life, cell death and oogenesis. Dev Biol 296:150-163.

Williams JM, Owens WA, Turner GH, Saunders C, Dipace C, Blakely RD, France CP, Gore JC, Daws LC, Avison MJ, Galli A (2007) Hypoinsulinemia regulates amphetamine-induced reverse transport of dopamine. PLoS Biol 5:e274.

Wise RA (2004) Dopamine, learning and motivation. Nat Rev Neurosci 5:483-494.

Wisor JP, Nishino S, Sora I, Uhl GH, Mignot E, Edgar DM (2001) Dopaminergic role in stimulant-induced wakefulness. J Neurosci 21:1787-1794.

Wolf ME, Roth RH (1990) Autoreceptor regulation of dopamine synthesis. Ann N Y Acad Sci 604:323-343.

Wood S, Sage JR, Shuman T, Anagnostaras SG (2014) Psychostimulants and cognition: a continuum of behavioral and cognitive activation. Pharmacol Rev 66:193-221.

Woodward JJ, Wilcox RE, Leslie SW, Riffee WH (1986) Dopamine uptake during fast-phase endogenous dopamine release from mouse striatal synaptosomes. Neuroscience Letters 71:106-112.

Wu S, Bellve KD, Fogarty KE, Melikian HE (2015) Ack1 is a dopamine transporter endocytic brake that rescues a trafficking-dysregulated ADHD coding variant. Proc Natl Acad Sci U S A 112:15480-15485.

Wu S, Fagan RR, Uttamapinant C, Lifshitz LM, Fogarty KE, Ting AY, Melikian HE (2017) The Dopamine Transporter Recycles via a Retromer-Dependent Postendocytic Mechanism: Tracking Studies Using a Novel Fluorophore-Coupling Approach. J Neurosci 37:9438-9452.

Wu X, Gu HH (2003) Cocaine affinity decreased by mutations of aromatic residue phenylalanine 105 in the transmembrane domain 2 of dopamine transporter. Mol Pharmacol 63:653-658.

Xie T, Ho MCW, Liu Q, Horiuchi W, Lin CC, Task D, Luan H, White BH, Potter CJ, Wu MN (2018) A Genetic Toolkit for Dissecting Dopamine Circuit Function in Drosophila. Cell Rep 23:652-665.

Yamashita A, Singh SK, Kawate T, Jin Y, Gouaux E (2005) Crystal structure of a bacterial homologue of Na+/Cl--dependent neurotransmitter transporters. Nature 437:215-223.

Yang JW, Larson G, Konrad L, Shetty M, Holy M, Jantsch K, Kastein M, Heo S, Erdem FA, Lubec G, Vaughan RA, Sitte HH, Foster JD (2019) Dephosphorylation of human dopamine transporter at threonine 48 by protein phosphatase PP1/2A up-regulates transport velocity. J Biol Chem 294:3419-3431.

Yang T, Xu X, Kernan T, Wu V, Colecraft HM (2010) Rem, a member of the RGK GTPases, inhibits recombinant CaV1.2 channels using multiple mechanisms that require distinct conformations of the GTPase. J Physiol 588:1665-1681.

Zhang H, Li S, Wang M, Vukusic B, Pristupa ZB, Liu F (2009) Regulation of dopamine transporter activity by carboxypeptidase E. Mol Brain 2:10.

Zhang L, Wahlin K, Li Y, Masuda T, Yang Z, Zack DJ, Esumi N (2013) RIT2, a neuron-specific small guanosine triphosphatase, is expressed in retinal neuronal cells and its promoter is modulated by the POU4 transcription factors. Mol Vis 19:1371-1386.

Zhang X, Niu M, Li H, Xie A (2015) RIT2 rs12456492 polymorphism and the risk of Parkinson's disease: A meta-analysis. Neurosci Lett 602:167-171.

Zhou Q, Li J, Wang H, Yin Y, Zhou J (2011) Identification of nigral dopaminergic neuron-enriched genes in adult rats. Neurobiol Aging 32:313-326.

Zhu S, Zhao C, Wu Y, Yang Q, Shao A, Wang T, Wu J, Yin Y, Li Y, Hou J, Zhang X, Zhou G, Gu X, Wang X, Bustelo XR, Zhou J (2015) Identification of a Vav2-dependent mechanism for GDNF/Ret control of mesolimbic DAT trafficking. Nat Neurosci 18:1084-1093.

Zhu SJ, Kavanaugh MP, Sonders MS, Amara SG, Zahniser NR (1997) Activation of protein kinase C inhibits uptake, currents and binding associated with the human dopamine transporter expressed in Xenopus oocytes. J Pharmacol Exp Ther 282:1358-1365.